Focal-Plane-Array FTIR Imaging

李耀昌
Yao-Chang Lee
NSRRC, Taiwan
yclee@nsrrc.org,tw

Outline

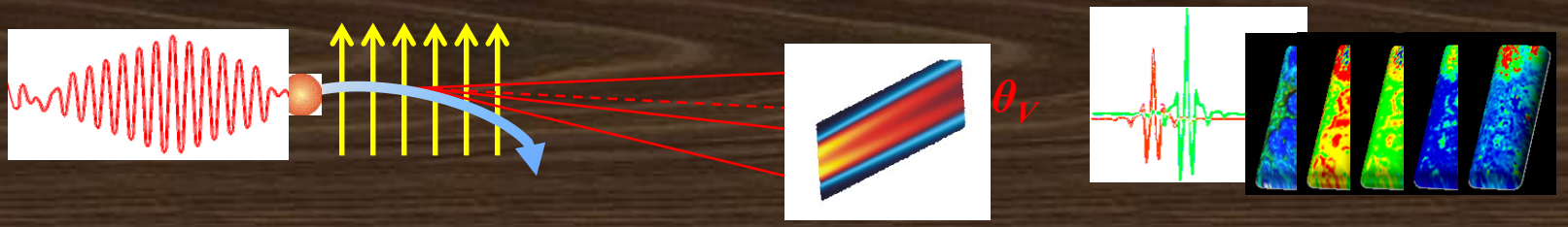

I. IR Beamline and End-Station

II. Principle of FTIR MicroSpectroscopy, Imaging, and IR Nanoscopy

III. Basic Principles of FTIR Spectroscopy

IV. The Principle of ATR-FTIR, and GIRA-FTIR

V. AI-Driven Spectral Imaging Analysis

VI. Summary

I. Introduction of Infrared Beamline and ES

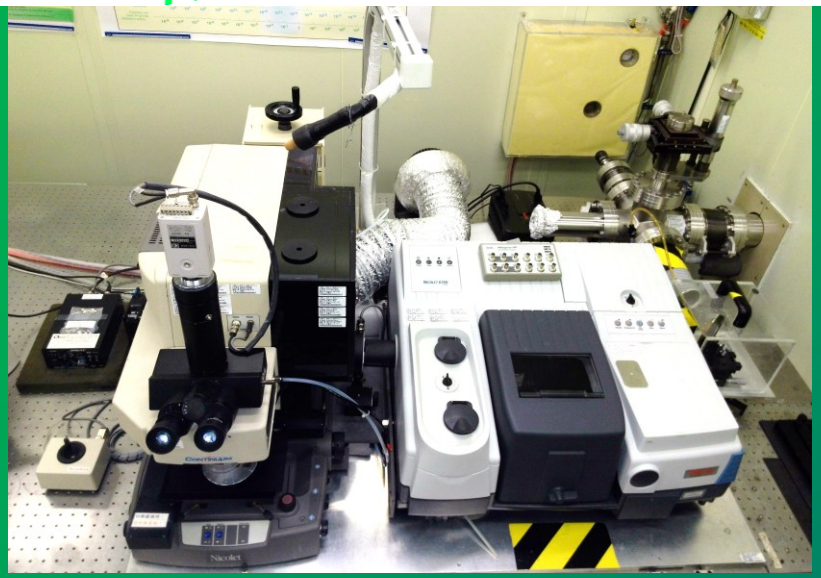

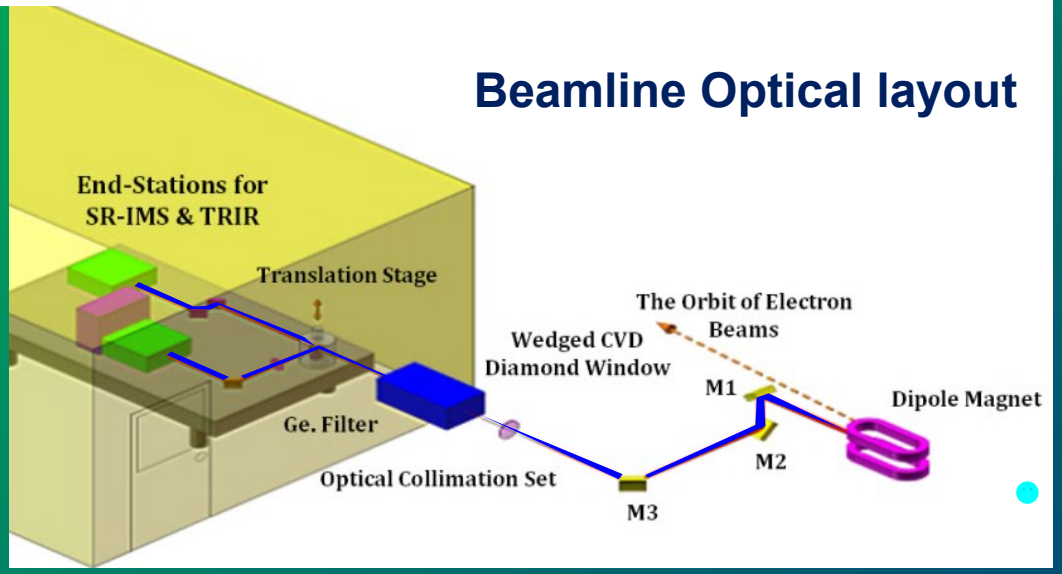

1. Spectral Resolution: 0.125 cm^{-1}
2. Lateral Resolution: 8 x 8 μm^2

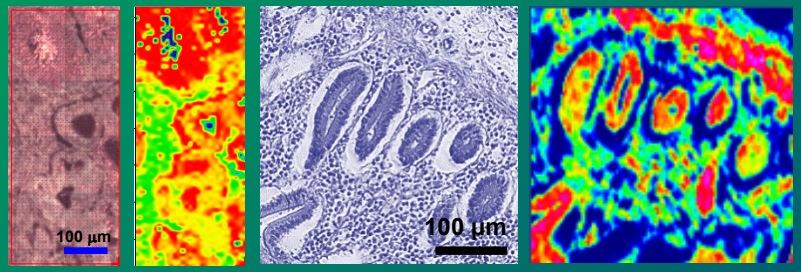

IR and Visible images of Human colon sections

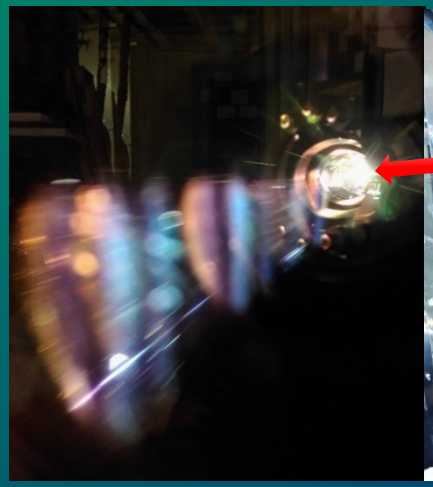

Synchrotron beam

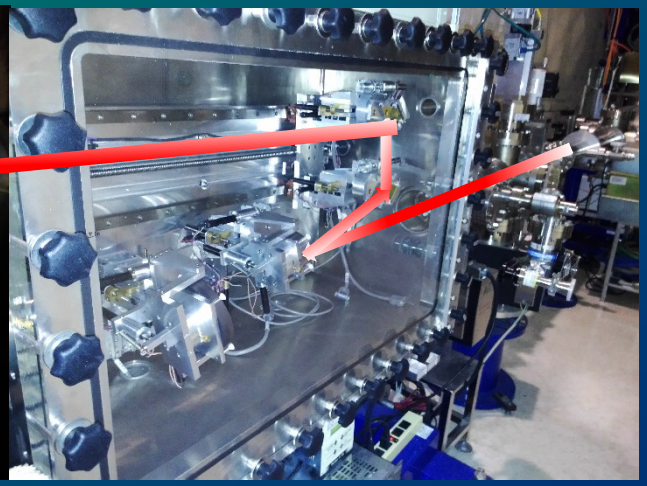

Beamline and Optical collimation Set

I. Introduction of Infrared Beamline and ES (Cont.)

Bruker Hyperion 3000
(Off-Line)
FT-IR imaging station
allows an area of 170 × 170 μm² to be imaged simultaneously.

Spectral resolution: 0.125 cm^{-1}
Lateral resolution: 15 μm @ 1000 cm^{-1}

Thermo-Nicolet Continμm
(On-Line)
Synchrotron-based FT-IR mapping station
MCT single element detector

Spectral resolution: 0.125 cm^{-1}
Lateral resolution: 8 μm @ 1000 cm^{-1}

II. Basic Principle of FTIR MicroSpectroscopy, Imaging, and IR Nanoscopy

Focal-Plane-Array FT-IR imaging system
Bruker Hyperion 300

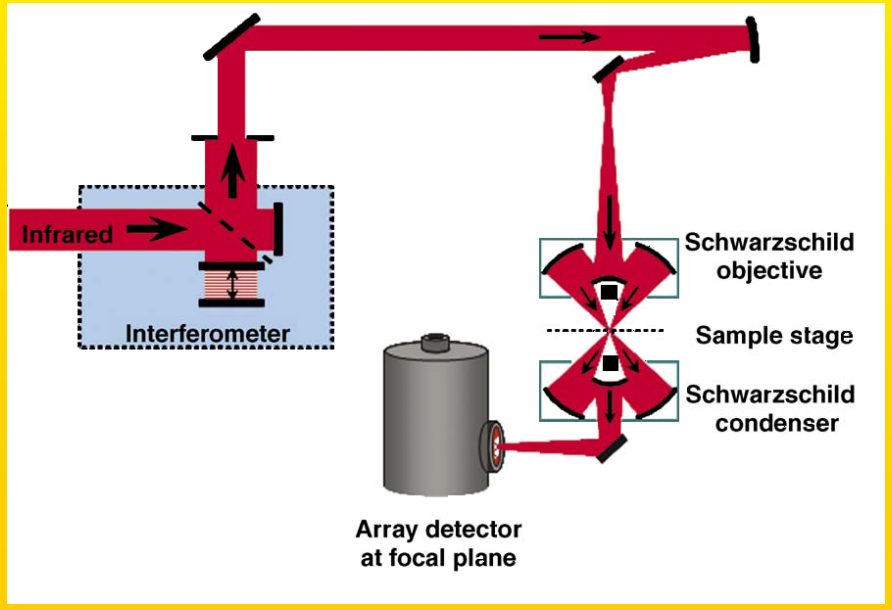

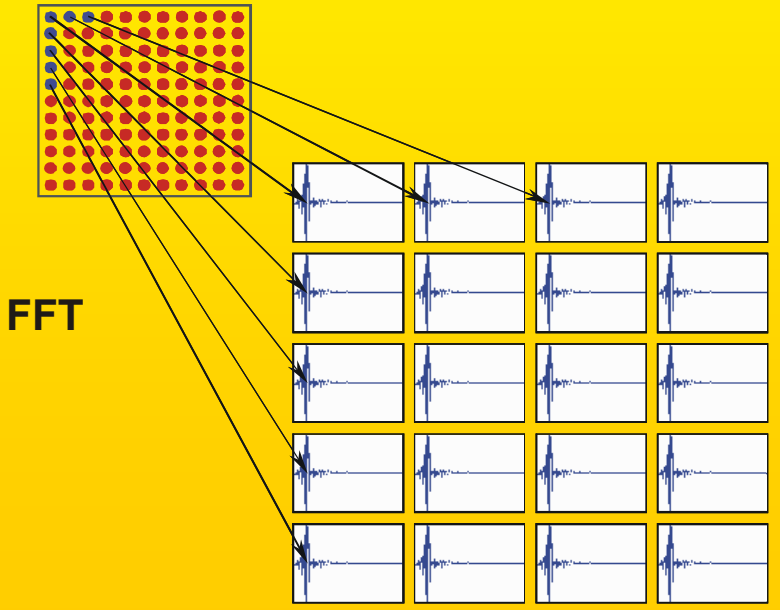

Optical layout of FPA-base FT-IR imaging system

• FTIR MicroSpectroscopy

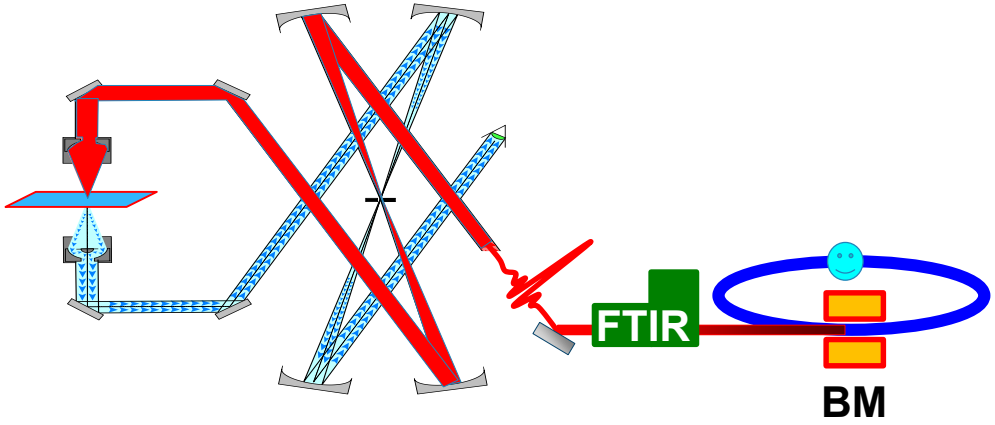

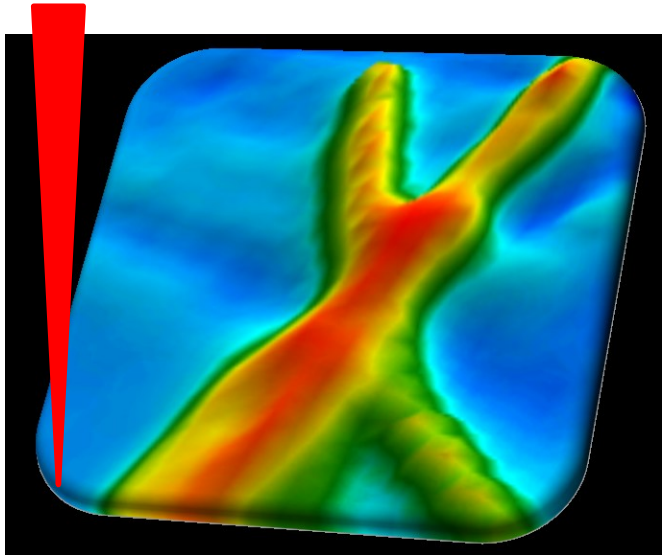

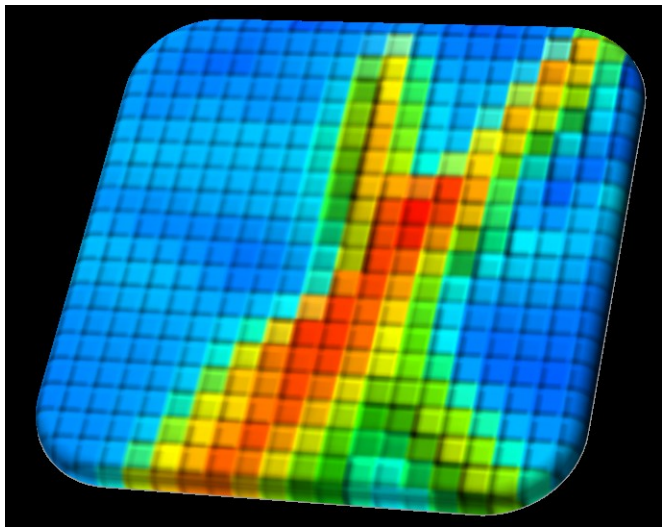

roscopy is defined by the size of focused beam on sample surface.

Infrared Beam Profile of Synchrotron IR and Globar IR

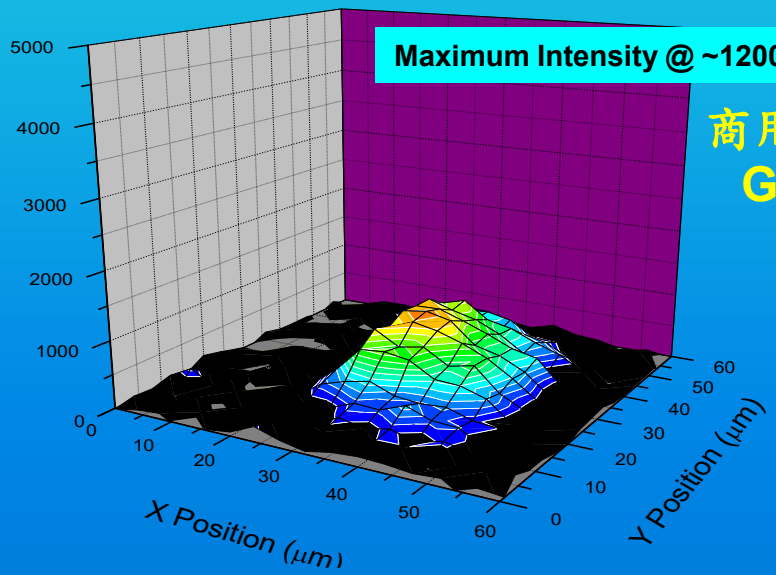

商用紅外光源
Globar IR

Beam Size: 50 x 30 μm²

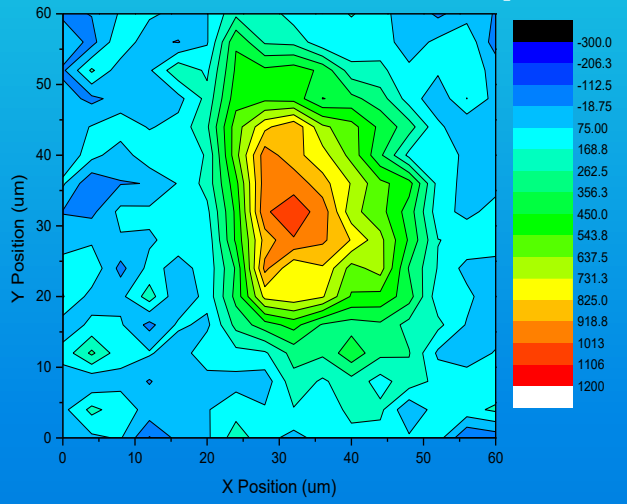

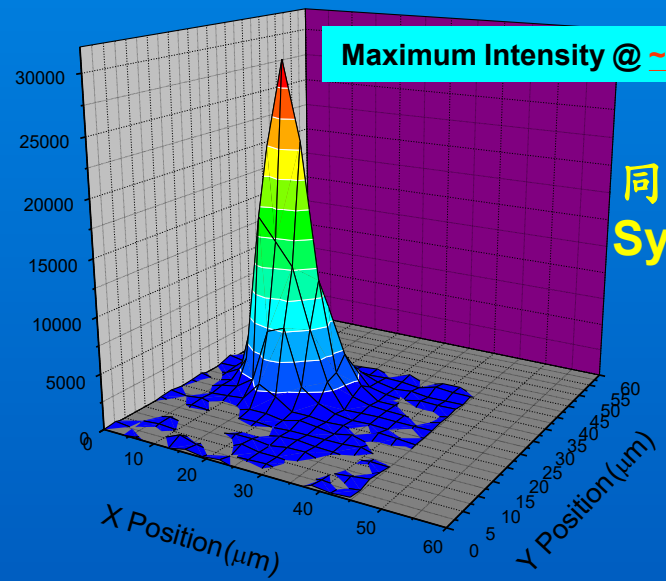

同步輻射紅外光
Synchrotron IR

Beam Size:13 x 10 μm²

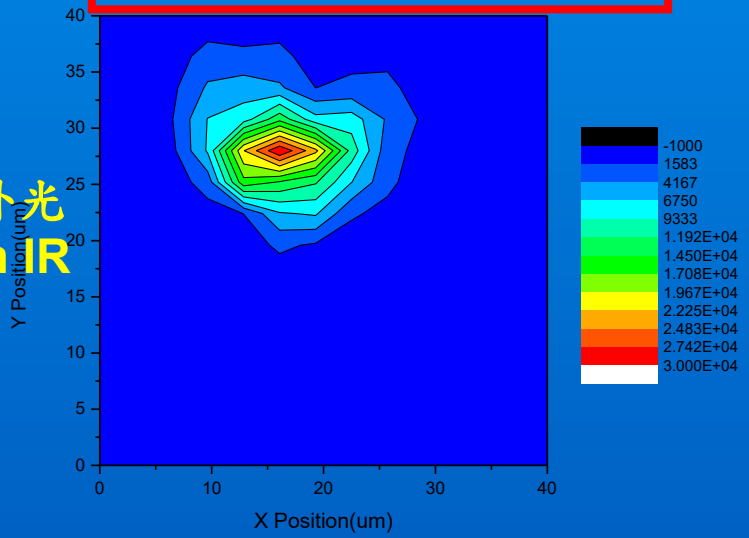

Confocal IR microscope

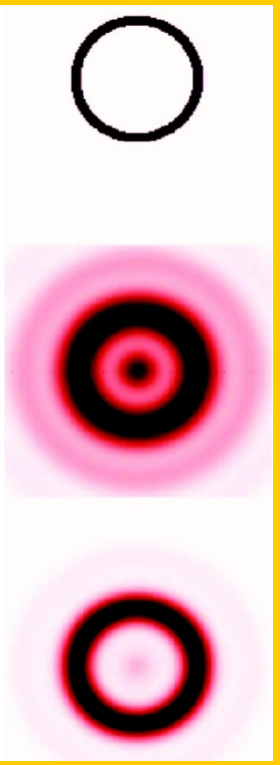

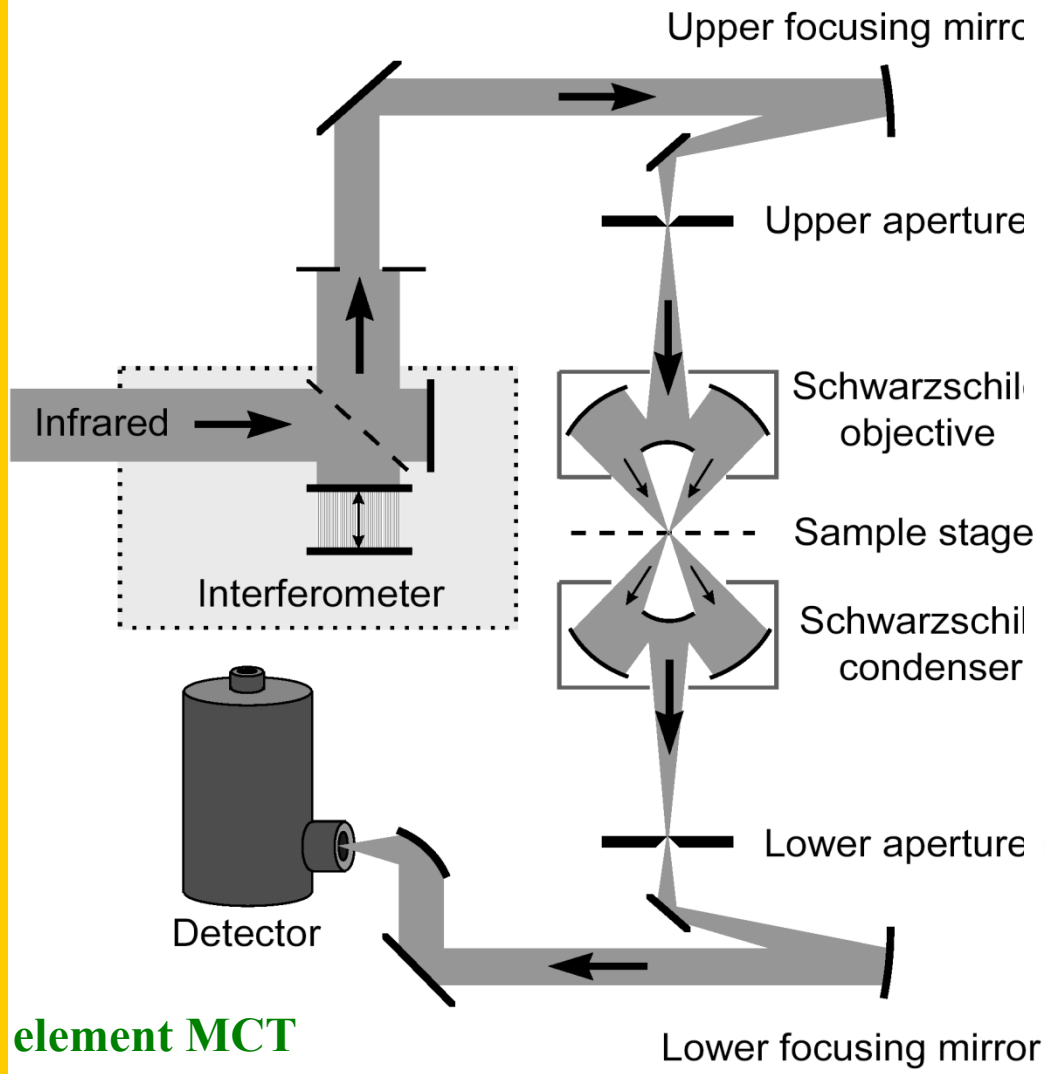

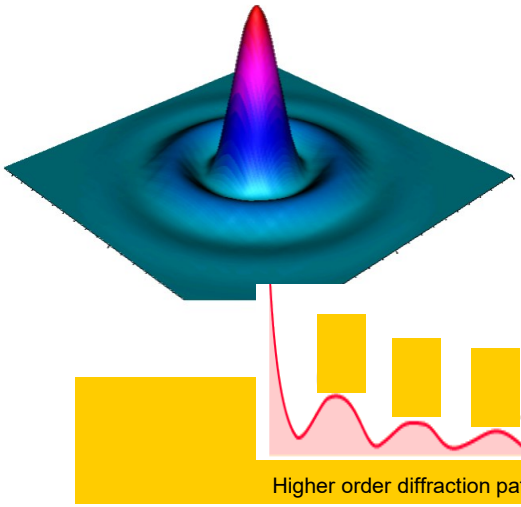

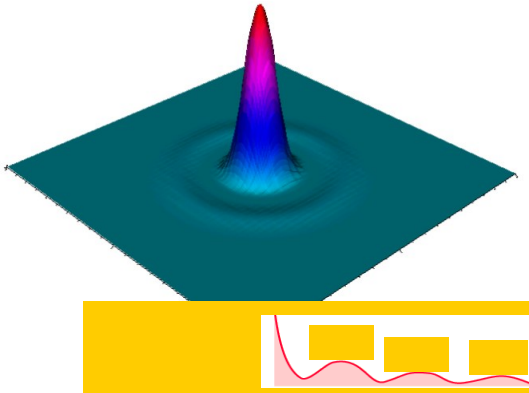

Single element MCT

Lateral Resolution and Sampling in FTIR Mapping and FPA Imaging

FTIR image pixel size or mapping step size is not equal to the true lateral resolution.

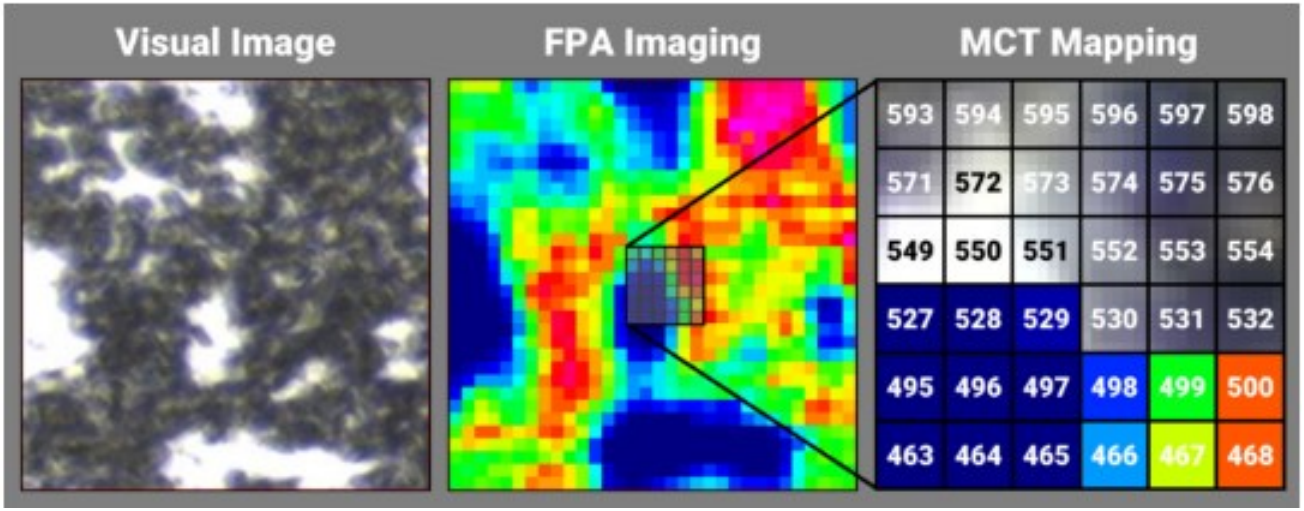

Rayleigh Criteria

$$d = 1.22\lambda/(2 * N.A.)$$

d: diffraction-limited lateral resolution
λ: IR wavelength
N.A. = n * sinθ: numerical aperture of the objective

https://www.opticsblog.bruker.com/ftir-mapping-vs-imaging-explaining-the-differences/

Lateral Resolution versus Wavenumber in Confocal IR Microscopy

900 cm^{-1}

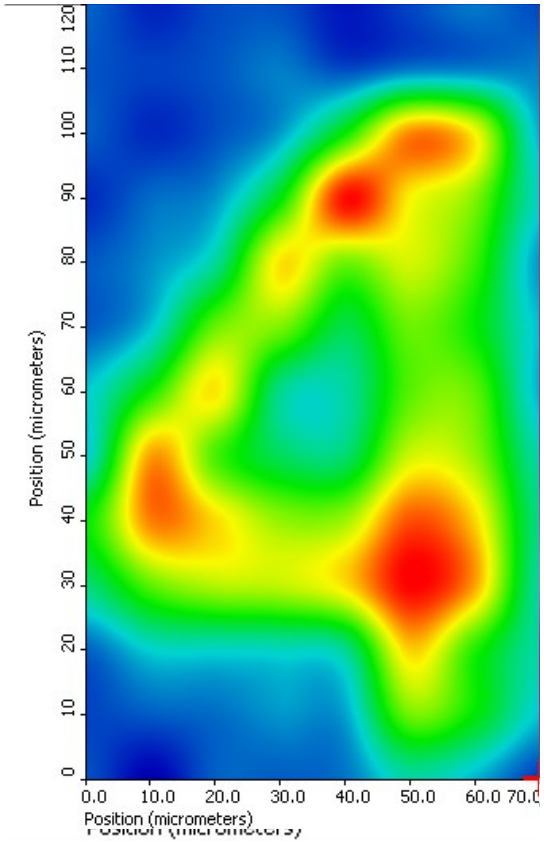

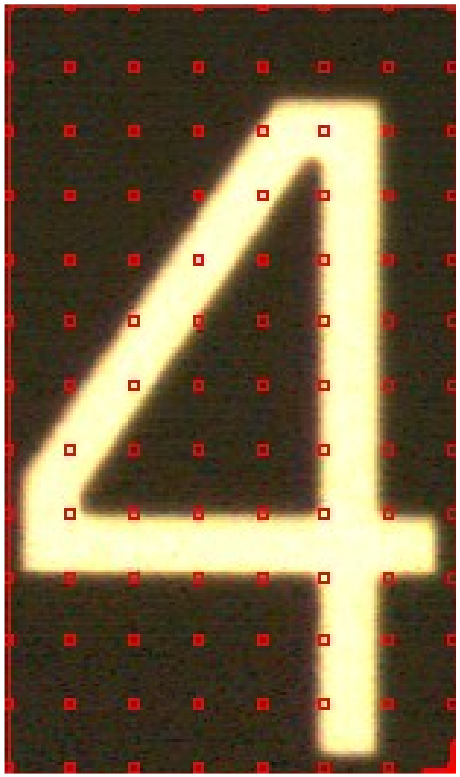

Verification of the wavenumber dependence of apparent lateral resolution in confocal IR microscopy using a USAF 1951 resolution target.

FTIR Mapping vs FPA Imaging

Item	MCT Mapping	FPA Imaging
Detector	Single-element MCT 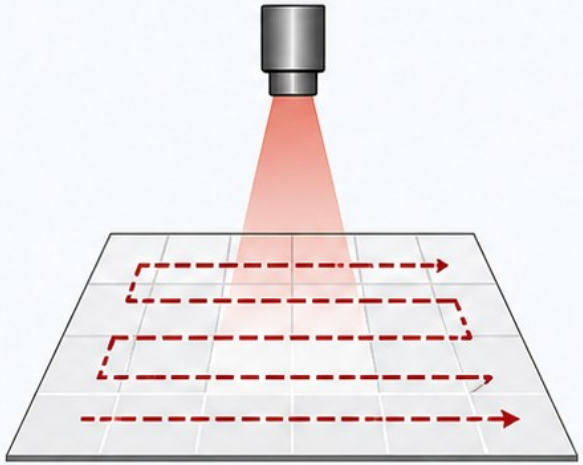	Focal plane array 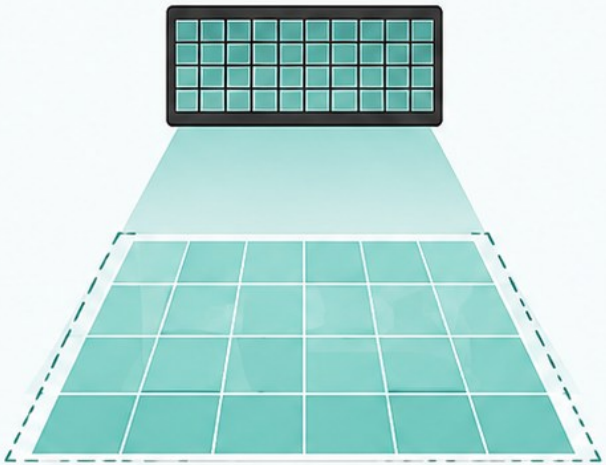
Acquisition	Point-by-point raster scan	Parallel acquisition
Spatial sampling	Step size / aperture size	Detector pixel projection
Advantage	Flexible, high S/N with SR-IR	Fast chemical imaging
Limitation	Slow	Pixel size and optical sampling limitations

Spectral Data Preprocessing Workflow

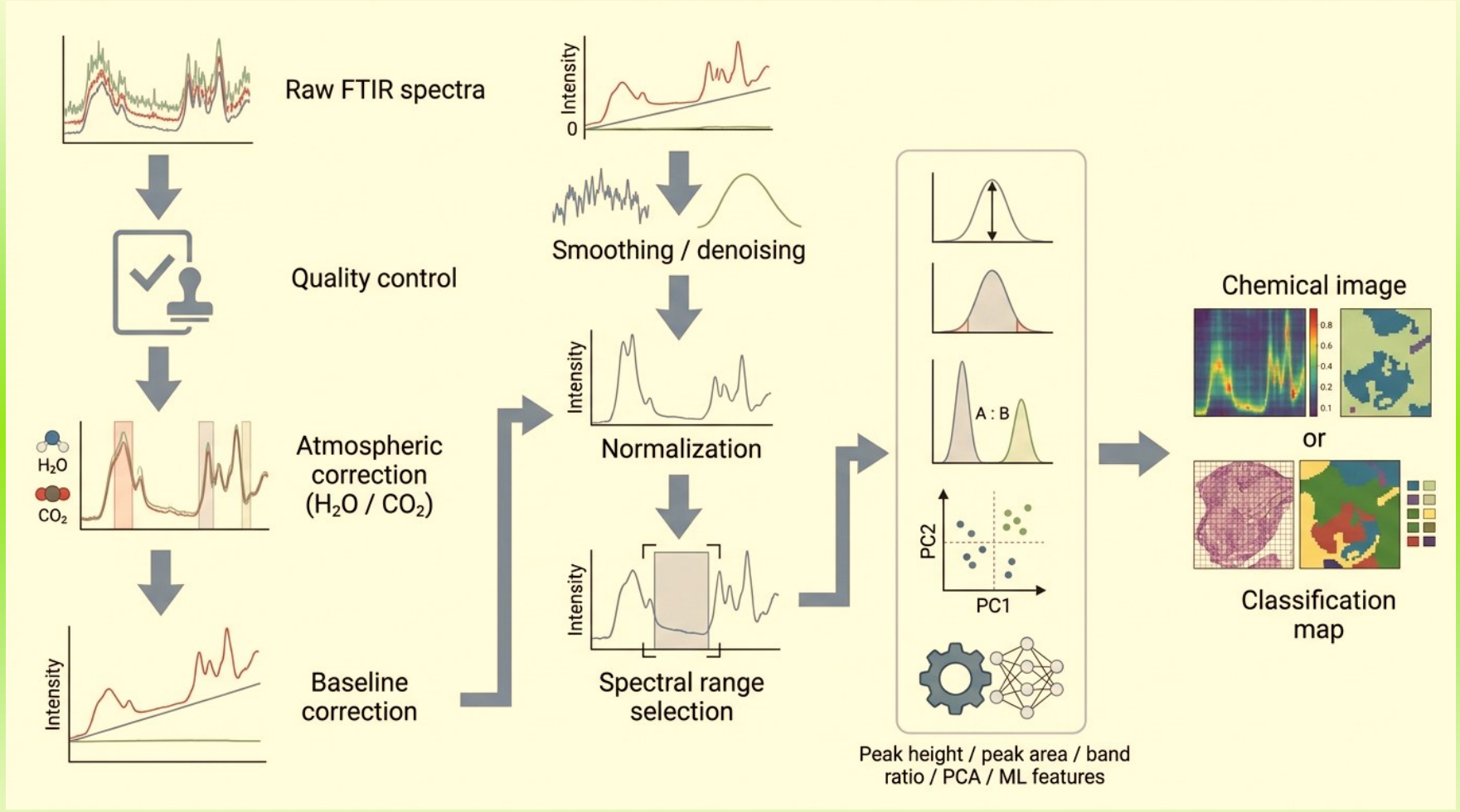

Workflow for FTIR spectral data preprocessing and feature extraction for chemical imaging and classification.

From FTIR Spectra to Biomolecular Chemical Images

Human Colon Tissue Section

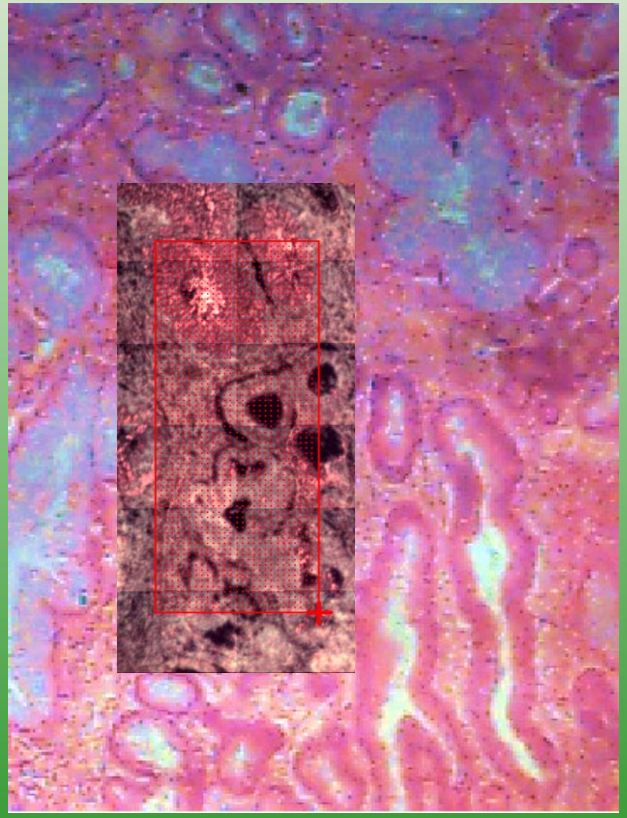

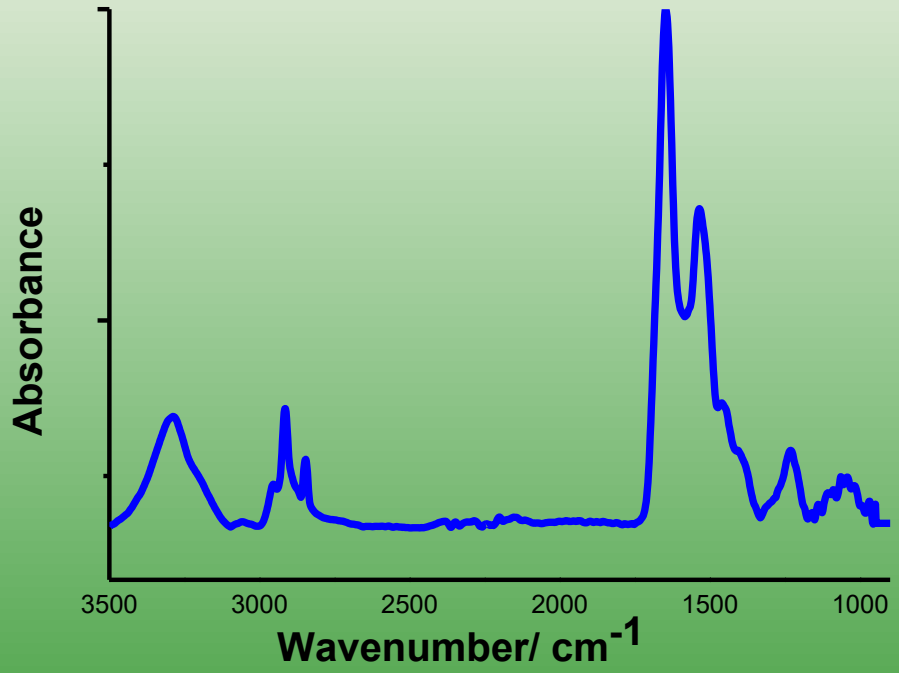

Lipid

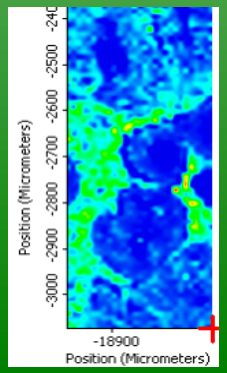

Protein

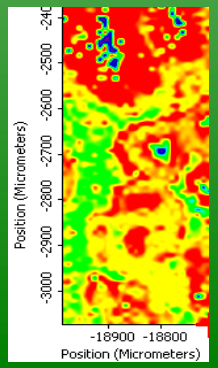

DNA/ RNA

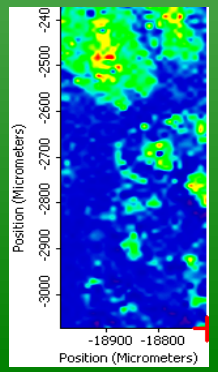

Carbohydrates

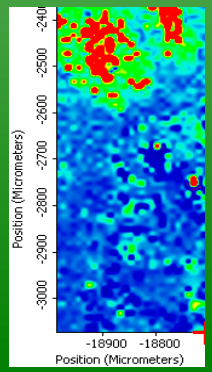

Applications and Highlights

Paleontology: Collagen Remains
195 Myr Dinosaurs Embryo and Rib; 2.89 Myr Mummy Fossil

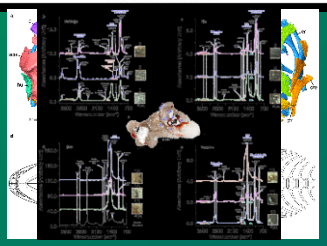

***Nature* 496**, 210–214 (**2013**).
Nature Communications, **8**, 14220 (**2017**)
Discover 2018 Top 100 Science Stories, Ranked No. 12
Nature volume 653, 117–123 (2026).

Medicine:
Cancer Screening and Chronic Disease Diagnosis

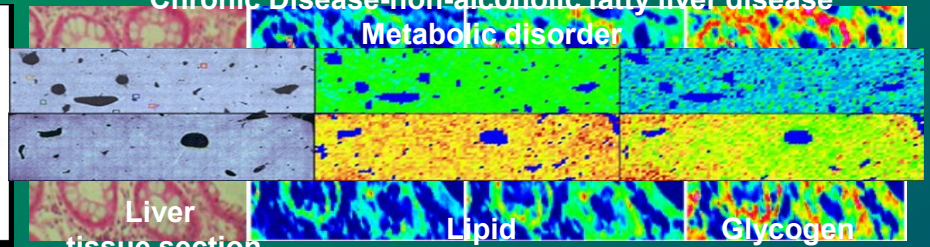

Analyst, **148(3)**, 643-653 (2023)
***US patent*, US-8-354,222 B2, (2013) ; *Japan patent*, 2009-119309, (2013) ; *R.O.C. patent*, No. 404931, (2013).**

Biocomponent Analysis:
Butterfly scales

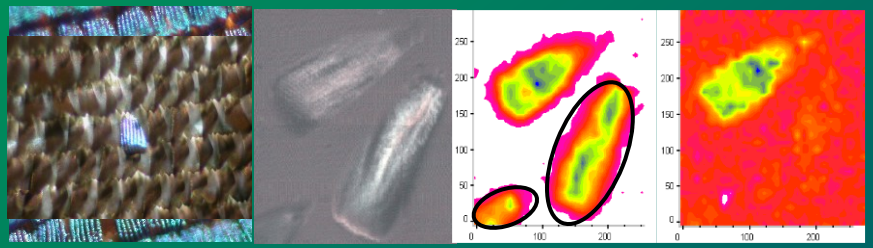

Cosmetic and Forensic science (drug abuse):
Human hair

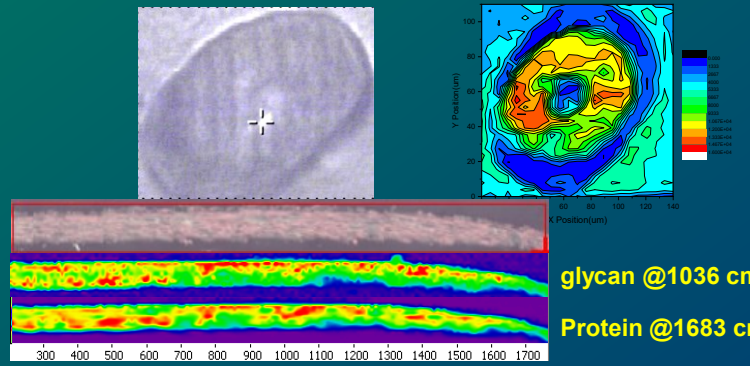

Environment Science
Organic Contamination in Soil

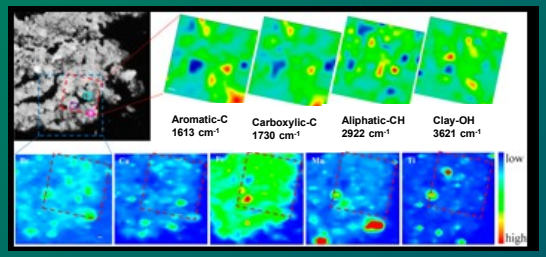

Science of the Total Environment, **624**, 210–214 (2018)
Journal of Hazardous Materials, **411**, 125129 (2021)

Industrial Application:
Quality Control of LED material

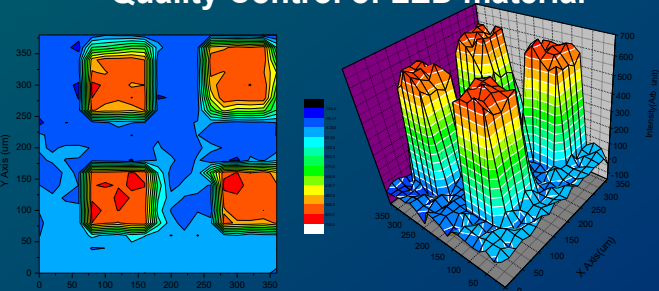

IR Nanoscopy: AFM coupled with FTIR Push Lateral Resolution to Nano Scale

Nano-FTIR

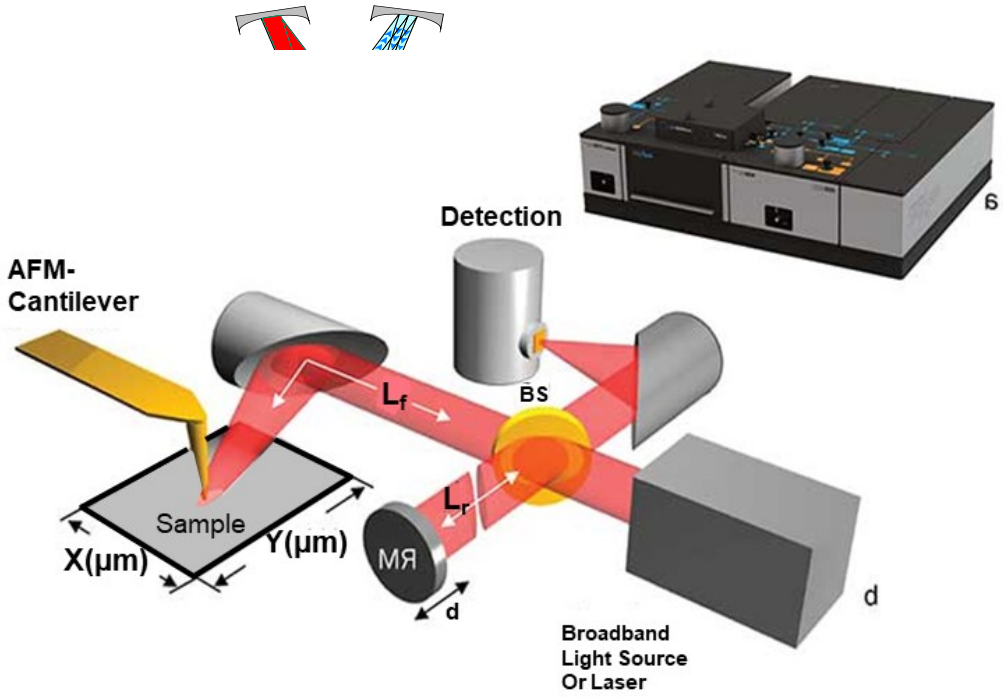

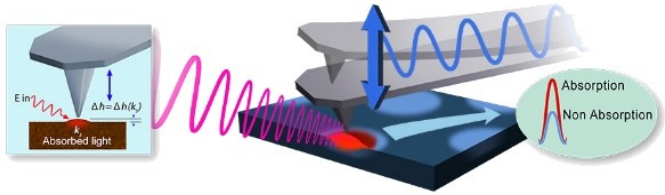

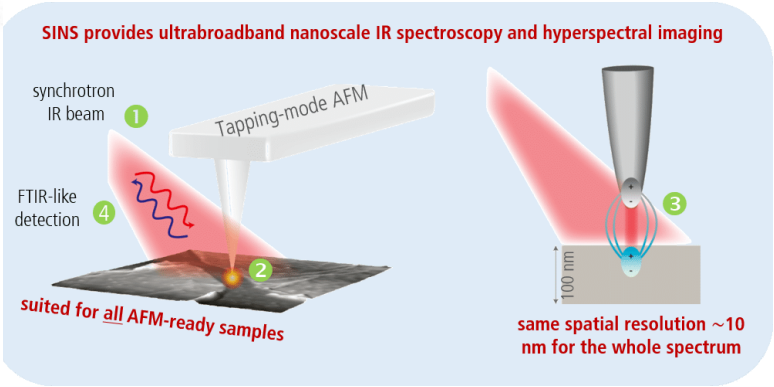

- **20~10 nm lateral resolution depended on Tip diameter**
- IR absorption spectroscopy & chemical imaging
- Highly interpretable spectra
- Excels for Polymers, Life Sciences, Inorganics, 2D Materials and Photonics

nano-IR

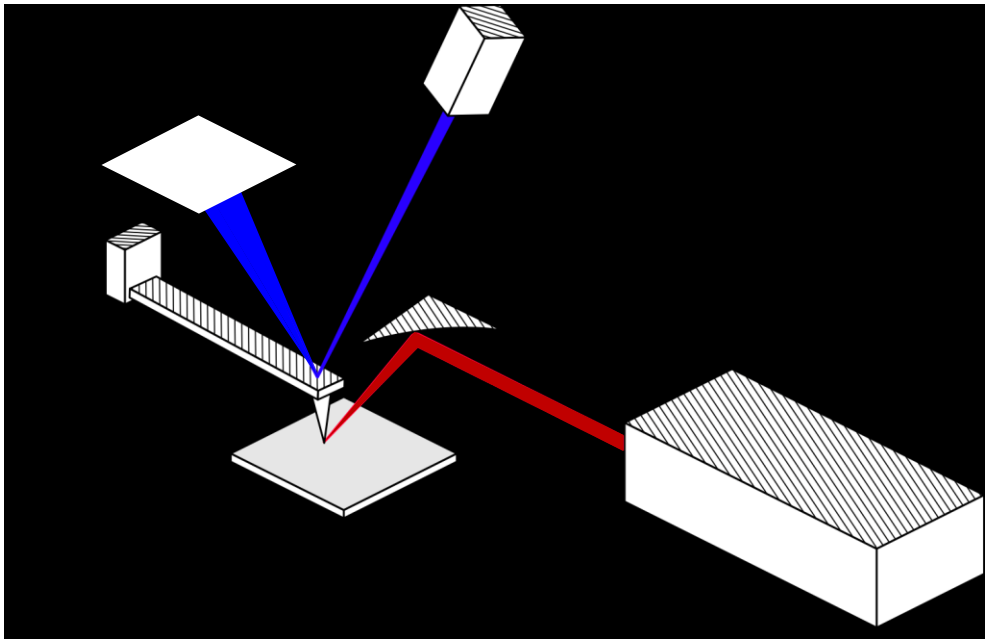

QCL

Because PiF-IR uses a narrowband QCL as a tunable source, the experimental setup is immensely simplified. Furthermore, the near-field signal is automatically isolated because IR measurements are made using mechanical force detection. **PiF-IR is both a near-field excitation and near-field detection technique as opposed to the near-field excitation, but far-field detection used for nano-FTIR**. Therefore, PiF-IR system is faster, easier to use, and provides better SNR via selective power control.

Applications of NanoIR

Polymer blends & Block Copolymers

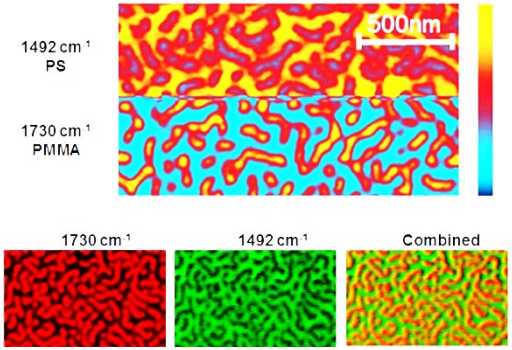

https://www.anasysinstrumentsinstruments.com/technology/tapping-afm-ir/

Multilayer films

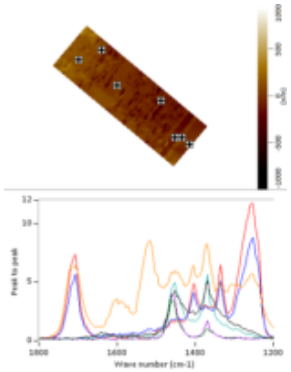

Nanofibers

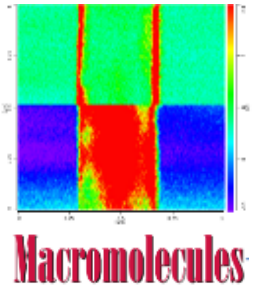

Macromolecules

2D Materials & Graphene

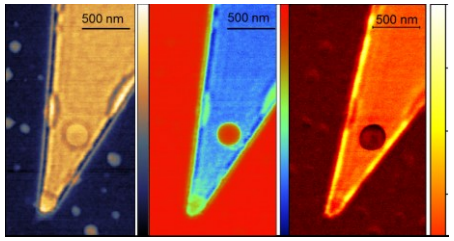

Sub-10 nm Spatial Resolution Chemical Imaging and Spectroscopy of a Graphene Wedge

Centrone et al., Analyst, 143, 3808 (2018)

Nano-Composites

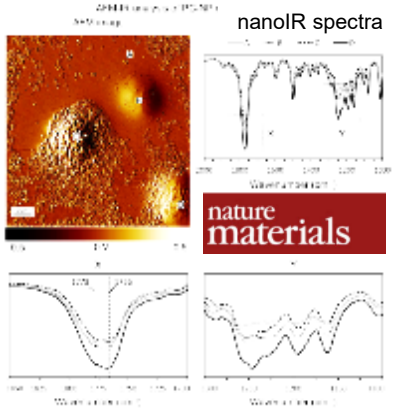

Organic nano-Contaminants

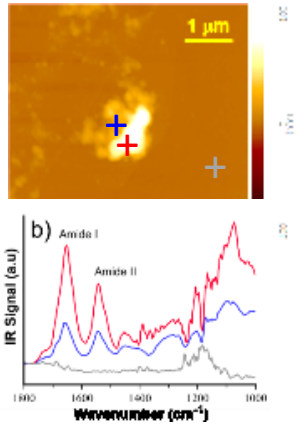

Life Science: Single protein molecule

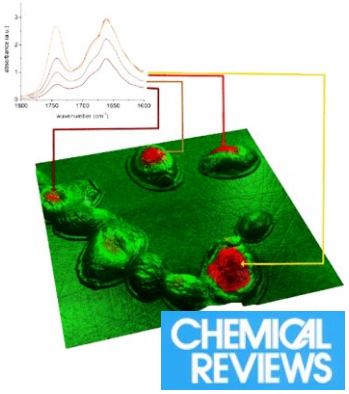

Chem. Rev.,117 (7), pp 5146–5173 (2017)

Perovskites & Solar Cells

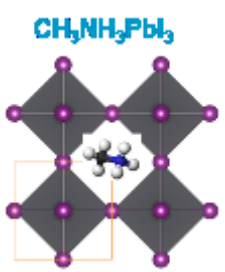

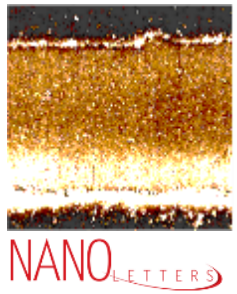

ECS Journal of Solid State Science and Technology
5 (4), 3018(2015)

III. Basic Principle of FTIR Spectroscopy

Vibrational Spectroscopy (VS) probes molecular vibrations

Vibrational spectroscopy

Infrared spectroscopy **Raman Spectroscopy**

Selection rule for transitions

Infrared : Molecular **dipole moment** must change during vibration

Raman : Molecular **polarizability** must **change** during vibration

IR spectroscopy is more sensitive than Raman spectroscopy

Two techniques are complimentary

The Infrared part of EM Spectrum and Units

Diagram of The Electromagnetic Spectrum with drawings, showing wavelengths (in meters), relative size of wavelengths, common name of waves, and energy of one photon (in electron volts). Source: NSRRC

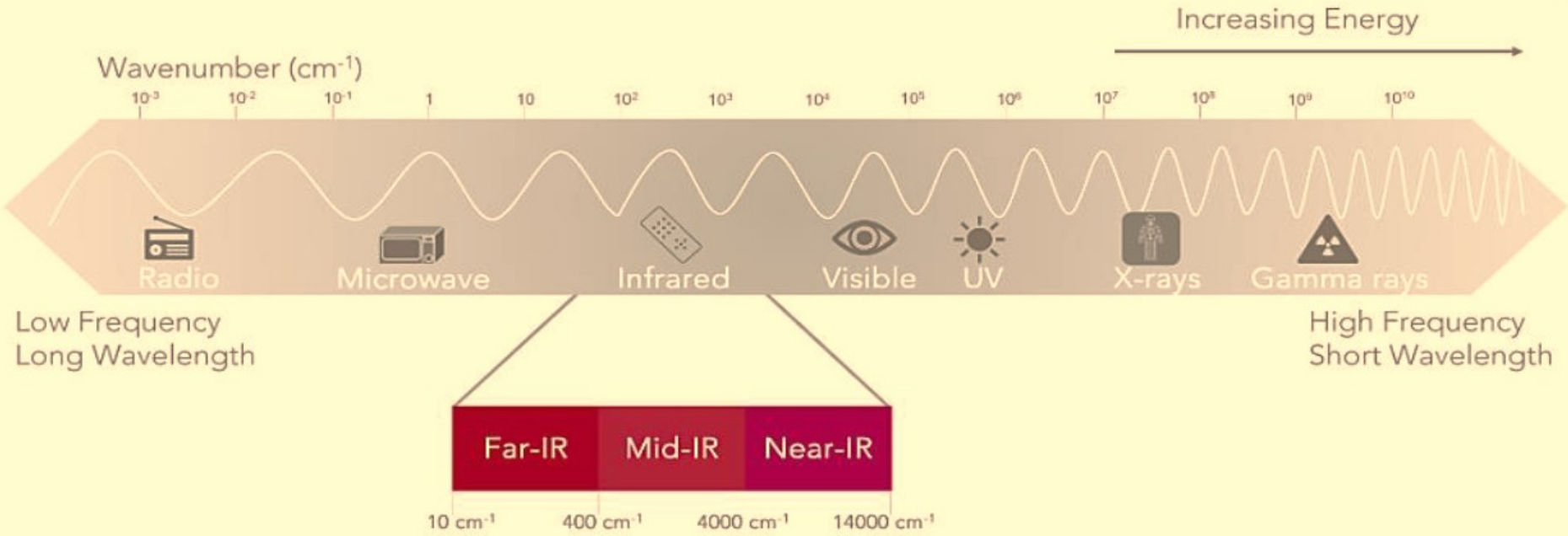

Frequently Use IR unit: wavenumbers (cm^{-1}) - the number of waves in a centimeter.
Wavelength: 10 micrometer (1000 cm^{-1})

1 eV ≈ 8065.456 cm^{-1}
1 THz ≈ 33 cm^{-1}
300 Kelvin ≈ 210 cm^{-1}
Wavenumber ≈ 0.695 x T (K)

Near-IR: 14000 – 4000cm^{-1}
Mid-IR: 4000 – 400 cm^{-1}
Far-IR: 400 – 5 cm^{-1}
NSRRC IR covers ~ 1 meV to 1 eV

IR Unit Conversions

Energy unit conversions:

1 cm^{-1} =		0.124 meV	0.030 THz	1.44 Kelvin
1 meV =	8.1 cm^{-1}		0.242 THz	11.6 Kelvin
1 THz =	33 cm^{-1}	4.14 meV		48 Kelvin
1 Kelvin =	0.70 cm^{-1}	0.086 meV	0.021 THz	

Conversions for microns (wavelength) to and from wavenumbers (cm^{-1}):

Y microns = 10^4 / (**X** cm^{-1})
X cm^{-1} = 10^4 / (**Y** microns)

Absorbance units:

A = log (1/T)

Where A is *Absorbance* and T is *Transmittance.*

Events Activated As EM Interact With Matter

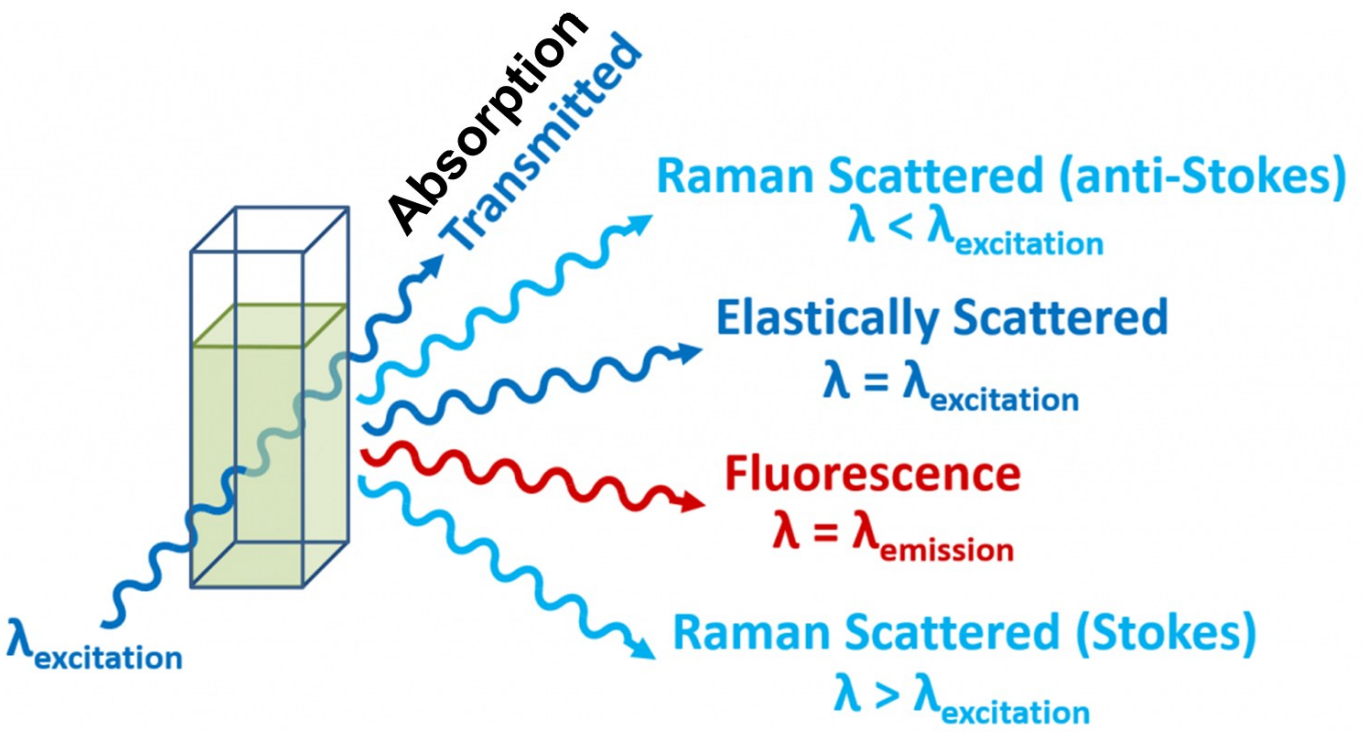

The figure shows how excitation light interacts with a sample, resulting in transmitted, elastically scattered, inelastically scattered (Raman Stokes and anti-Stokes), and fluorescence signals, each with distinct wavelength characteristics.

https://www.edinst.com/blog/raman-scattering-blog/

Absorbance (A), Reflectance (R), and Transmittance (T)

$$T = \frac{I_T}{I_0} \qquad R = \frac{I_R}{I_0}$$

$$A = -\log\left(\frac{I_T}{I_0}\right) = \log\left(\frac{1}{T}\right) \qquad A = -\log\left(\frac{I_R}{I_0}\right) = -\log(R) = \log\left(\frac{1}{R}\right)$$

$$A = 1 - R - T$$

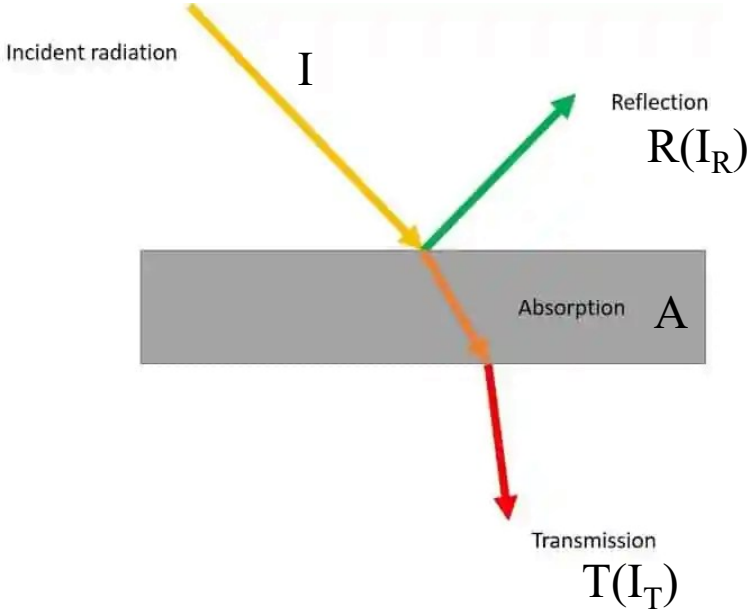

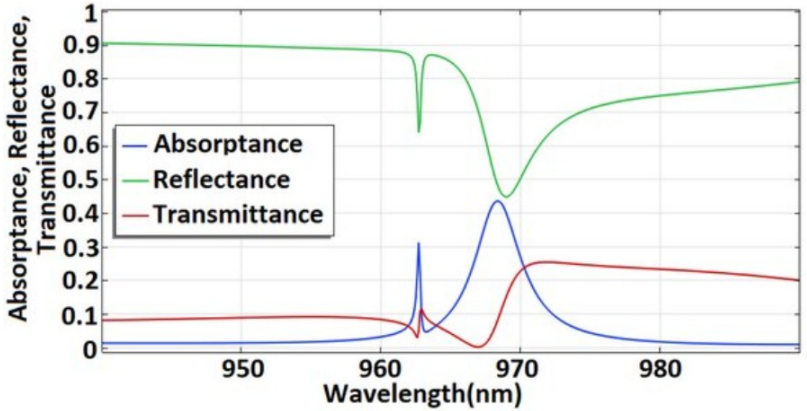

Optical Density (OD) or absorbance (A)

Absorbance (A) emphasizes absorption, while OD may include other losses.

https://www.researchgate.net/publication/370442060_A_Sensitive_Biosensor_Based_on_Plasmonic-Graphene_Configuration_for_Detection_of_COVID-19_Virus/figures?lo=1

Events Activated As EM interact with Matter in UV/Vis and mid-IR range

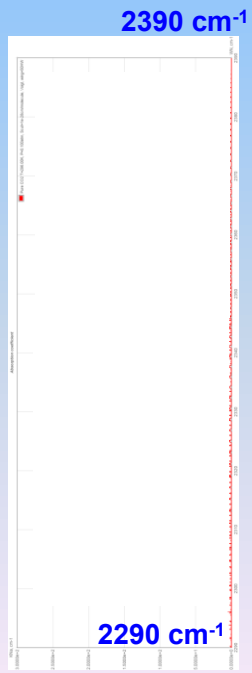

Potential Energy

Singlet

Vibration Relaxation
$10^{-11} \sim 10^{-14}$ s

Triplet

$10^{-14} \sim 10^{-11}$ s
Intersystem crossing

Singlet

UV/ VIS

Absorption
~ 10^{-15} s

$10^{-3} – 10^{0}$ s
Phosphorescence UV/ VIS

Fundamental Vibration Transition (IR)

Fluorescence
$10^{-9} \sim 10^{-6}$ s

Reaction Coordinate (Bond length, bond angle, or dihedral angle)

Origin of EM Absorption

Energy Region

X - Ray **Bond breaking/ Inner-shell ele**

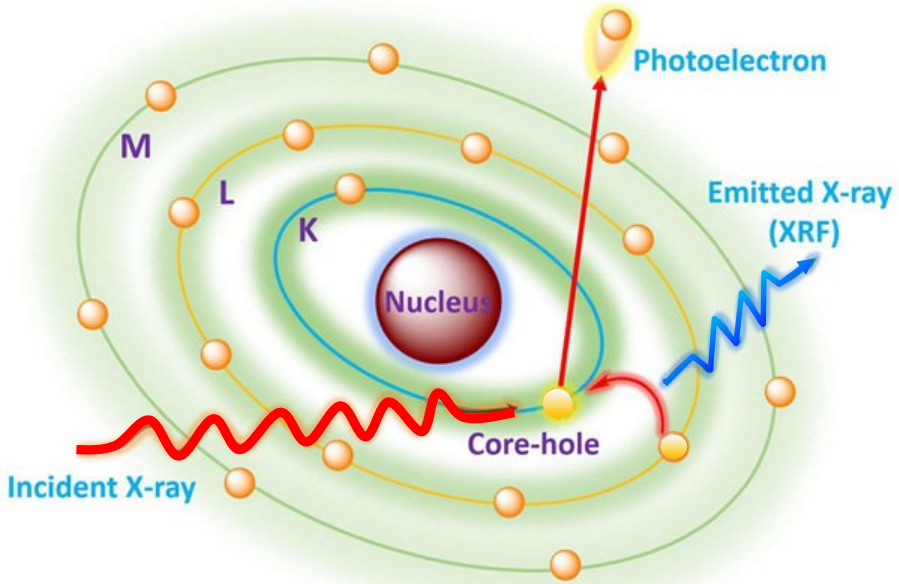

American Journal of Nuclear Medicine and Molecular Imaging 8(3), 169(2018)

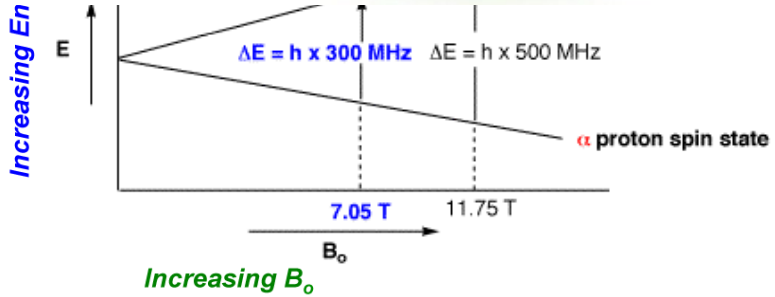

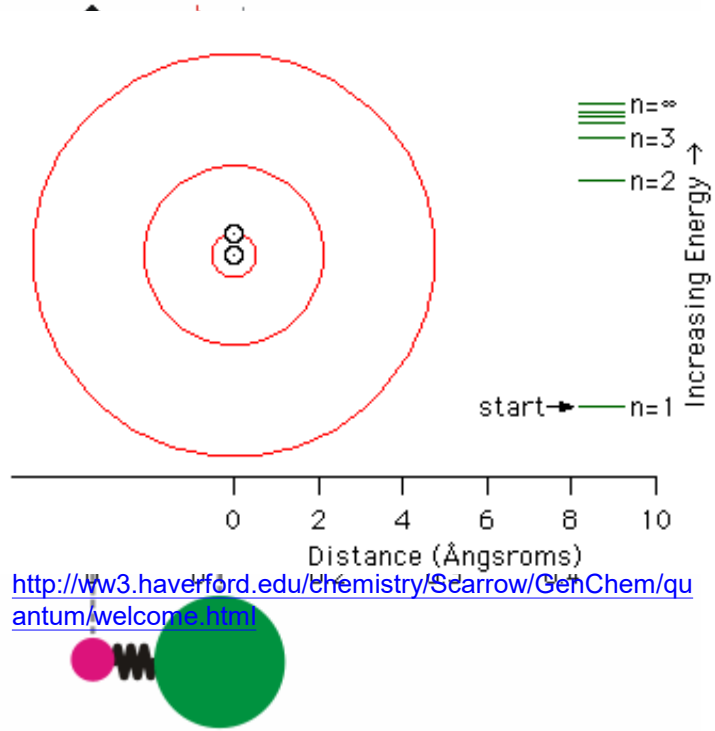

http://ww3.haverford.edu/chemistry/Scarrow/GenChem/quantum/welcome.html

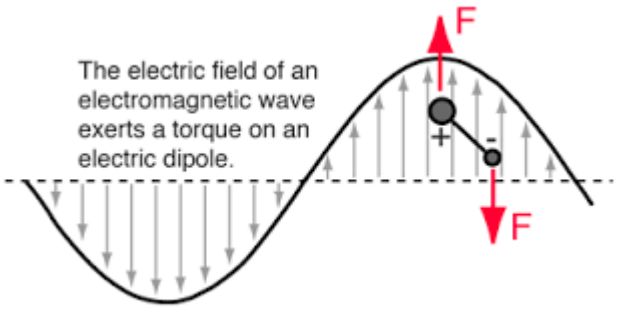

III. The Principle of FTIR Spectroscopy

- **Origin of absorption**

Infrared active vibrations (those that absorb IR radiation) must result in a ***change*** *of* ***dipole moment***

ex: OH with permanent dipole IR active

O_2, N_2, Cl_2 w/o IR **in**active

frequency(energy) *versus* **peak intensity**(amplitude)

Fig 10.2

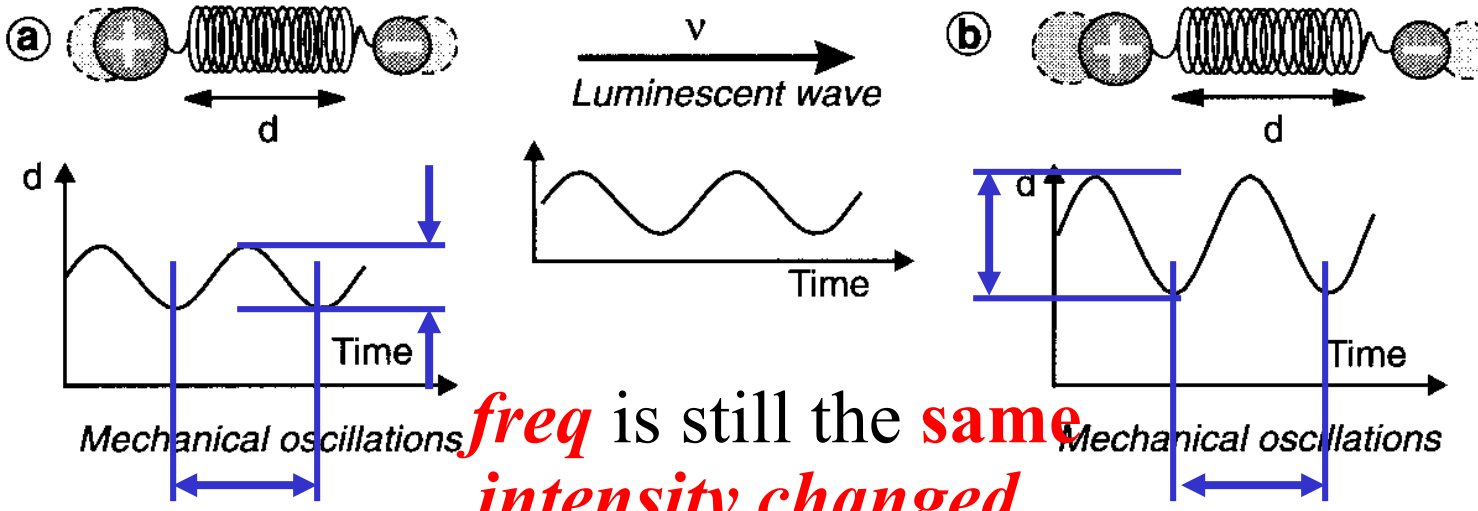

freq is still the **same**

intensity changed

Resonance Absorption

https://specac.com/theory-articles/molecular-vibrations-explained-animated-guides/

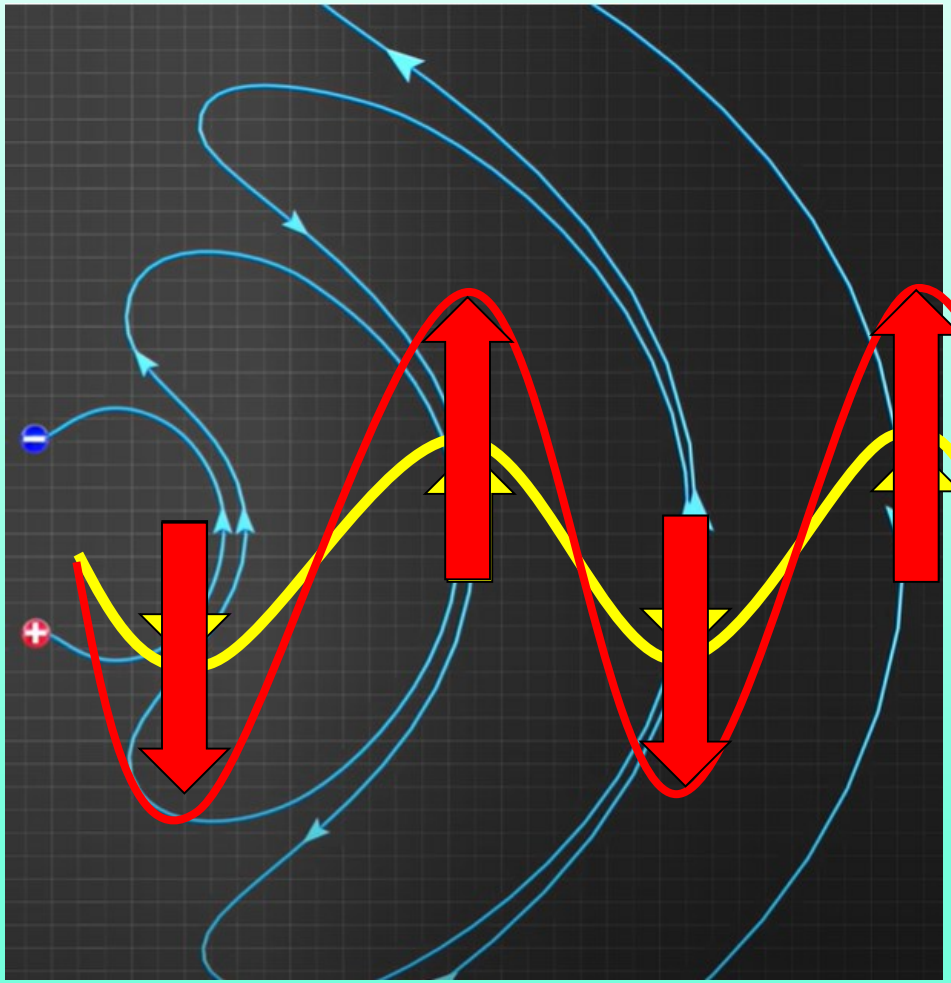

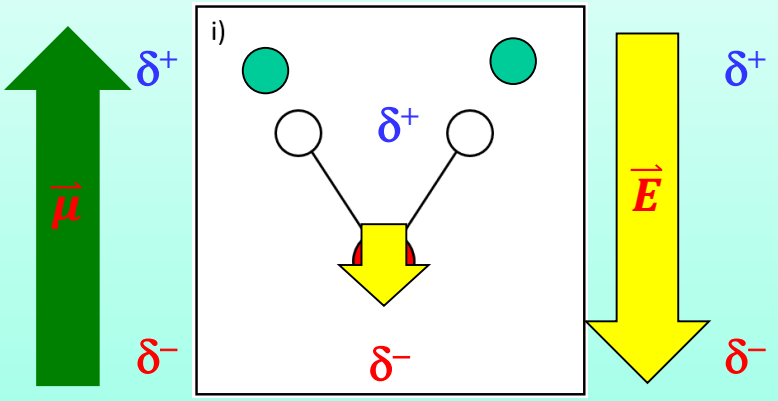

Natural Vibration
Vibrational Ground state

Vibrational Transition
Nuclear kinetic energy

Periodic oscillating electric field is generated by molecular Vibration oscillating with the electric field of EM wave in phase.

Dipole moment must change during vibration excitation (absorption)

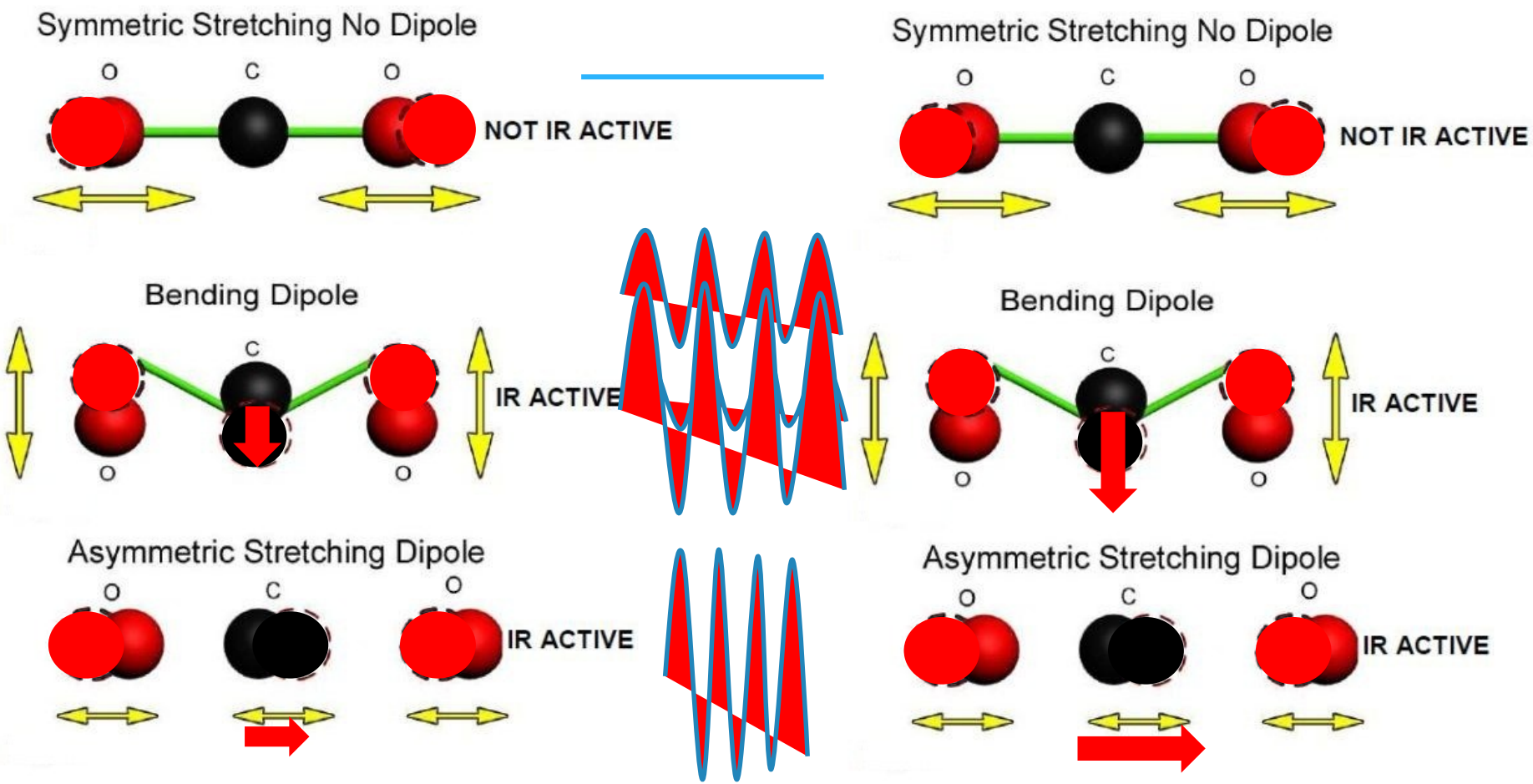

Specific mid-IR photon energy is absorbed by a vibration motion of a molecule.

http://www.azosensors.com/Article.aspx?ArticleID=544

Motions of Molecule (Thermal Motion)

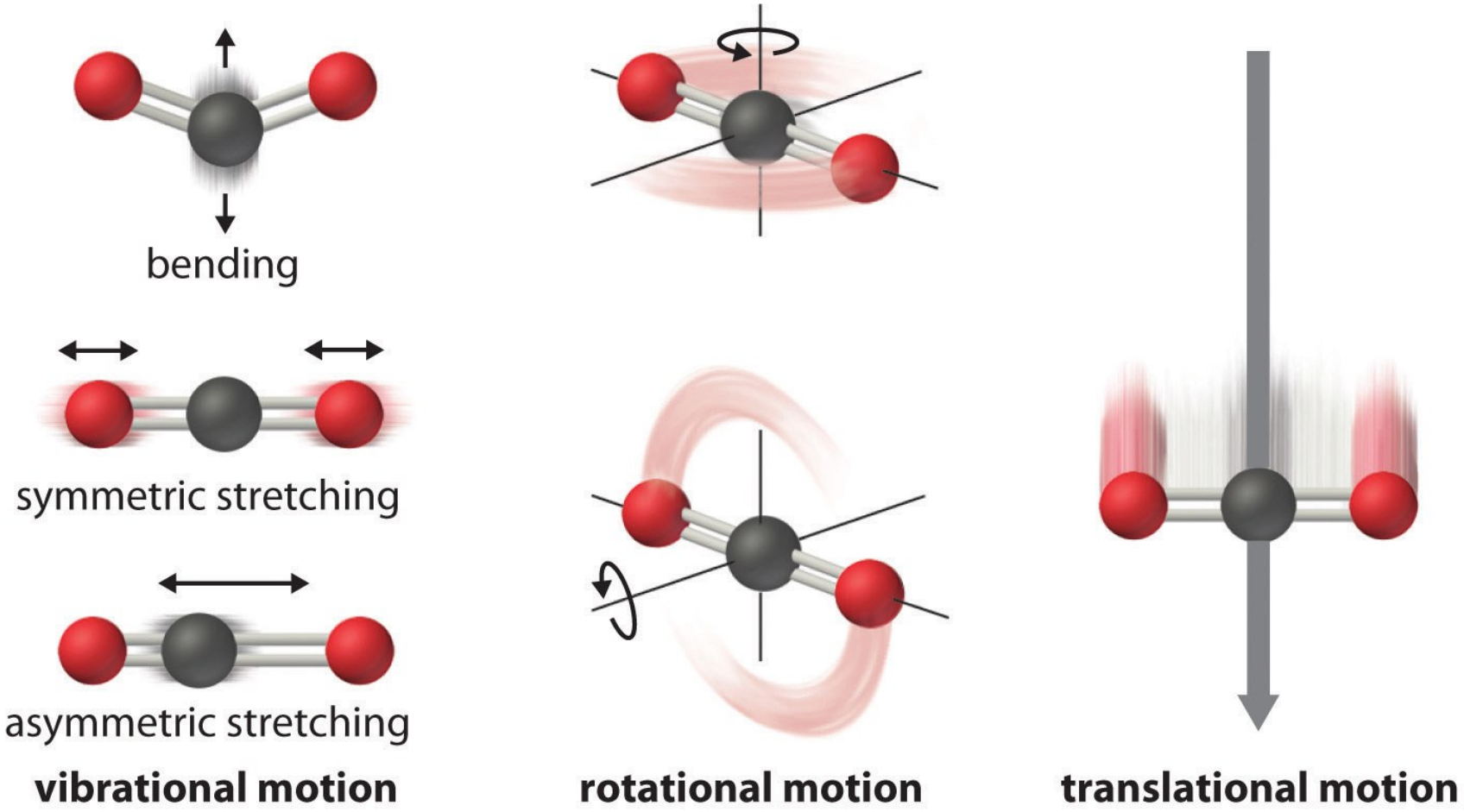

http://2012books.lardbucket.org/books/principles-of-general-chemistry-v1.0m/s22-04-entropy-changes-and-the-third-.html

Functional Groups and Fingerprint in a FTIR Spectrum

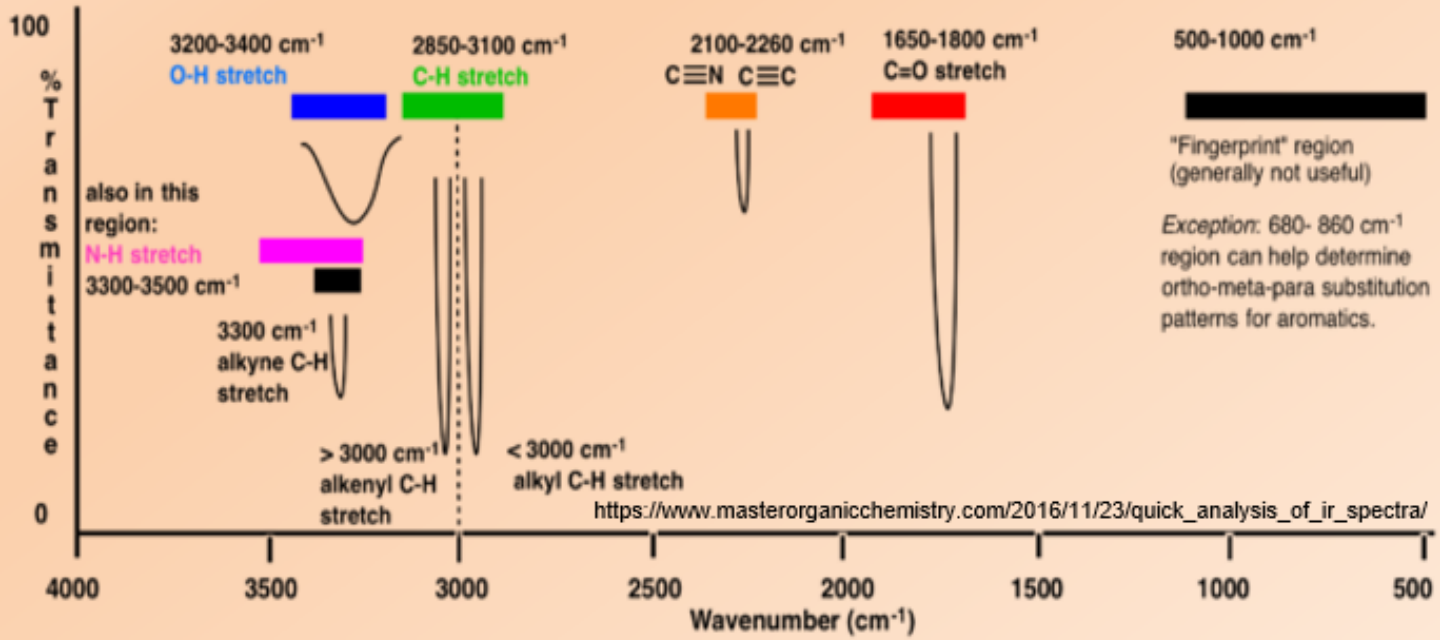

Distinct IR Markers of Cellular Components

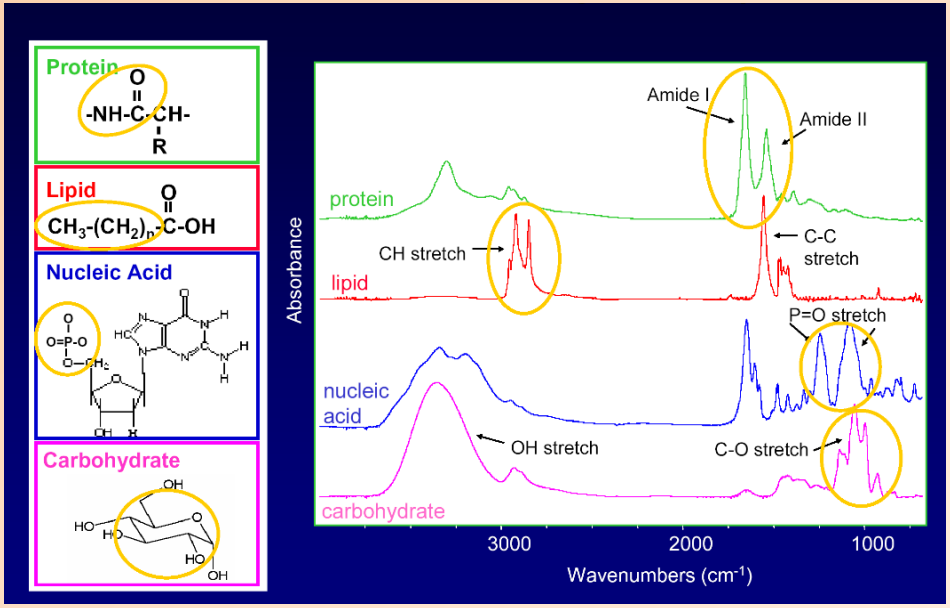

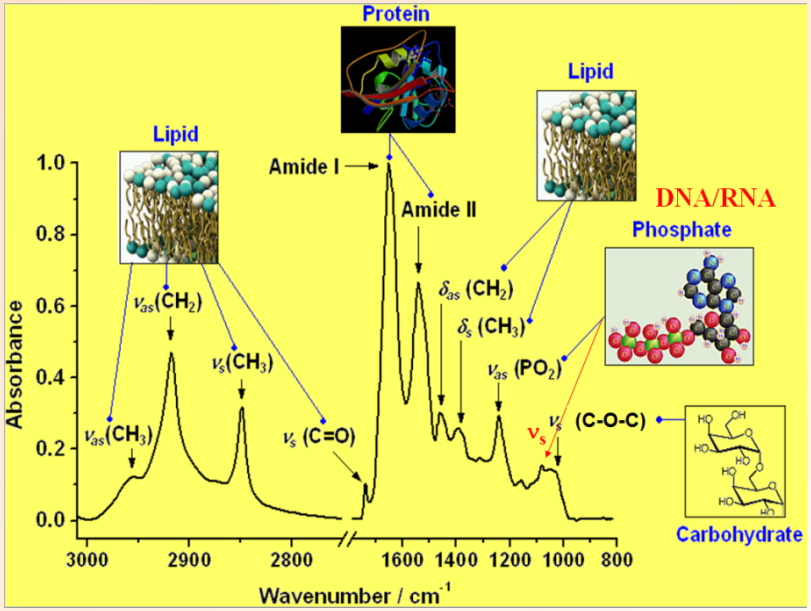

basic organic functional group
reference chart

NAME	C-H	C=C	C≡C	Ring	C-O	O-H	C=O	N-H	C≡N
Aliphatic									
Methyl	2960								
Methylene	2930								
Unsaturated									
Alkenes	3050	1640							
Vinyl	910	1640							
Vinylidene	890	1640							
Cis	700	1640							
Trans	965	1670							
Alkynes	3200		2200						
Aromatics									
Mono	750			700					
Ortho	750			---					
Meta	782			700					
Para	817			---					
Oxygen Groups									
Ether					1100				
Alcohol					1100	3350			
Carbonyl Groups									
Aldehyde	2700						1730		
Ketone							1700		
Ester					1200		1740		
Carboxylic Acid						3100	1720		
Nitrogen Groups									
Amide							1640	3200	
Amine								3300	
Nitrile									2250

FUNCTIONAL GROUP REPRESENTATION

Methyl			
CH_3-	**Methylene**	**Alkene**	**Alkyne**
Vinyl	- CH_2-	C=C	C≡C
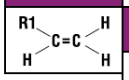	**Vinylidene**	**Cis**	**Trans**
	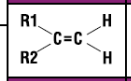	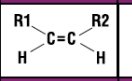	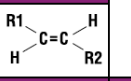
Mono	**Ortho**	**Meta**	**Para**
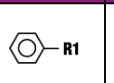	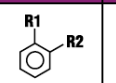	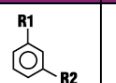	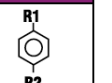
	Aldehyde	**Ketone**	**Ester**
	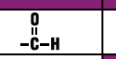	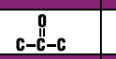	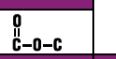
		Ether	**CarbAcid**	**Alcohol**
		C-O-C	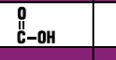	C-O-H
		Amide	**Amine**	**Nitrile**
		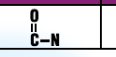	C-N	C≡N

RELATIVE PEAK INTENSITIES

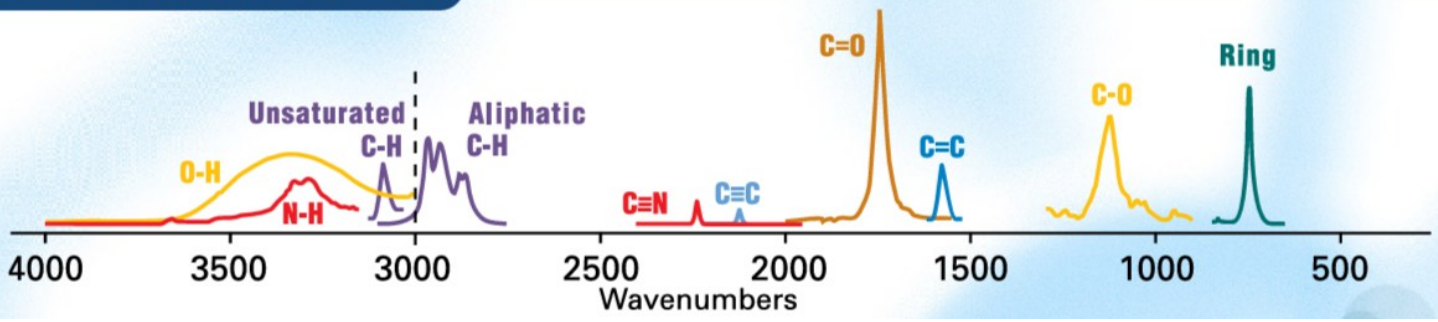

The Fingerprint Region of IR Spectrum of a Sample

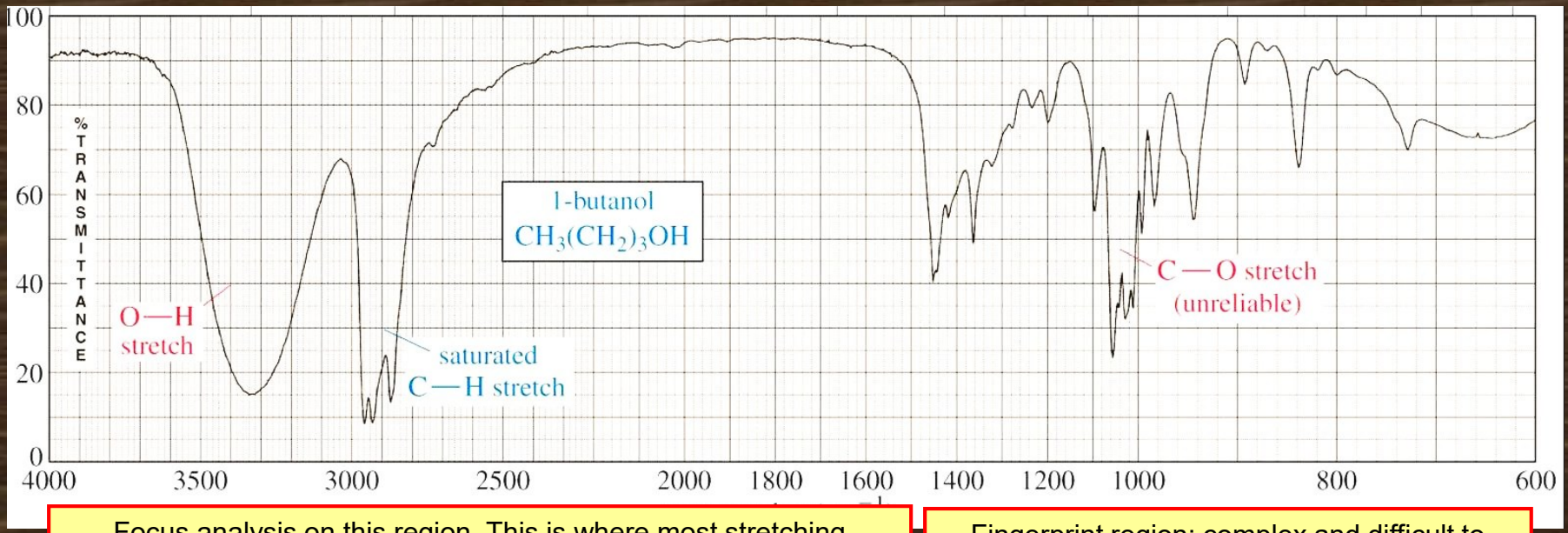

Focus analysis on this region. This is where most stretching frequencies appear.

Fingerprint region: complex and difficult to interpret reliably.

Although the entire IR spectrum can be used as a fingerprint for the purposes of comparing molecules, the **1400 - 600 cm^{-1}** range is called the **fingerprint region**. This is normally a complex area showing many bands, frequently overlapping each other.

Graphics source: Wade, Jr., L.G. *Organic Chemistry*, 6th ed. Pearson Prentice Hall Inc., 2006

IR Spectra of Hydrocarbons (Alkanes, Alkene and Alkynes)

IR spectra of Hydrocarbons display only C-C, C=C, C≡C and C-H bond vibrations. Of these the most useful information are the **C-H bands**, which appear in the range of **3000-2800 cm^{-1}**. Since most organic molecules have such bonds, most organic molecules displays those bands in their spectrum.

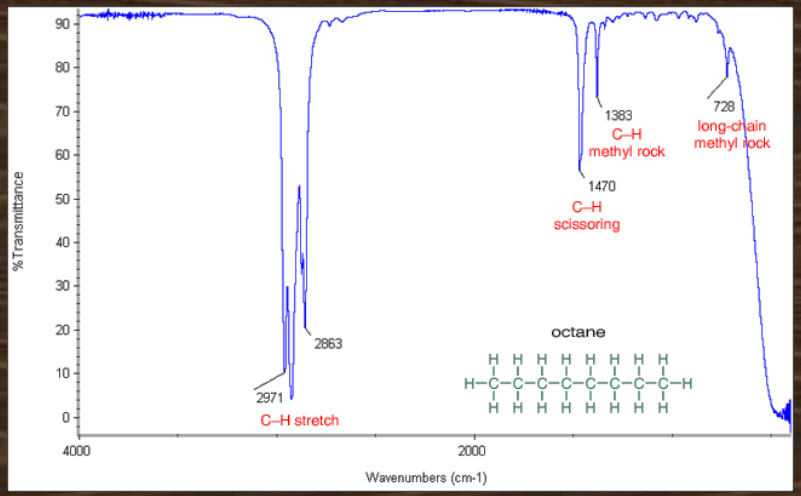

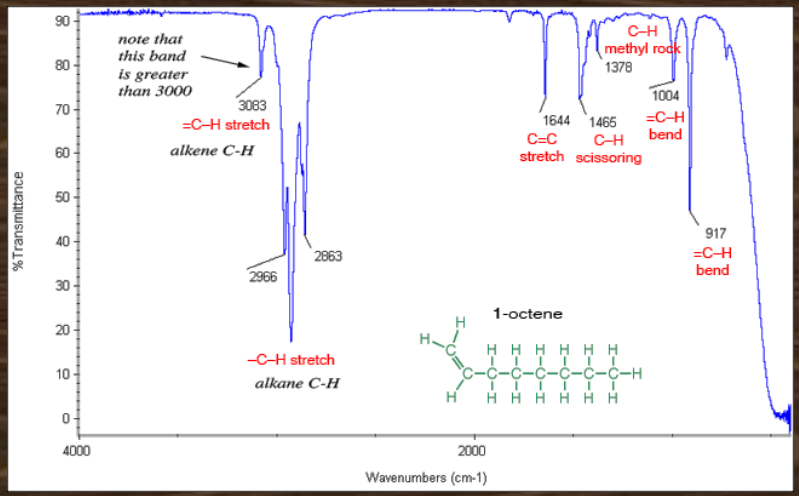

https://orgchemboulder.com/Spectroscopy/irtutor/tutorial.shtml

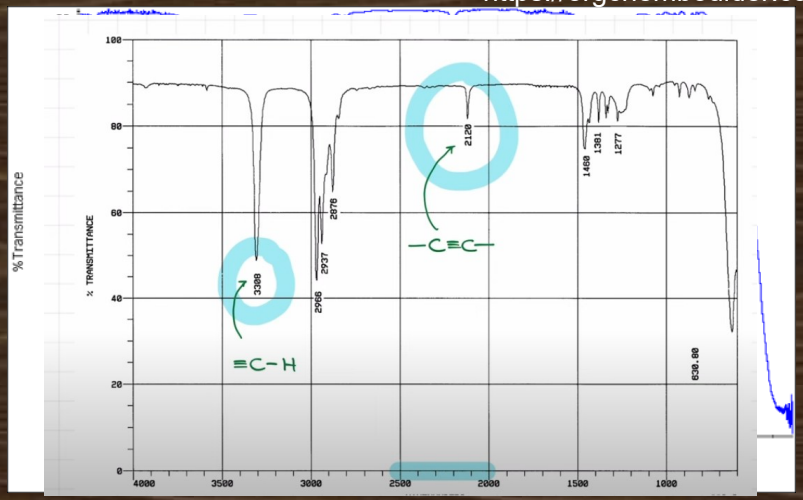

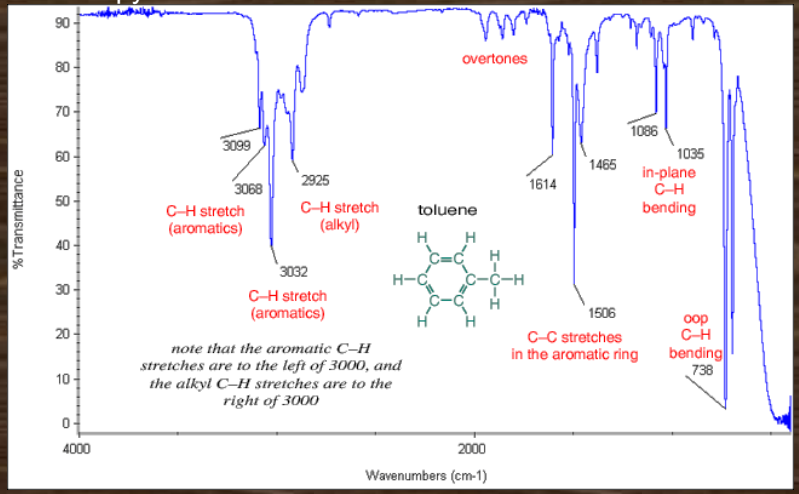

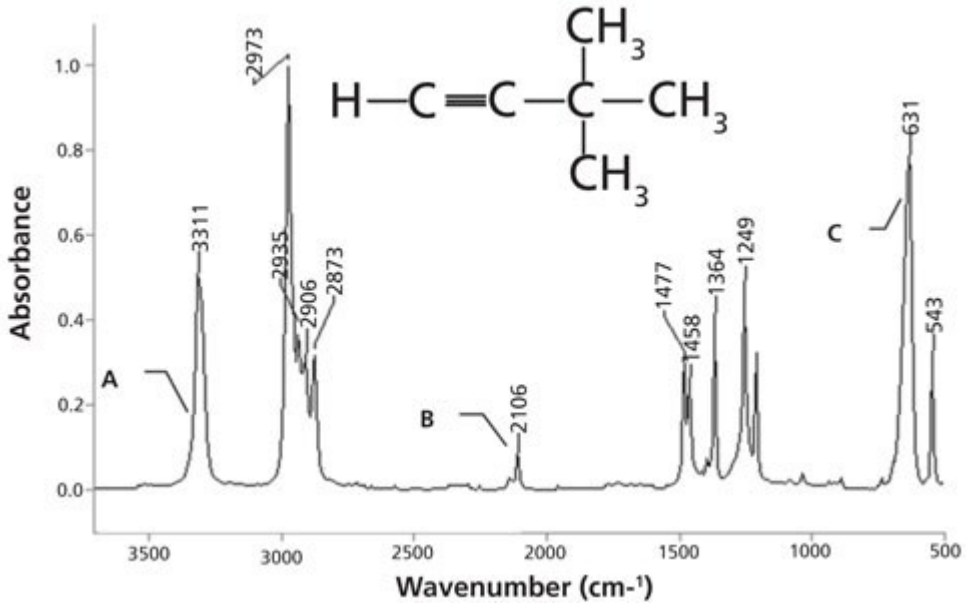

Table II: Peak assignments for spectrum shown in Figure 5		
A	3311	≡C-H stretch
B	2106	C≡C stretch
C	631	C-H wag

http://www.spectroscopyonline.com/ir-spectral-interpretation-potpourri-carbohydrates-and-alkynes?pageID=3

IR Spectra of Alcohol, Ketone, Aldehyde, and Carboxylic Acid

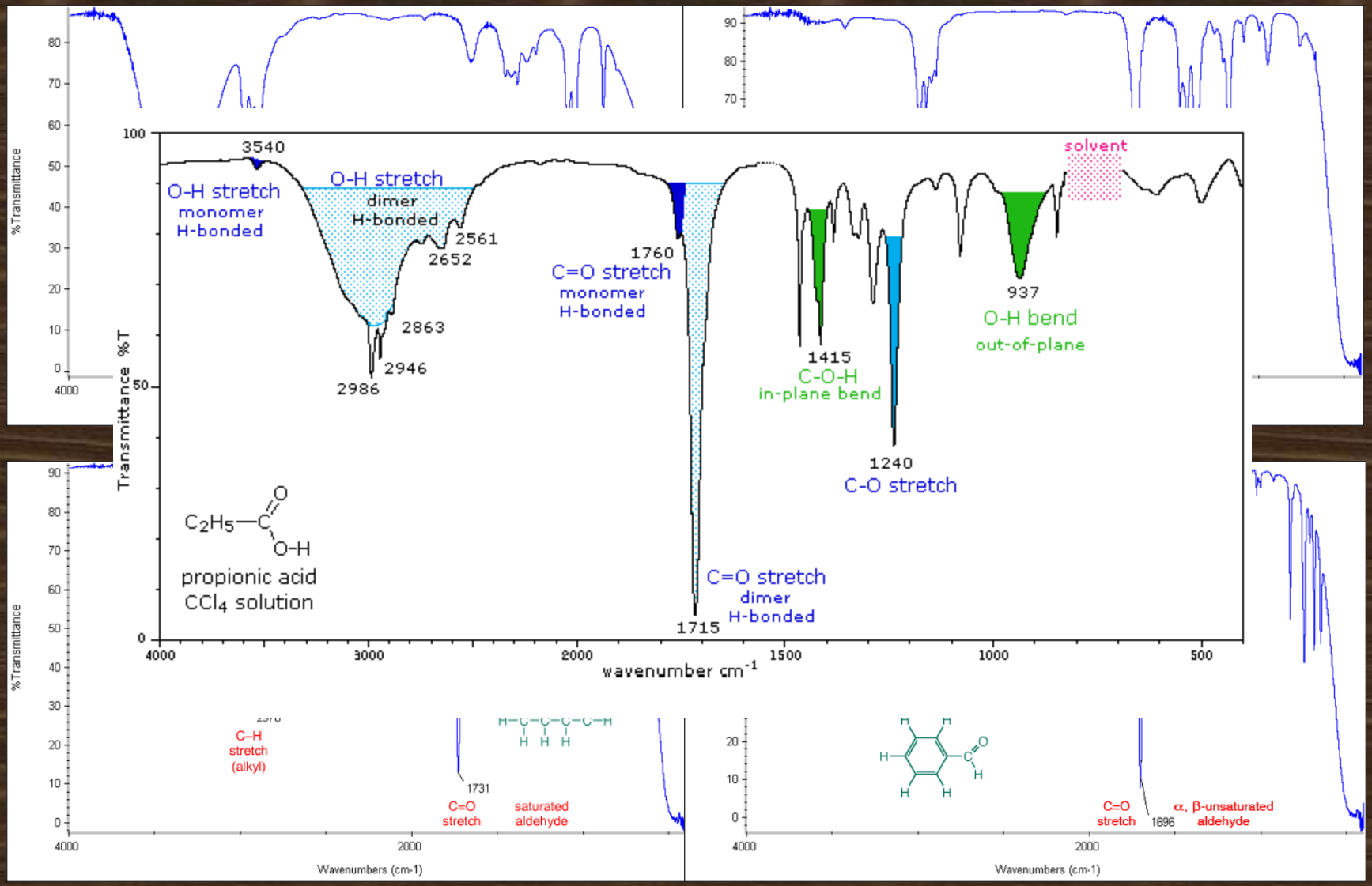

https://www2.chemistry.msu.edu/faculty/reusch/virttxtjml/spectrpy/infrared/irspec1.htm

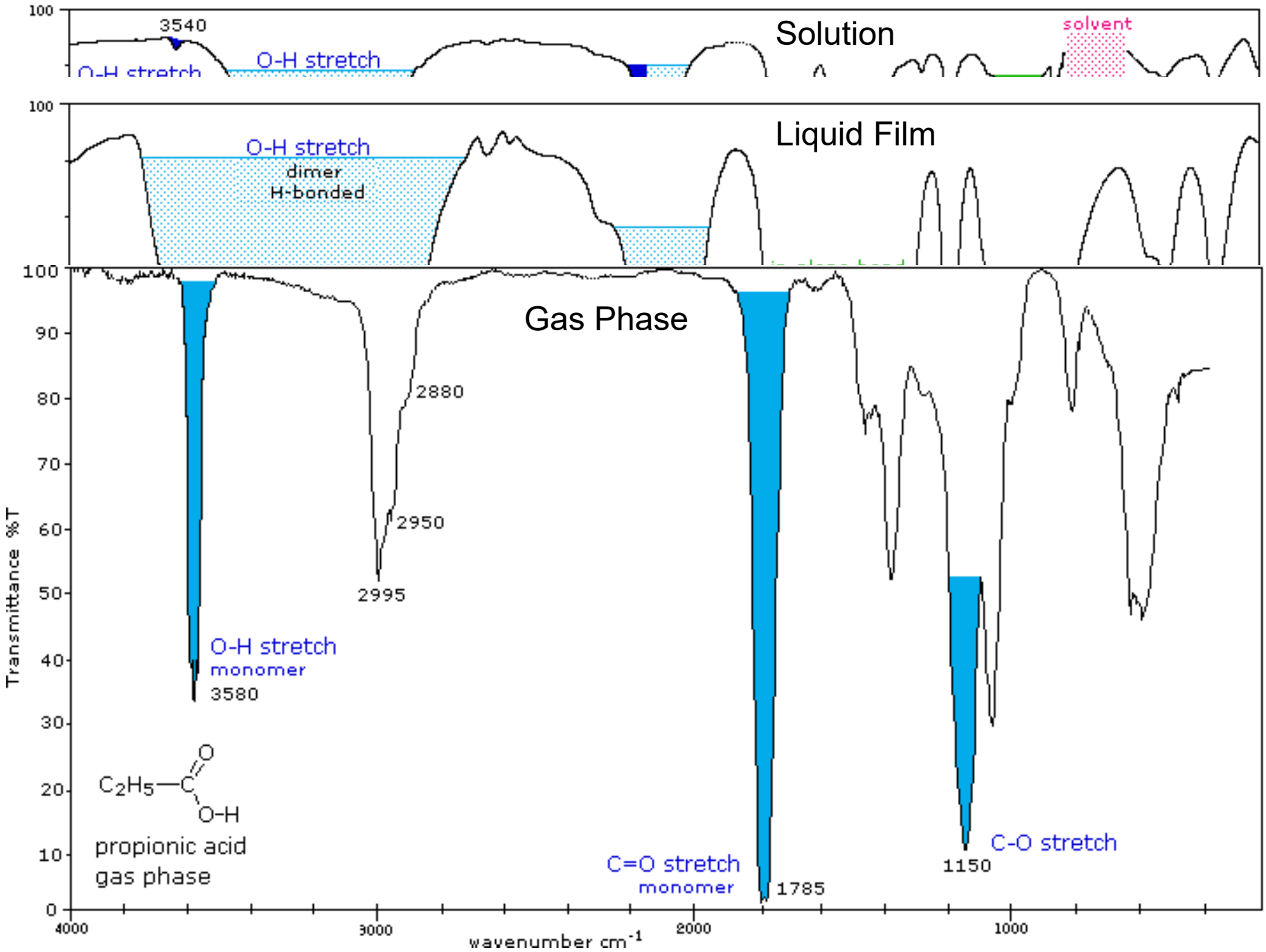

IR Spectra of Ester

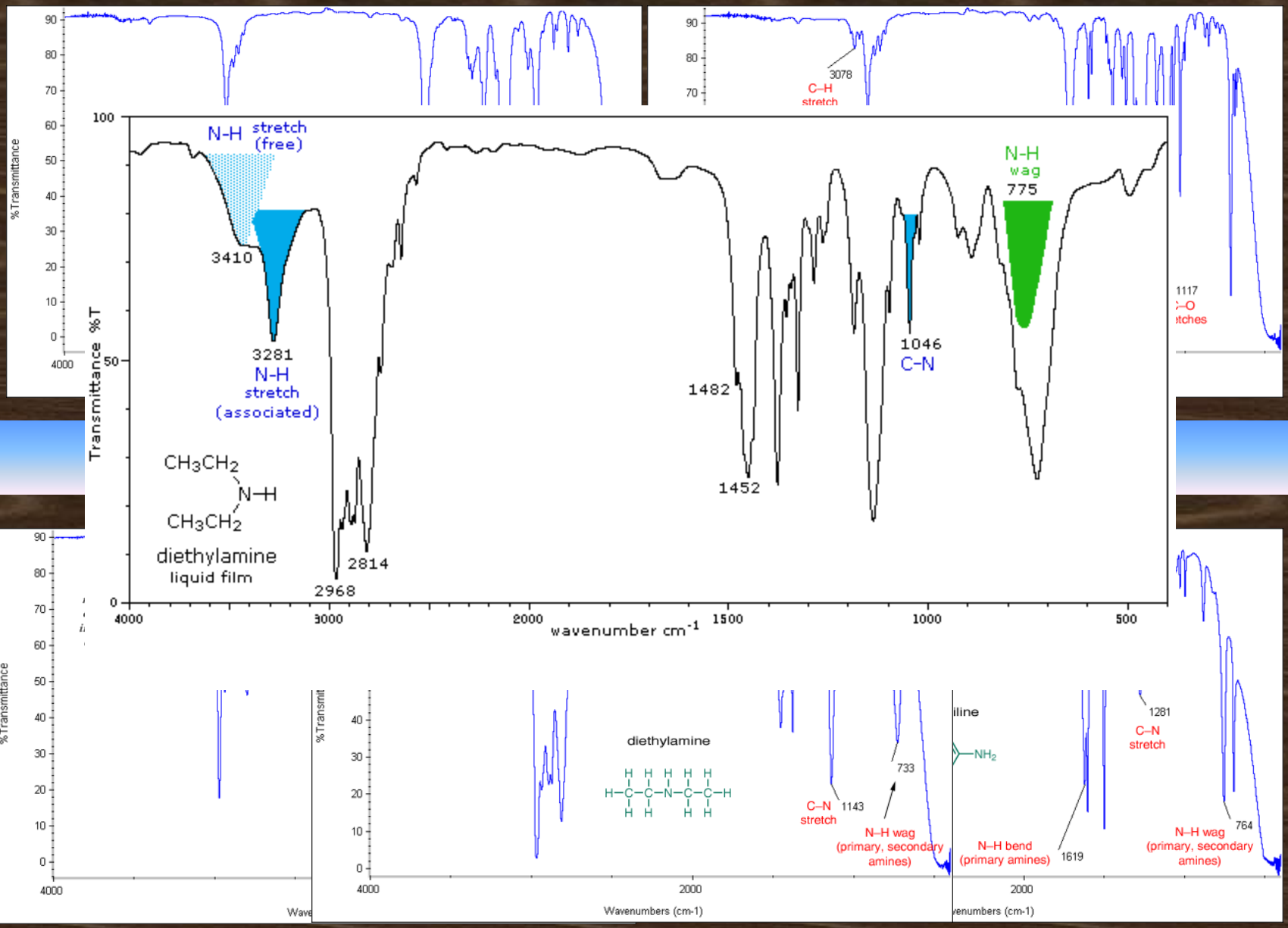

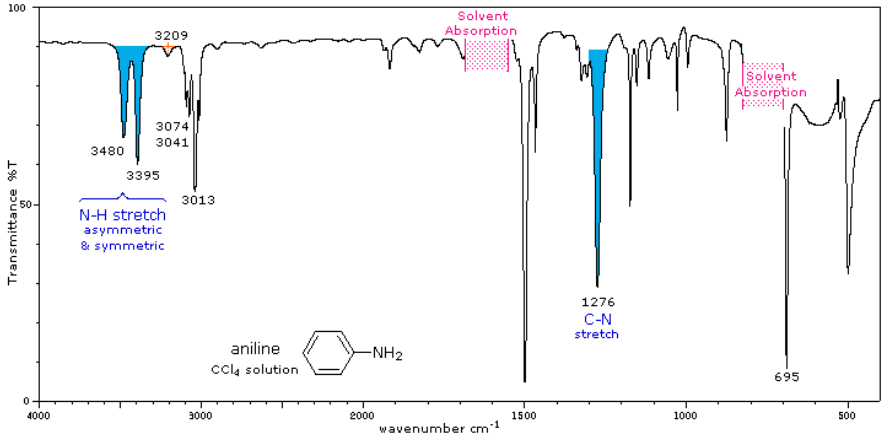

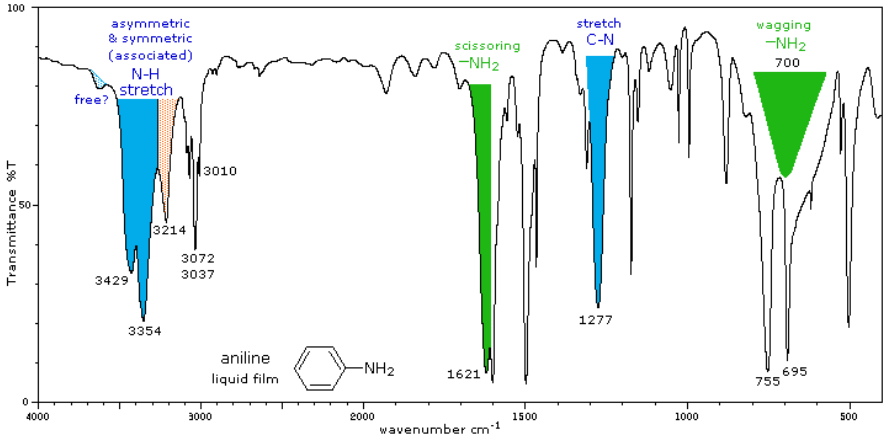

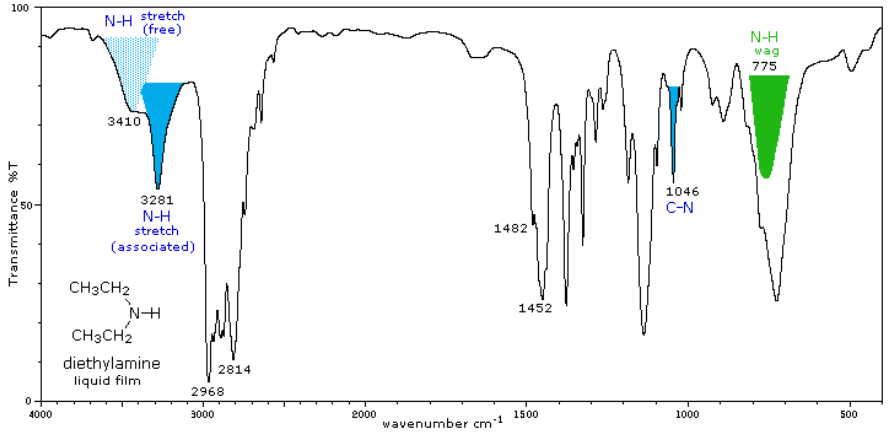

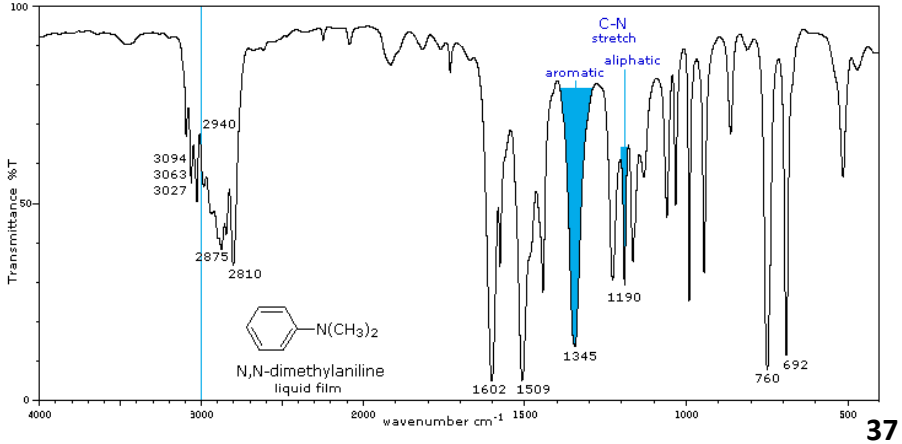

https://chem.libretexts.org/LibreTexts/Athabasca_University/Chemistry_360%3A_Organic_Chemistry_II/Chapter_24%3A_Amines_and_Heterocycles/24.10_Spectroscopy_of_Amines

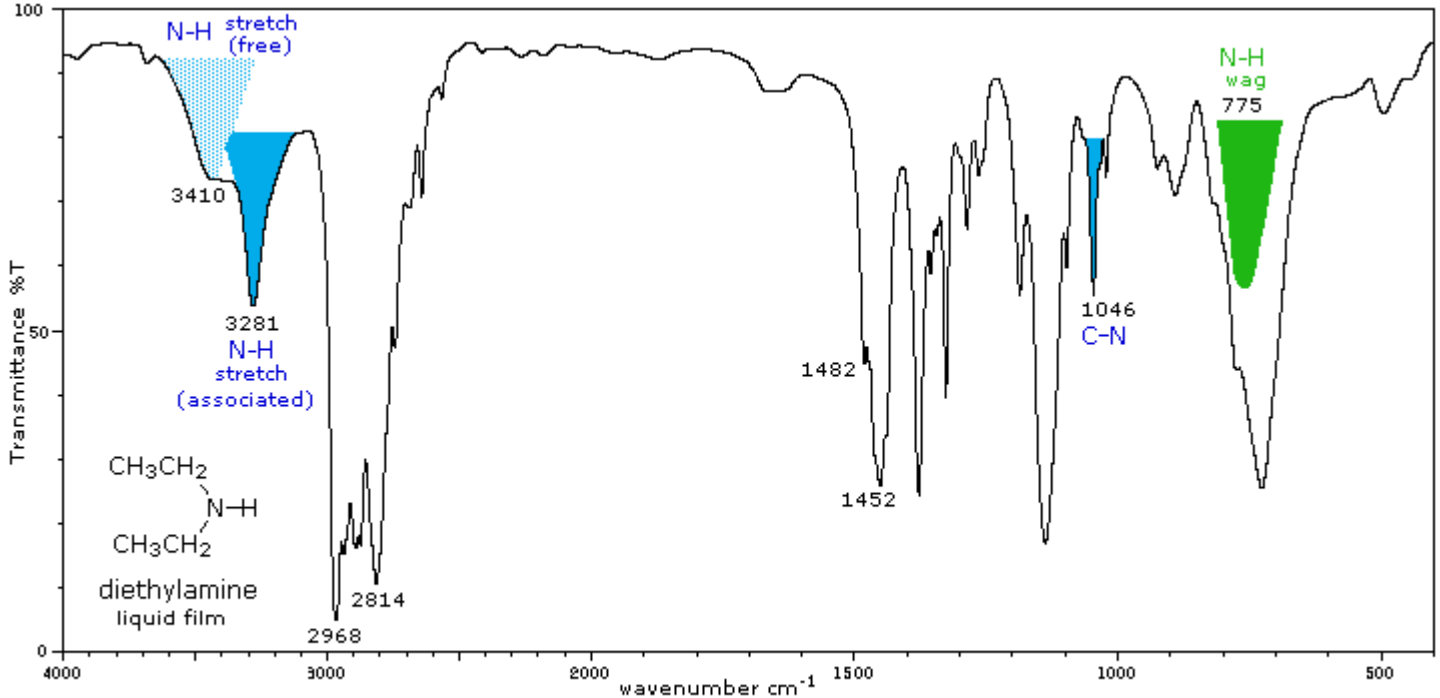
N-H stretch (free)
3410
3281
N-H stretch (associated)
N-H wag
775
1046
C-N
1482
1452
2968
2814
CH3CH2
N–H
CH3CH2
diethylamine
liquid film
Transmittance %T
wavenumber cm-1
4000
3000
2000
1500
1000
500
100
50
0

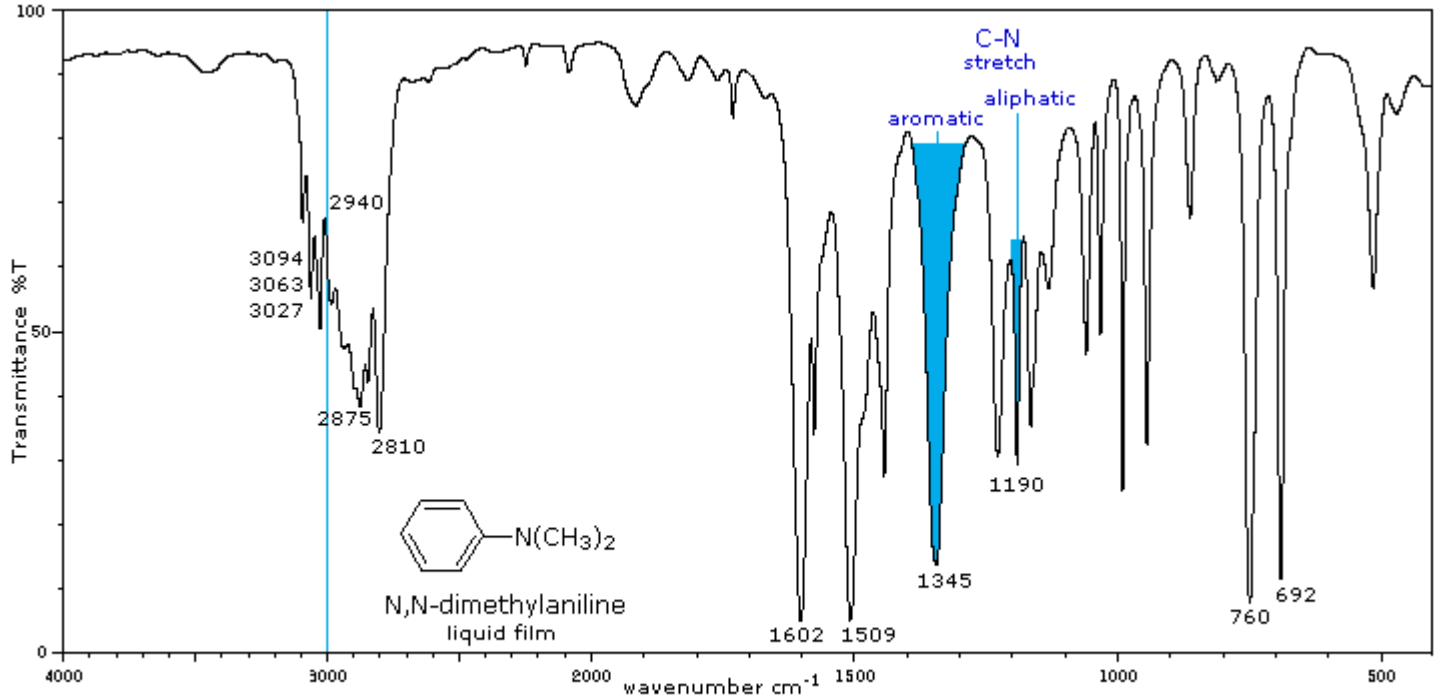
C-N stretch
aromatic
aliphatic
2940
3094
3063
3027
2875
2810
1190
1345
760
692
1602
1509
N(CH3)2
N,N-dimethylaniline
liquid film
Transmittance %T
wavenumber cm-1
4000
3000
2000
1500
1000
500
100
50
0

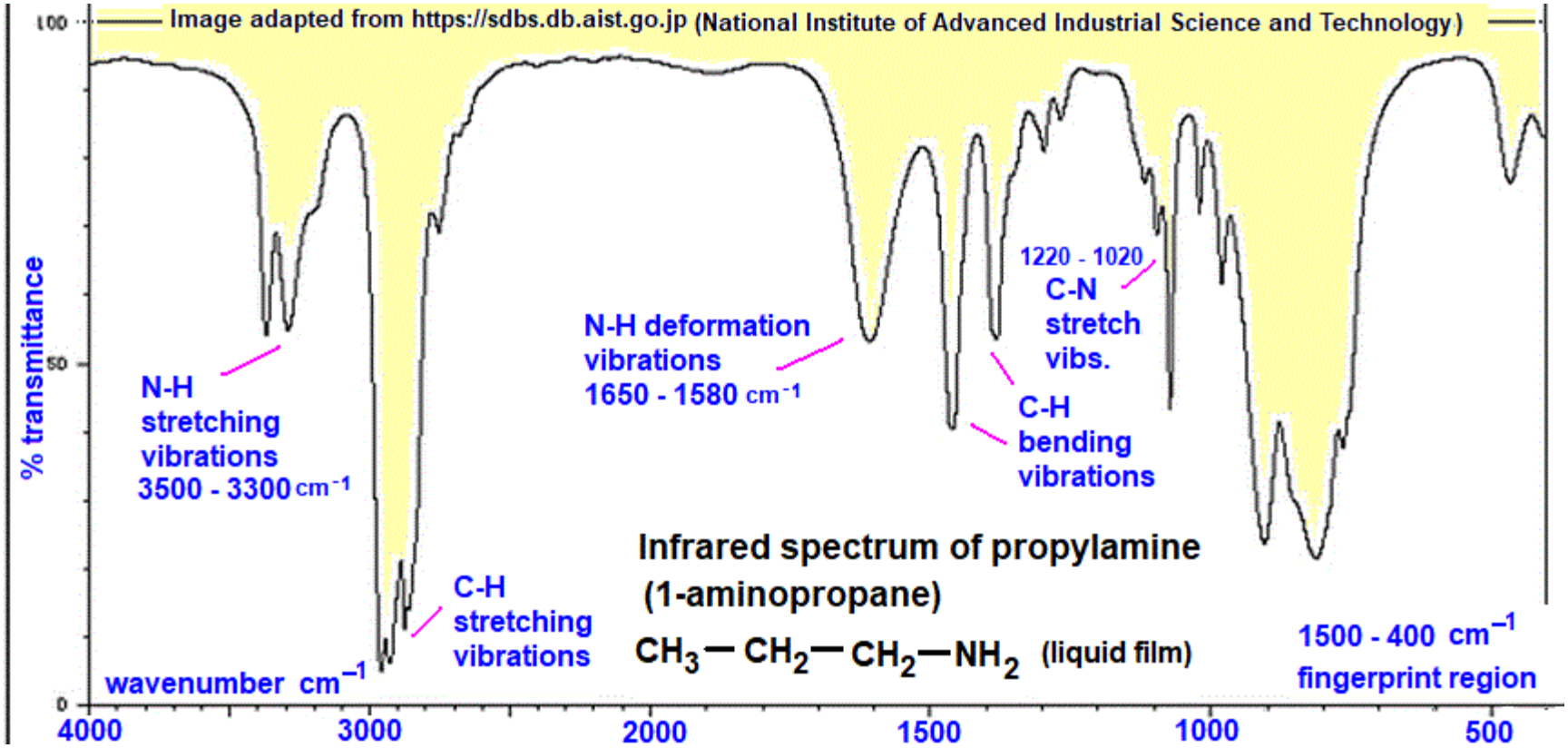

https://www.docbrown.info/page06/spectra/propylamine-ir.htm

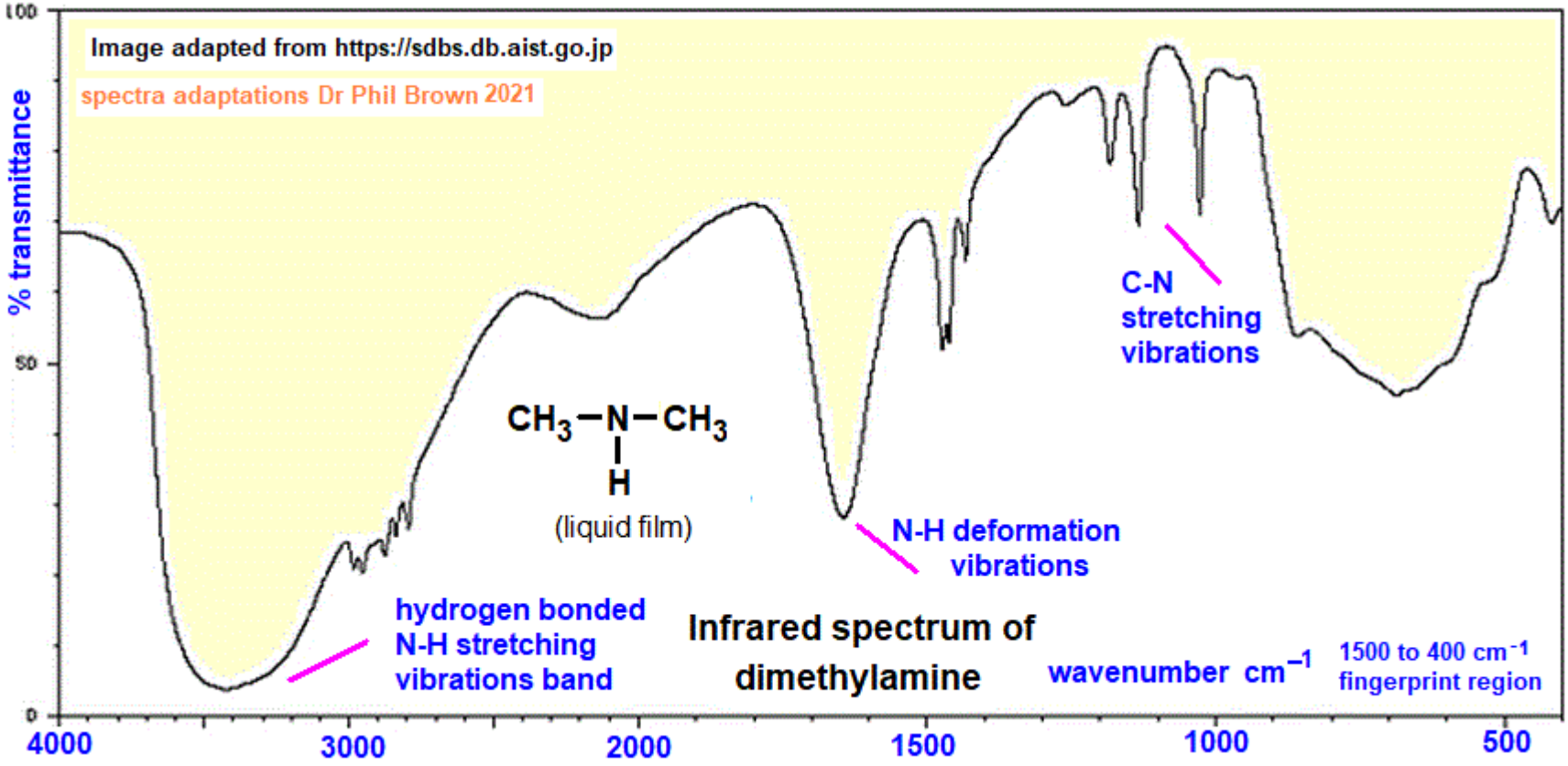

https://docbrown.info/page06/spectra2/dimethylamine-ir.htm

IR Spectra of Aromatics

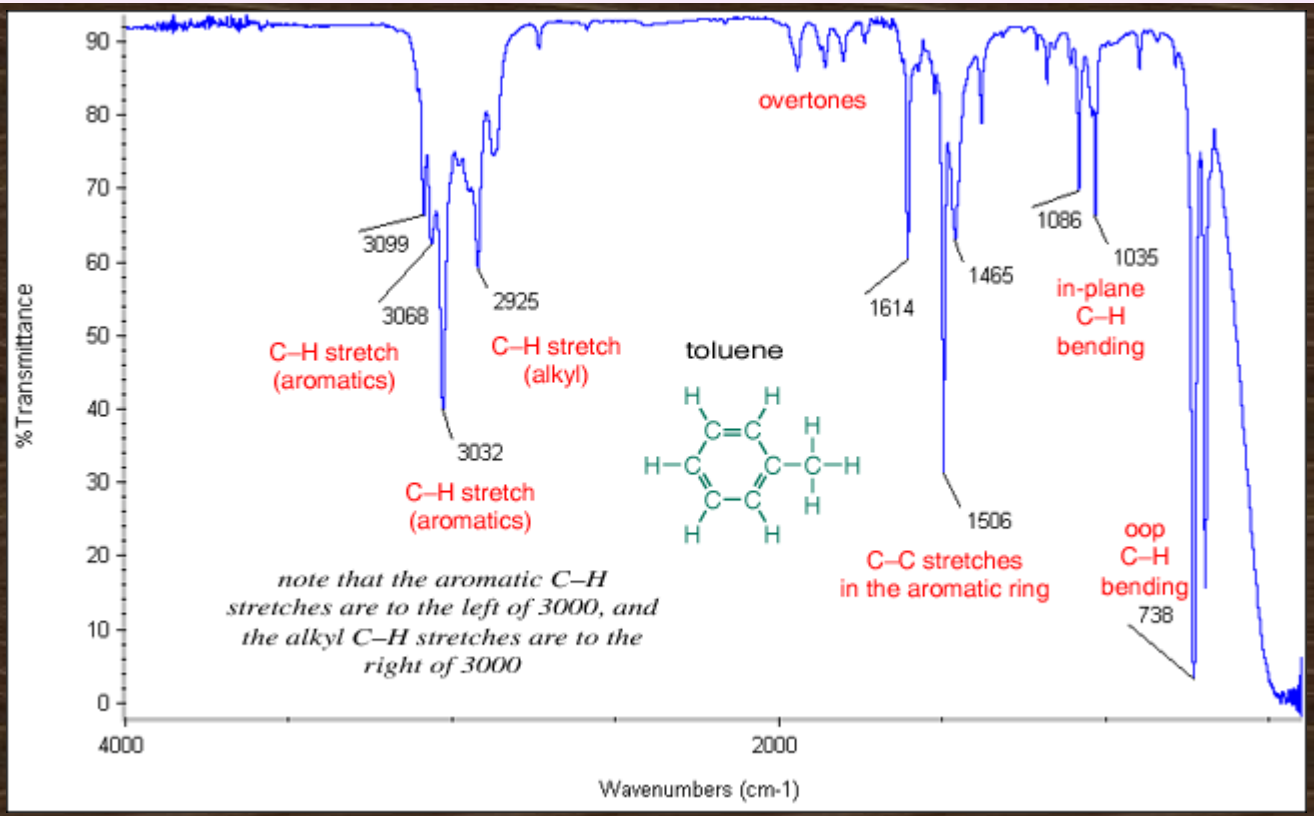

C–H stretch from 3100-3000 cm^{-1}
overtones, weak, from 2000-1665 cm^{-1}
C–C stretch (in-ring) from 1600-1585 cm^{-1}
C–C stretch (in-ring) from 1500-1400 cm^{-1}
C–H "oop" from 900-675 cm^{-1}

The spectrum of toluene is shown below. Note the =C–H stretches of aromatics (3099, 3068, 3032) and the –C–H stretches of the alkyl (methyl) group (2925 is the only one marked). The characteristic overtones are seen from about 2000-1665. Also note the carbon-carbon stretches in the aromatic ring (1614, 1506, 1465), the in-plane C–H bending (1086, 1035), and the C–H oop (738).

IR Spectra of Nitro group

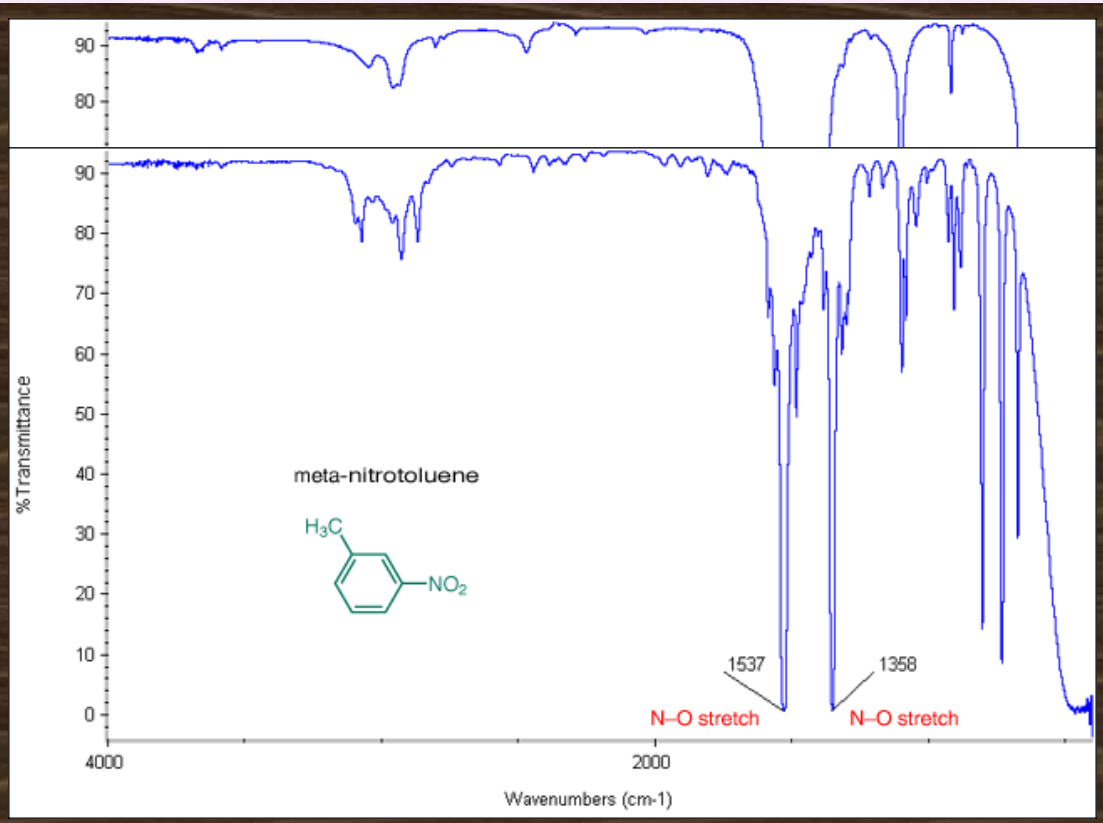

The N–O stretching vibrations in nitro-alkanes occur near 1550 cm^{-1} (asymmetrical) and 1365 cm^{-1} (symmetrical), the band at 1550 cm^{-1} being the stronger of the two.
If the nitro group is attached to an aromatic ring, the N–O stretching bands shift to down to slightly lower wavenumbers: 1550-1475 cm^{-1} and 1360-1290 cm^{-1}.

Summary:
- N–O asymmetric stretch from 1550-1475 cm^{-1}
- N–O symmetric stretch from 1360-1290 cm^{-1}

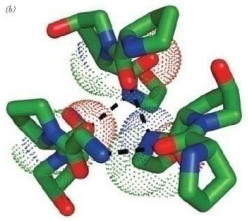

Secondary Structure

- Defined as the local conformation of protein backbone
- Primary Structure —folding— Secondary Structure
- α helix and β sheet

Secondary Structure

Regular Secondary Structure (α-helices, β-sheets)

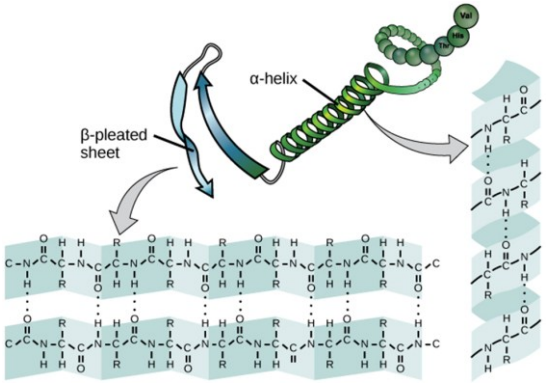

Irregular Secondary Structure (Tight turns, Random coils, bulges)

https://www.khanacademy.org/science/biology/macromolecules/proteins-and-amino-acids/a/orders-of-protein-structure

Primary structure

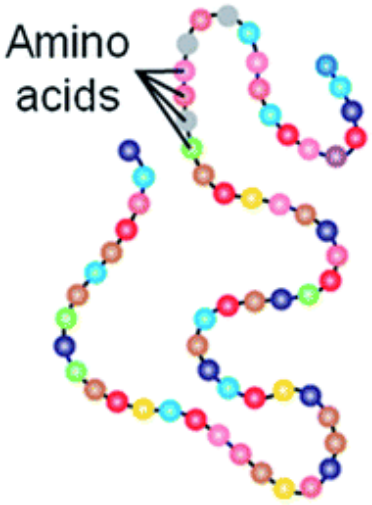

Secondary structure

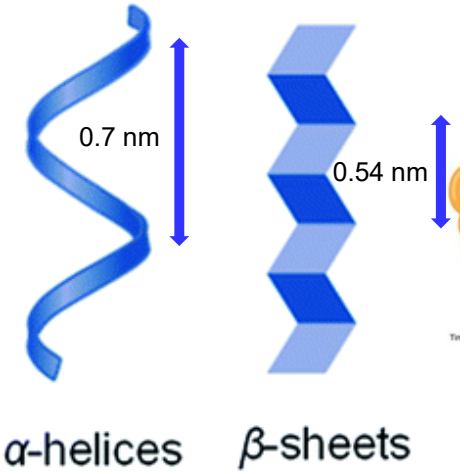

Tertiary structure

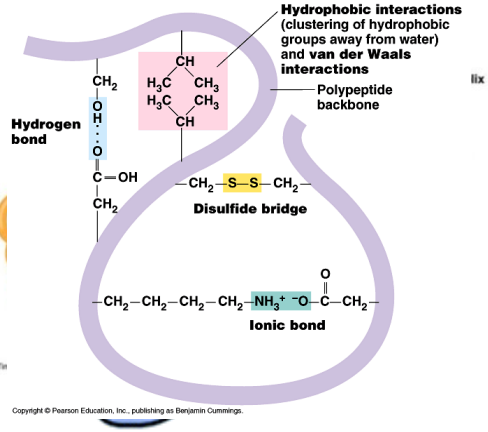

Quaternary structure

eets

ices

https://www.toppr.com/en-ar/content/concept/advanced-knowledge-of-structure-of-protein-200359/

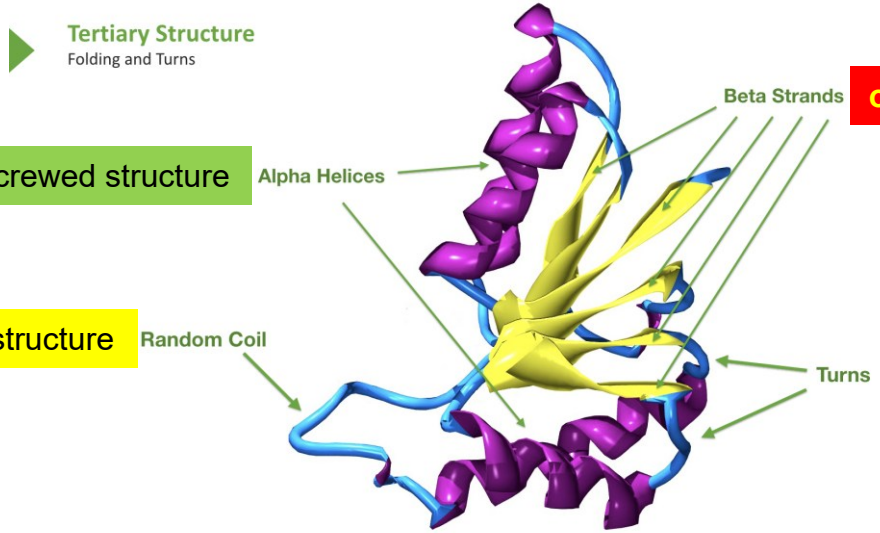

β-Sheet: A β-sheet is a common secondary structure in proteins, formed by linking two or more β-strands side by side through hydrogen bonds. The β-strands in a β-sheet can be either parallel (running in the same direction) or antiparallel (running in opposite directions). β-sheets are often depicted as flat arrows pointing in the direction of the polypeptide chain. They provide structural stability and are often found in the core of proteins.

β-Strand: A β-strand is a single stretch of polypeptide chain that is almost fully extended. It typically consists of 5-10 amino acids. In a protein, multiple β-strands come together to form a β-sheet through hydrogen bonding between the backbone atoms of the strands. While β-strands themselves are not stable structures, their stability comes from the formation of β-sheets.

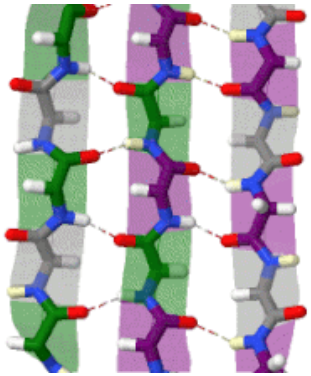

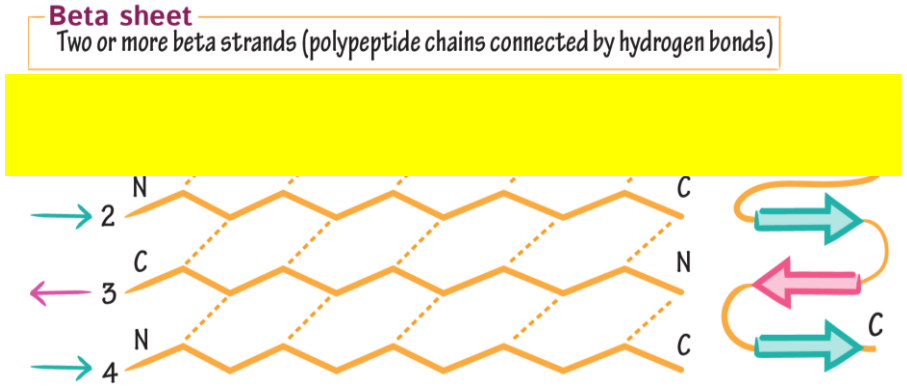

https://en.wikipedia.org/wiki/Beta_sheet

https://ditki.com/course/biochemistry/glossary/biochemical-pathway/beta-sheets-aka-beta-pleated-sheets

β-sheets

The hydrogen bonds in antiparallel β-sheets are linear, while the hydrogen bonds in **parallel** β-sheets are non-linear.

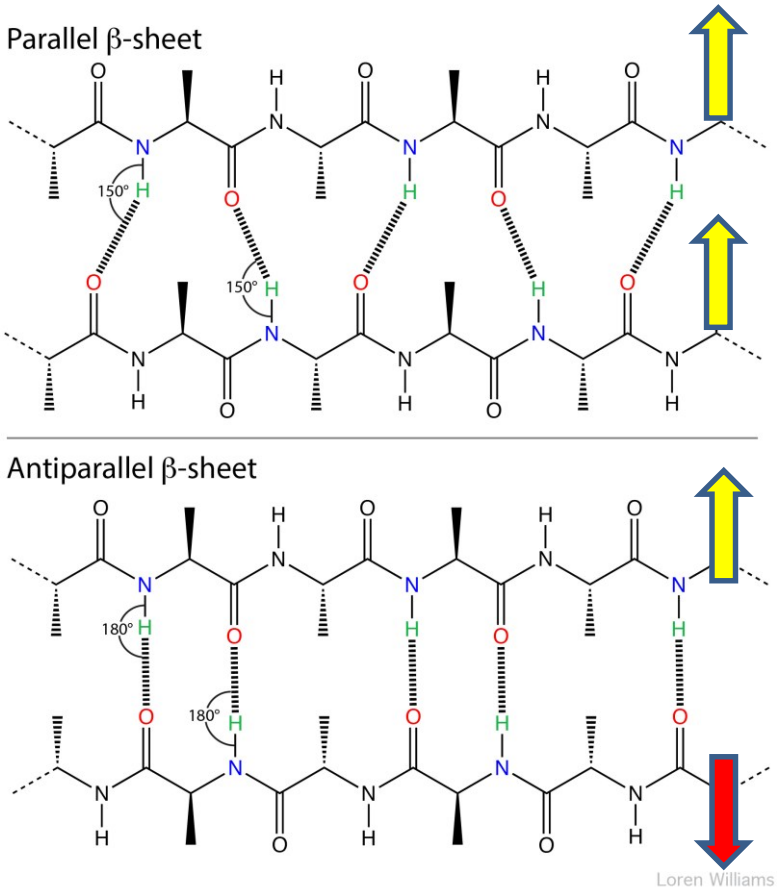

β-strand

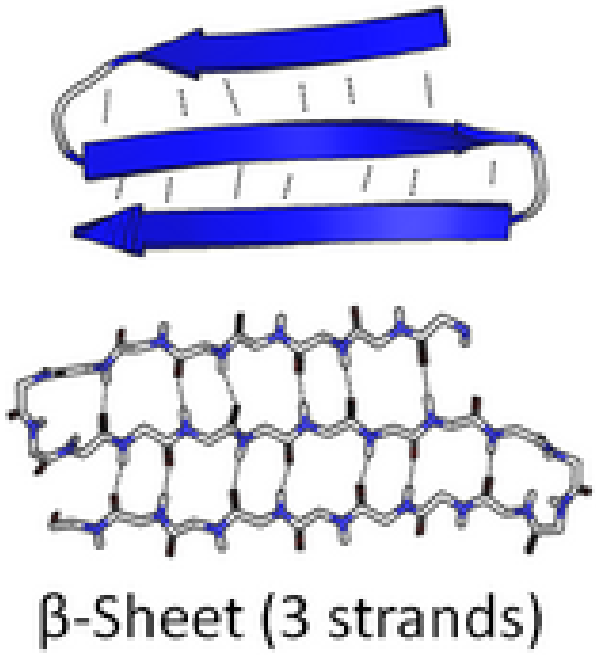

Figure illustrates the **non-linearity of parallel β-sheet hydrogen bonds** and the **linearity of antiparallel β-sheet hydrogen bonds**.

https://www.x-mol.com/groups/Dong/news/1653

Vibrational Coupling in β-Sheets Determines Amide I Spectral Features

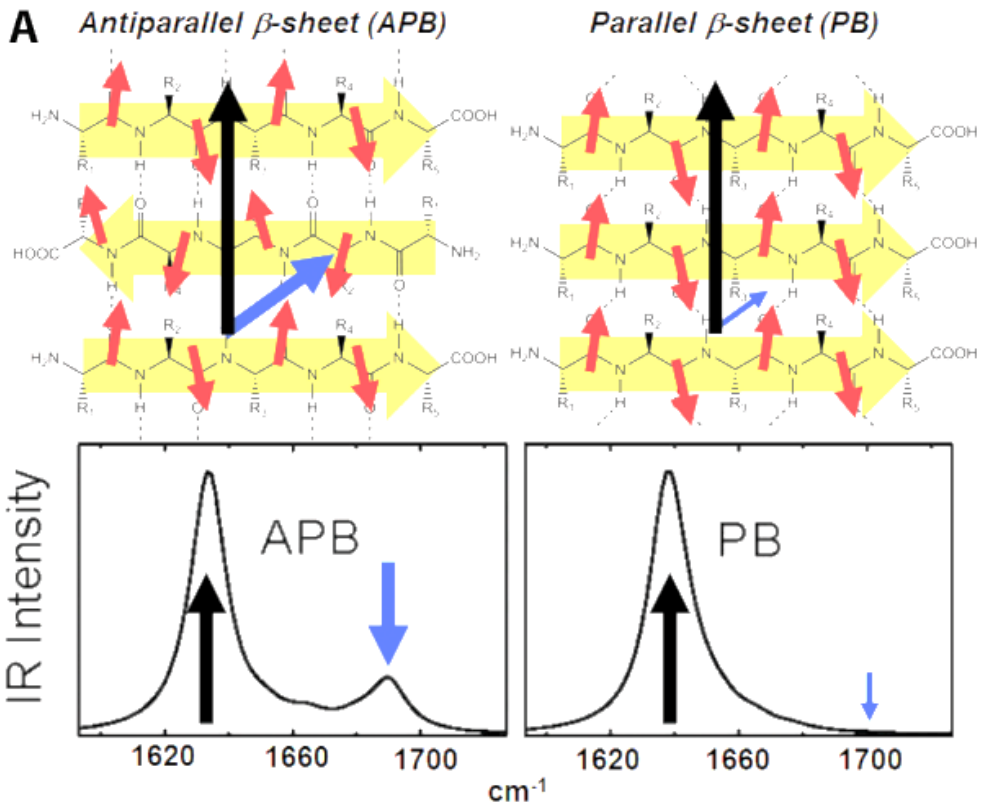

Vibrational coupling between transition dipole moments causes excitonic delocalization within β-sheets, producing collective normal modes. In IR spectra, β-sheets show a strong low-frequency mode common to both parallel and antiparallel structures, while the high-frequency mode differs in strength and position, being more prominent in antiparallel β-sheets.

Recommended Conservative Assignment

Wavenumber region	Recommended assignment
1610–1640 cm^{-1}	β-sheet / aggregated β-sheet
1640–1650 cm^{-1}	Random coil / unordered structure
1650–1660 cm^{-1}	α-helix
1660–1680 cm^{-1}	β-turn / turns
1680–1700 cm^{-1}	β-turns and/or the high-frequency component of antiparallel β-sheet

References

1) 1,692 cm_{-1} (β-turns, or the high-frequency component of anti-parallel β-sheets)
2) 1,678 cm^{-1} (parallel β-sheets)
3) 1,661 cm^{-1} (α-helix)
4) **1,645 cm^{-1} (random coils)**
5) **1,630 cm^{-1} (β-sheet / aggregated β-sheet low-frequency component)**
6) 1,610 cm^{-1} (aromatic rings)

e-PS, 6, 129(2009)

nature protocols,10, 3, 385(2015)

TABLE 1 | Deconvoluted amide I band frequencies and assignments to secondary structure for protein in D_2O and H_2O media.

H_2O[a]		D_2O[b]	
Mean frequencies	Assignment	Mean frequencies	Assignment
1,624 ± 1.0	β-sheet	1,624 ± 4.0	β-sheet
1,627 ± 2.0	β-sheet	1,631 ± 3.0	β-sheet
1,633 ± 2.0	β-sheet	1,637 ± 3.0	β-sheet
1,638 ± 2.0	β-sheet	1,641 ± 2.0	3_{10}-helix
1,642 ± 1.0	β-sheet	1,645 ± 4.0	Random
1,648 ± 2.0	Random	1,653 ± 4.0	α-helix
1,656 ± 2.0	α-helix	1,663 ± 4.0	β-turn
1,663 ± 3.0	3_{10}-helix	1,671 ± 3.0	β-turn
1,667 ± 1.0	β-turn	1,675 ± 5.0	β-sheet
1,675 ± 1.0	β-turn	1,683 ± 2.0	β-turn
1,680 ± 2.0	β-turn	1,689 ± 2.0	β-turn
1,685 ± 2.0	β-turn	1,694 ± 2.0	β-turn
1,691 ± 2.0	β-sheet		
1,696 ± 2.0	β-sheet		

[a]Data are from Dong and colleagues[6,47,48,54].
[b]Data are from Susi and colleagues[4,5,13,46].

1) **1,690 cm^{-1} (β-turns and/or high-frequency component of antiparallel β-sheet),**
2) 1,680 cm^{-1} (β-turns and/or possible antiparallel β-sheet component),
3) 1,668 cm^{-1} (β-turns),
4) 1,658 cm^{-1} (α-helix),
5) **1,647 cm^{-1} (unordered),**
6) 1,638 cm^{-1} (triple helix),
7) **1,625 cm^{-1} (β-sheet / aggregated β-sheet low-frequency component),**
8) 1,612 cm^{-1} (aggregated β-sheet / strongly hydrogen-bonded β-sheet).

Anal Bioanal. Chem., 386,1961 (2006)

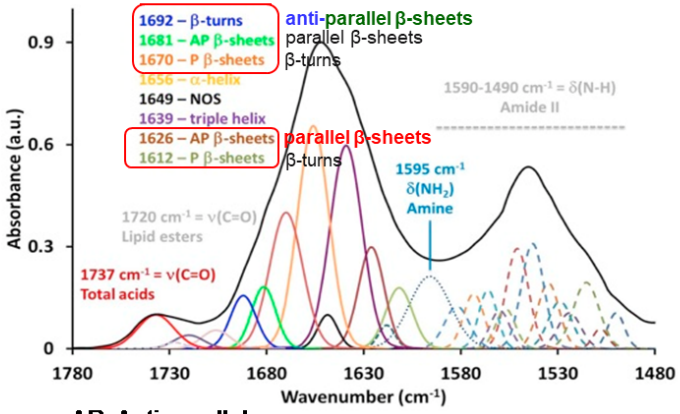

AP: Anti-parallel
P: Parallel

Trends in Analytical Chemistry, 82, 443(2016)

1) 1,715 cm^{-1}, esters,
2) **1,690 cm^{-1}, (β-turns and/or high-frequency component of antiparallel β-sheet),**
3) 1,679 cm^{-1}, parallel β-strand (in a β-sheet structure),
4) **1,668 cm^{-1}, β-turn,**
5) 1,656 cm^{-1}, α-helix,
6) **1,647 cm^{-1}, unordered structure,**
7) 1,638 cm^{-1}, triple helix,
8) **1,628 cm^{-1}, (β-sheet / aggregated β-sheet low-frequency component),**
9) **1,617 cm^{-1}, (aggregated β-sheet / strongly hydrogen-bonded β-sheet),**
10) 1,592 cm^{-1}, amine, (N–H),

TRENDS in Biotechnology, 24 ,10(2006)

OMNIC Peak Fitting Analysis of Polystyrene Film FTIR Spectrum

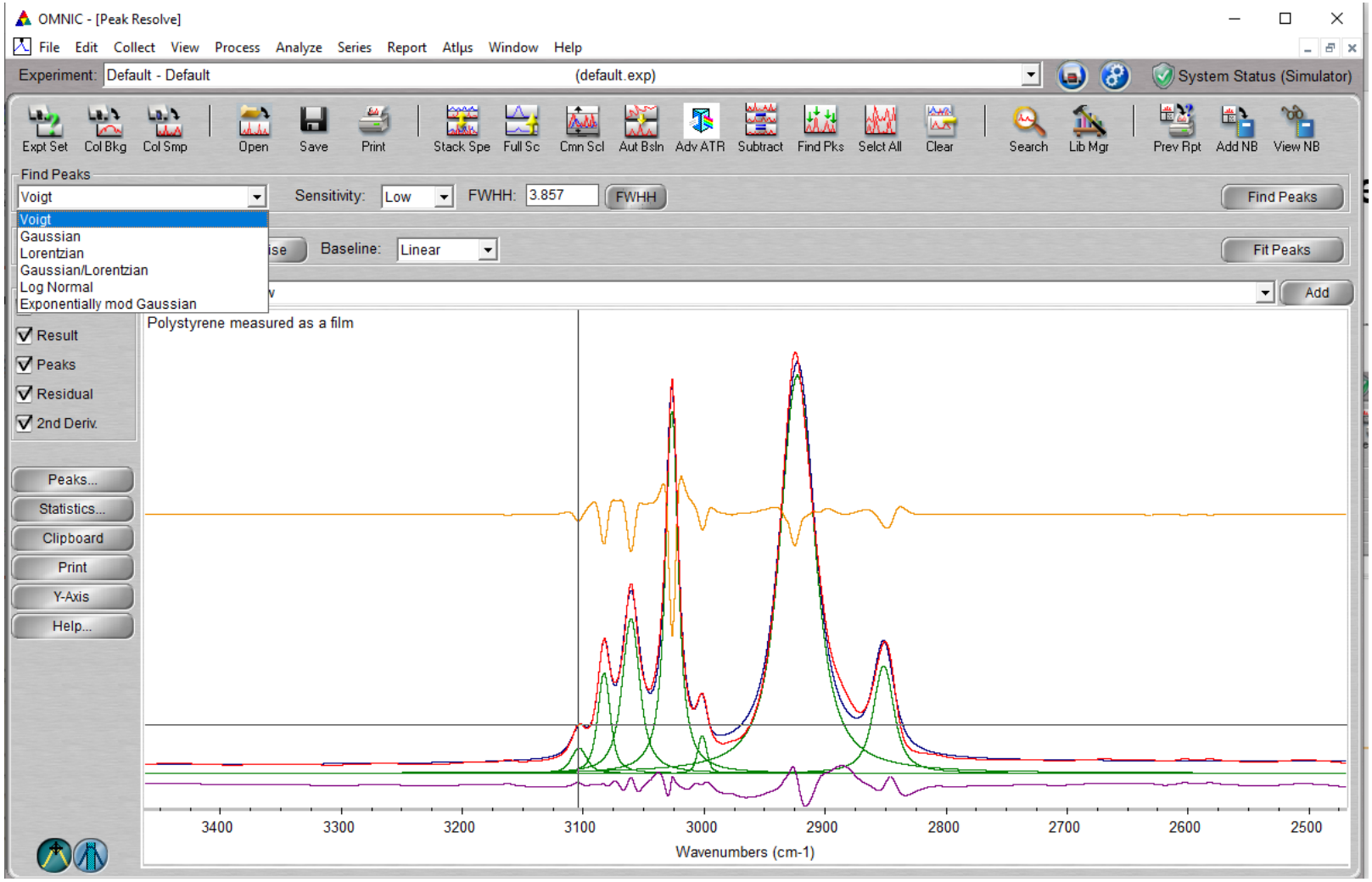

Key Concepts and Parameters of Line Shapes and Peak Fitting in Vibrational Spectroscopy (IR/Raman)

Key Concepts and Parameters of Line Shapes and Peak Fitting in Vibrational Spectroscopy (IR/Raman)

Function	Description
Gaussian	Typical in solids; static environment; produces broader, symmetric peaks.
Lorentzian	Common in gases; sharp central peak with longer wings due to collisions and rotations.
Voigt	A convolution of Gaussian and Lorentzian shapes; often used for liquids, combining both features.
Gaussian/Lorentzian	Weighted sum or mix of Gaussian and Lorentzian; allows flexible fitting between the two extremes.
Log Normal	Asymmetric peak shape, often seen in [redacted]
Exponentially mod Gaussian	Gaussian profile modified by an exponential decay, used for asymmetric peaks often found in IR/Raman spectra.

Key Concepts and Parameters of Line Shapes and Peak Fitting in Vibrational Spectroscopy (IR/Raman)

Other Key Parameters	Description
Peak Position	Location of the peak maximum (center).
Intensity	Height of the peak; less accurate for concentration than area.
FWHH	Full width at half height; relates to dynamics and lifetime.
Peak Area	More reliably reflects molecular concentration than intensity alone.
Peak Width	Broader peaks indicate faster dynamics and shorter lifetimes.

Fourier Transform Spectrometers

- **Interferometer**

basic principle of measurements:

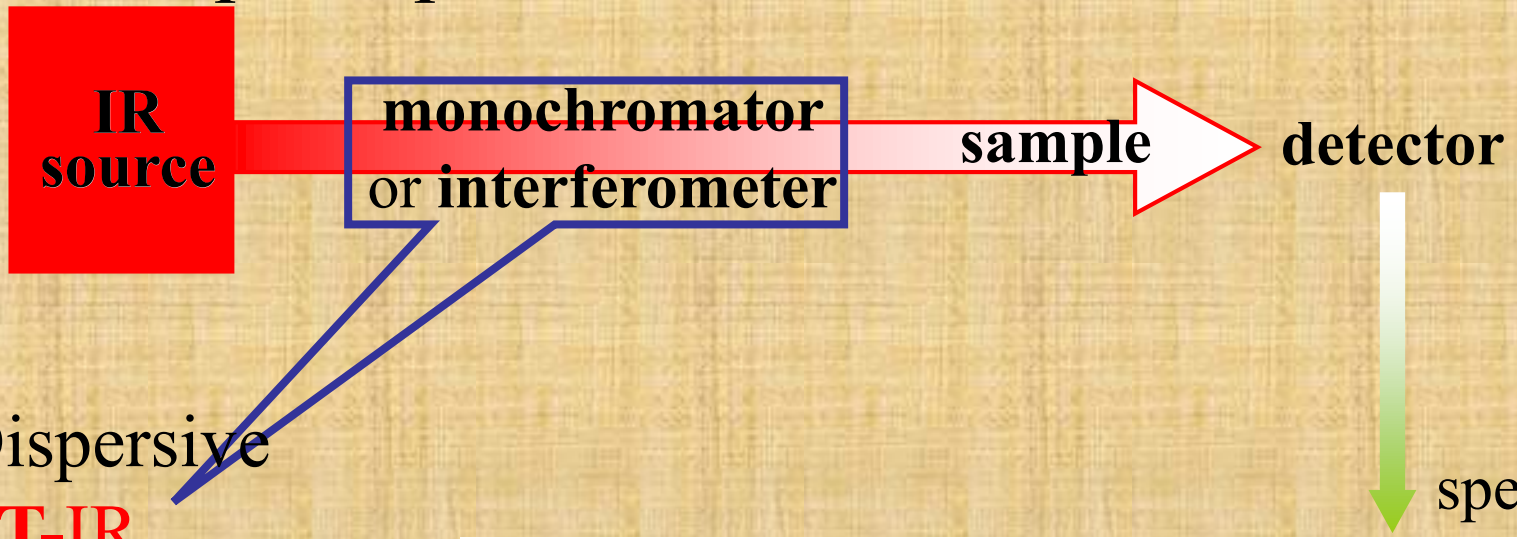

Dispersive

FT-IR

Non-dispersive

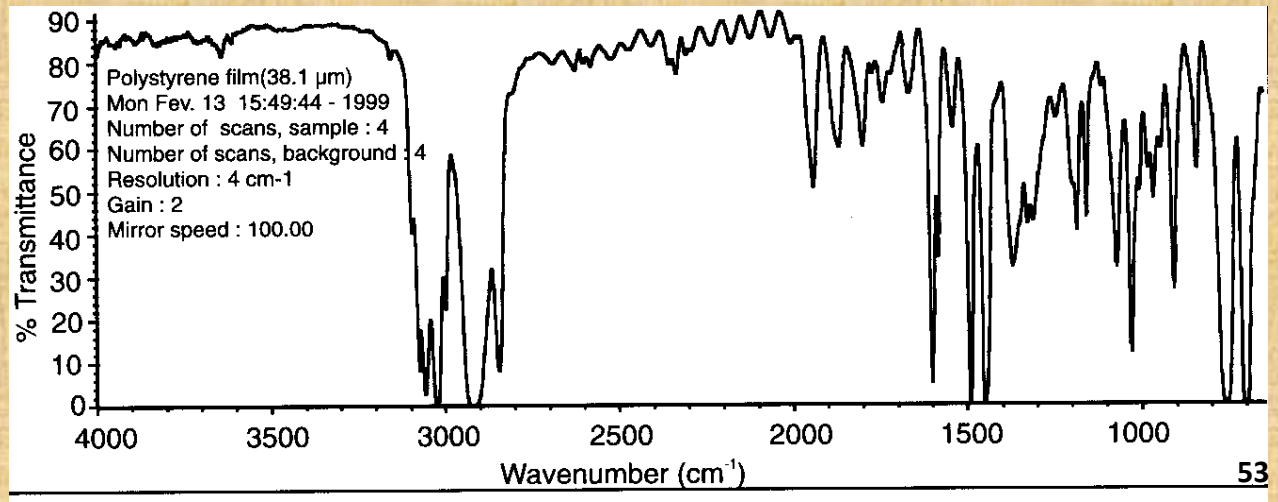

Fourier Transform IR

- **Interferometer**

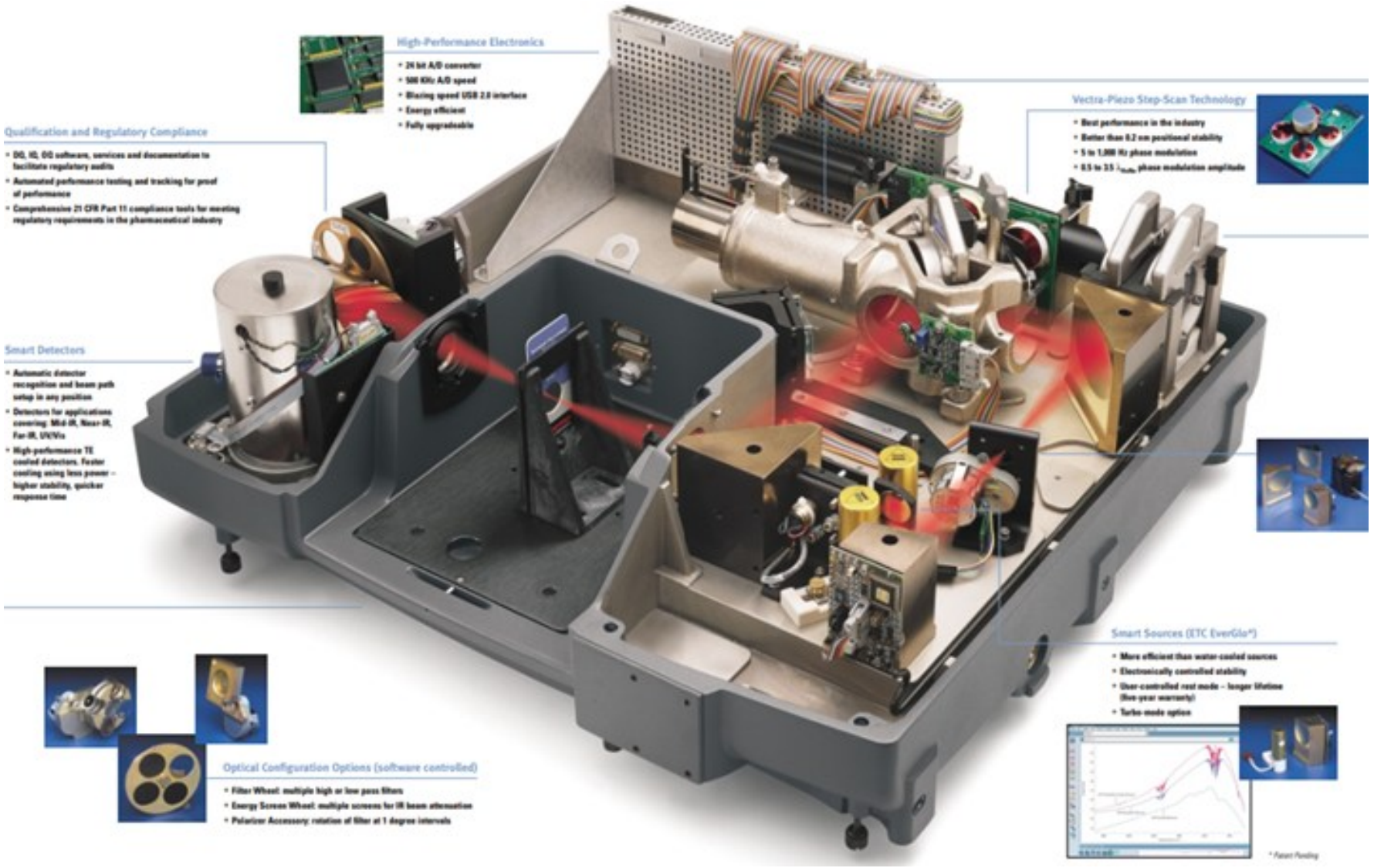

Fourier Transform IR

- **Interferometer**

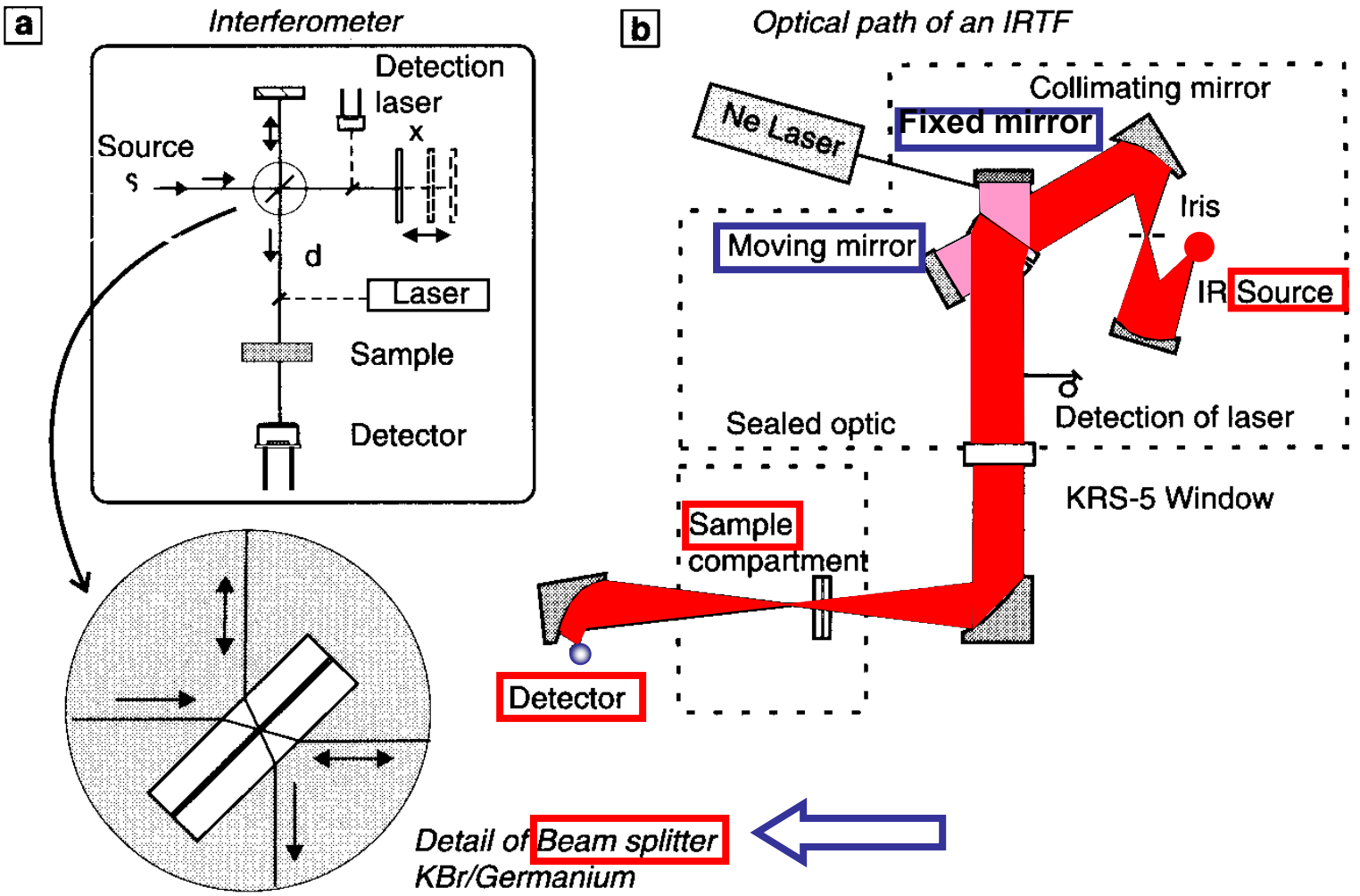

Fourier Transform IR

- **Interferometer: Michelson Interferometer**

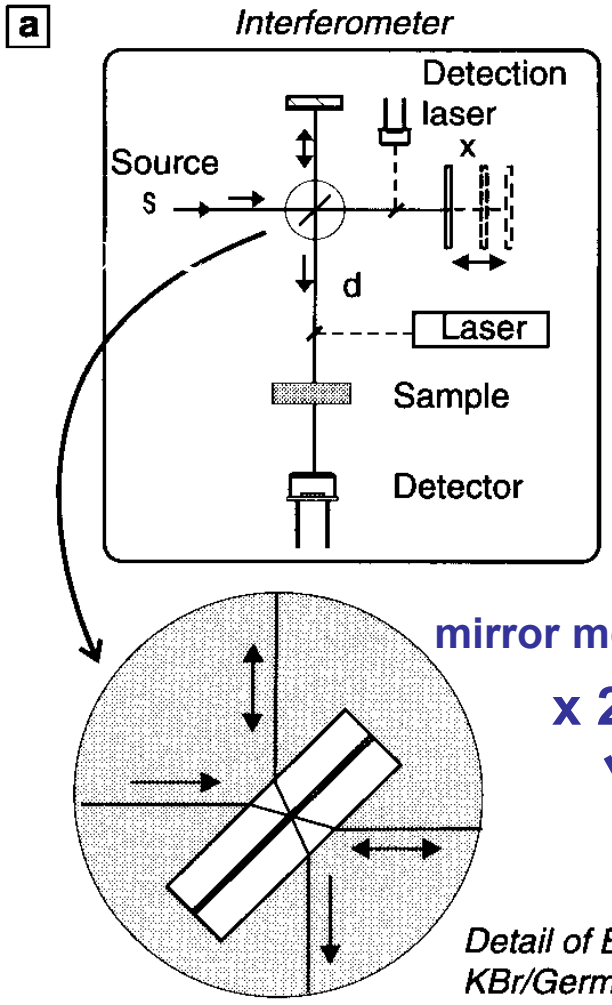

Q: what does the detector record when a beam with single wavelength transpasses the interferometer?

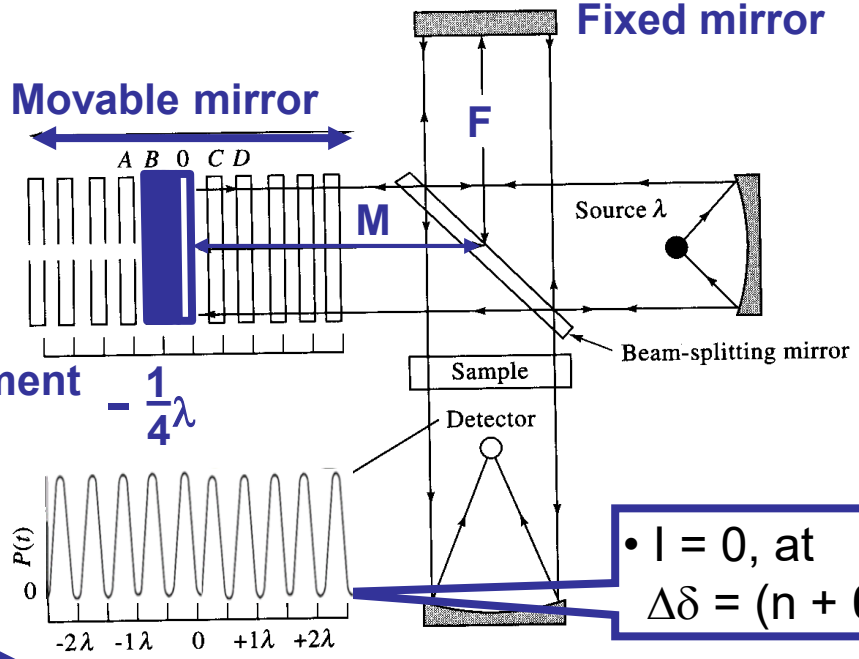

mirror movement $-\frac{1}{4}\lambda$

x 2

$-\frac{1}{2}\lambda$ difference in beam travel paths

180° out of phase, i.e. destructive

- I = 0, at $\Delta\delta = (n + \mathbf{0.5})\lambda$

Optical arrangement of a Fourier transform IR spectrometer

Modulation frequency

Region	Wave length μm
Near IR	0.75-2.5
Mid IR	2.5-25
Far IR	25-1000

$$\upsilon_{2.5} = \frac{c}{\lambda_{2.5}} = \frac{3*10^8}{2.5*10^{-6}} = 1.2*10^{14}\ \text{Hz}$$

$$\upsilon_{25} = \frac{c}{\lambda_{25}} = \frac{3*10^8}{25*10^{-6}} = 1.2*10^{13}\ \text{Hz}$$

λ : wave length of modulation frequency
τ : the period of bright/dark fringe
v_M : the velocity of movable mirror
f_{mo}: modulation frequency

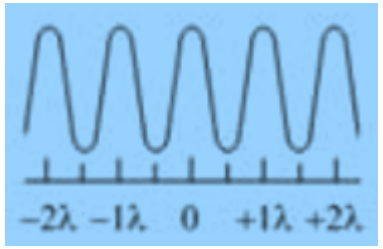

Signal frequency on detector

frequency of IR

$$v_M * \tau = \frac{\lambda}{2}$$

$$f_{mo} = \frac{1}{\tau} = \frac{2v_M}{\lambda} = \frac{2v_M}{c} * \upsilon$$

$$\lambda = \frac{c}{\upsilon}$$

2.5 μm → f_{mo}= 16 KHz
25 μm → f_{mo}= 1.6 kHz
(V_M=2.0 cm/s)

V_m(cm/s) 2.0 λ(μm) 10

1250 Hz

Calculate Fmo

Fourier Transform IR

- **Interferometer: Michelson Interferometer**

Q: the x-axis of IR spectra ?

frequency, *f*, $\bar{\nu}$

wavenumber, cm^{-1}

i.e. correlate δ with $\bar{\nu}$

Q: correlation between intensity P(δ) & λ of light source?

i.e. correlate δ with λ

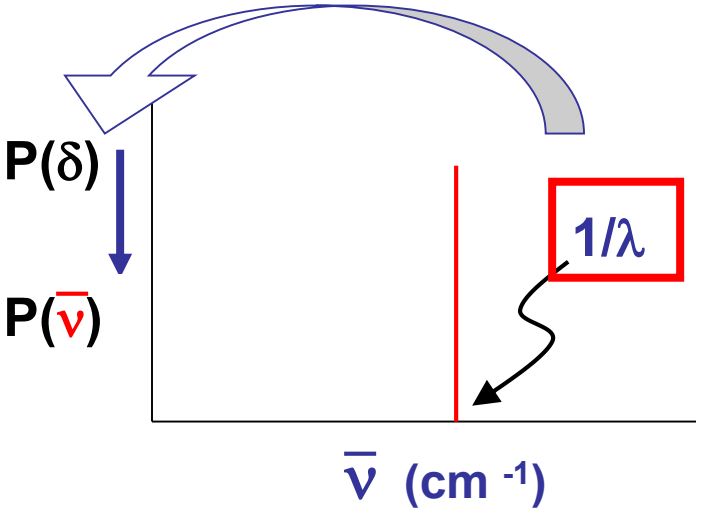

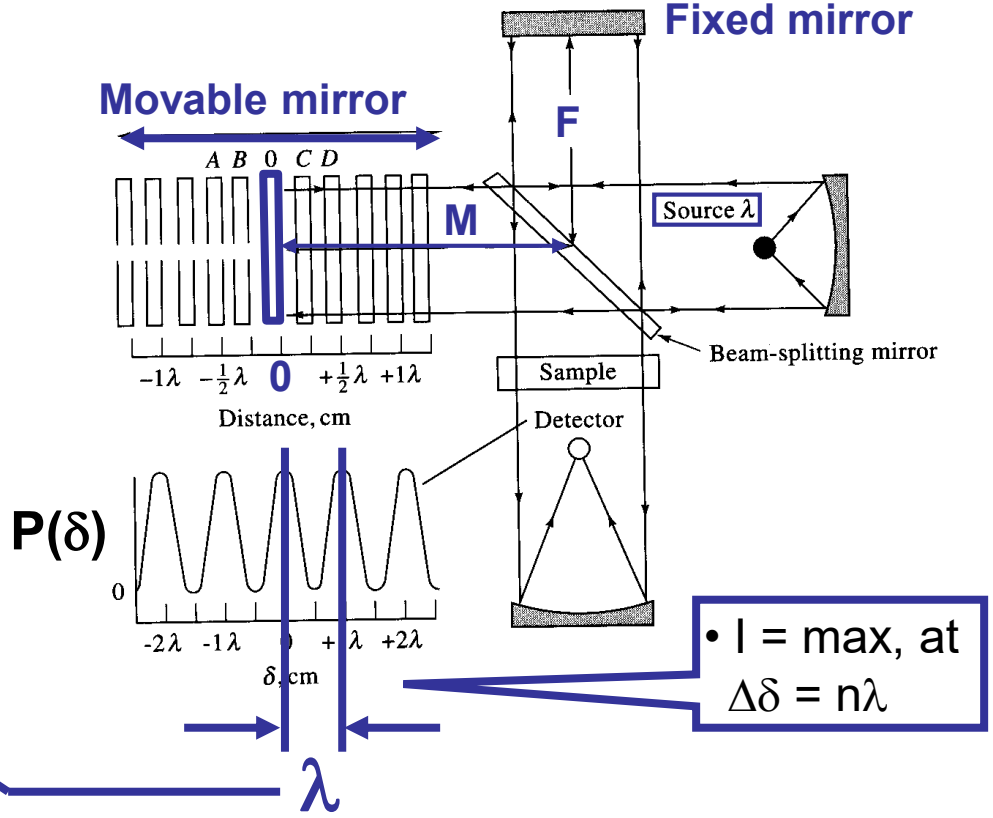

Fourier Transform IR

- **Interferometer:**

plot of
output power **P(δ)**
versus
difference in beam pathways, δ

interferogram

IR spectrum for monochromatic source i.e. single wavelength

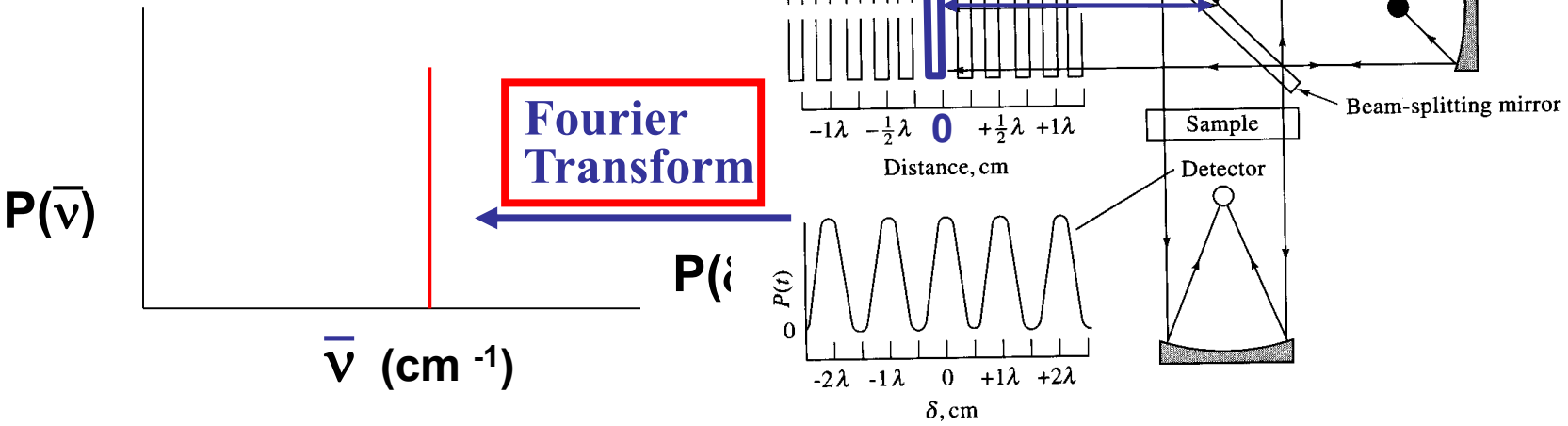

$$P(\delta) = \frac{1}{2} P(\bar{\nu}) \cos 2\pi f t$$

Fourier Transform IR

- **Interferometer:**

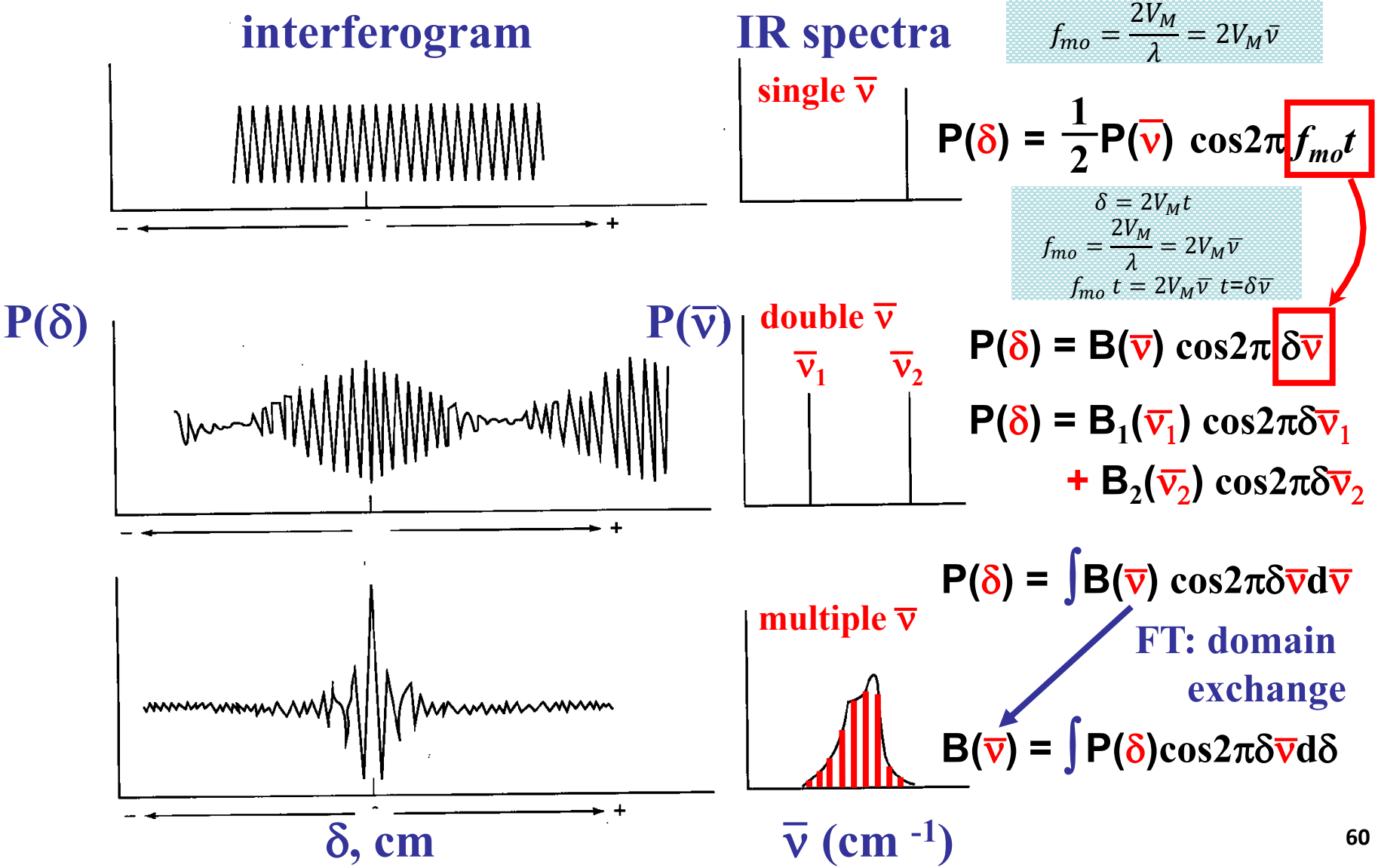

$$\omega = \frac{2\pi}{\tau} = 2\pi f_{mo}$$

$$f_{mo} = \frac{2V_M}{\lambda} = 2V_M\bar{\nu}$$

$$P(\delta) = \frac{1}{2}P(\bar{\nu})\cos 2\pi f_{mo}t$$

$$\delta = 2V_M t$$

$$f_{mo}\,t = 2V_M\bar{\nu}\;\; t=\delta\bar{\nu}$$

$$P(\delta) = B(\bar{\nu})\cos 2\pi\delta\bar{\nu}$$

$$P(\delta) = B_1(\bar{\nu}_1)\cos 2\pi\delta\bar{\nu}_1 + B_2(\bar{\nu}_2)\cos 2\pi\delta\bar{\nu}_2$$

$$P(\delta) = \int B(\bar{\nu})\cos 2\pi\delta\bar{\nu}\,d\bar{\nu}$$

FT: domain exchange

$$B(\bar{\nu}) = \int P(\delta)\cos 2\pi\delta\bar{\nu}\,d\delta$$

The Fourier Transform .com

$$\mathcal{F}\{g(t)\} = G(f) = \int_{-\infty}^{\infty} g(t)e^{-i2\pi ft}\,dt$$

$$\mathcal{F}^{-1}\{G(f)\} = g(t) = \int_{-\infty}^{\infty} G(f)e^{i2\pi ft}\,df$$

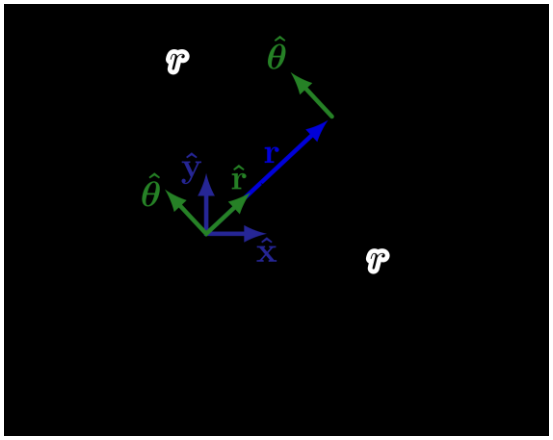

$\omega t = (2\pi f)\, t = \theta$

$$e^{i2\pi ft} = COS\,(2\pi ft) + i\sin(2\pi ft)$$

Counterclockwise

$$e^{-i2\pi ft} = COS\,(2\pi ft) - i\sin(2\pi ft)$$

Clockwise

https://www.youtube.com/watch?v=spUNpyF58BY

Fourier Transformation in FTIR:
From Interferogram to Spectrum

$$F(\omega) = \int_{-\infty}^{\infty} f(t) e^{j\omega t} \partial t$$

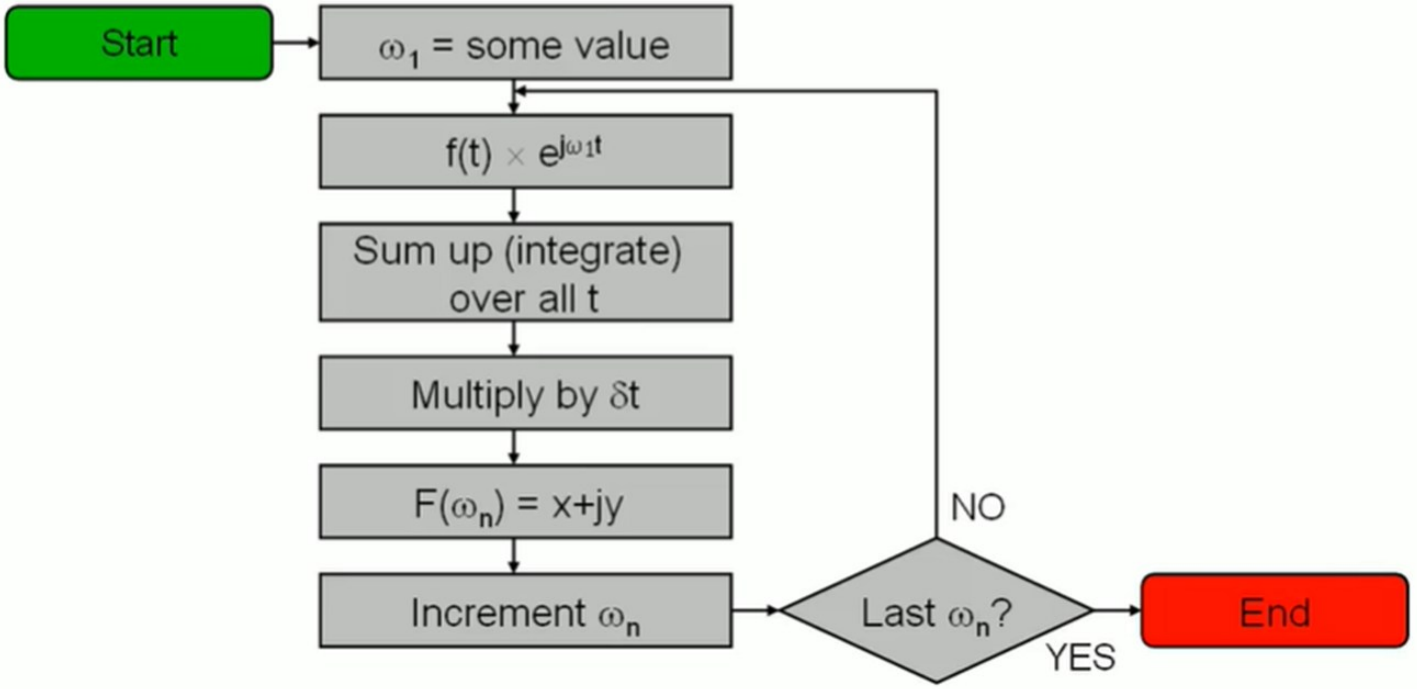

Fourier transformation decomposes an interferogram into its frequency components. By evaluating each frequency component sequentially, the optical-path-difference-domain signal is converted into an infrared spectrum in the wavenumber domain.

Role of the Imaginary Component in FTIR Phase Correction

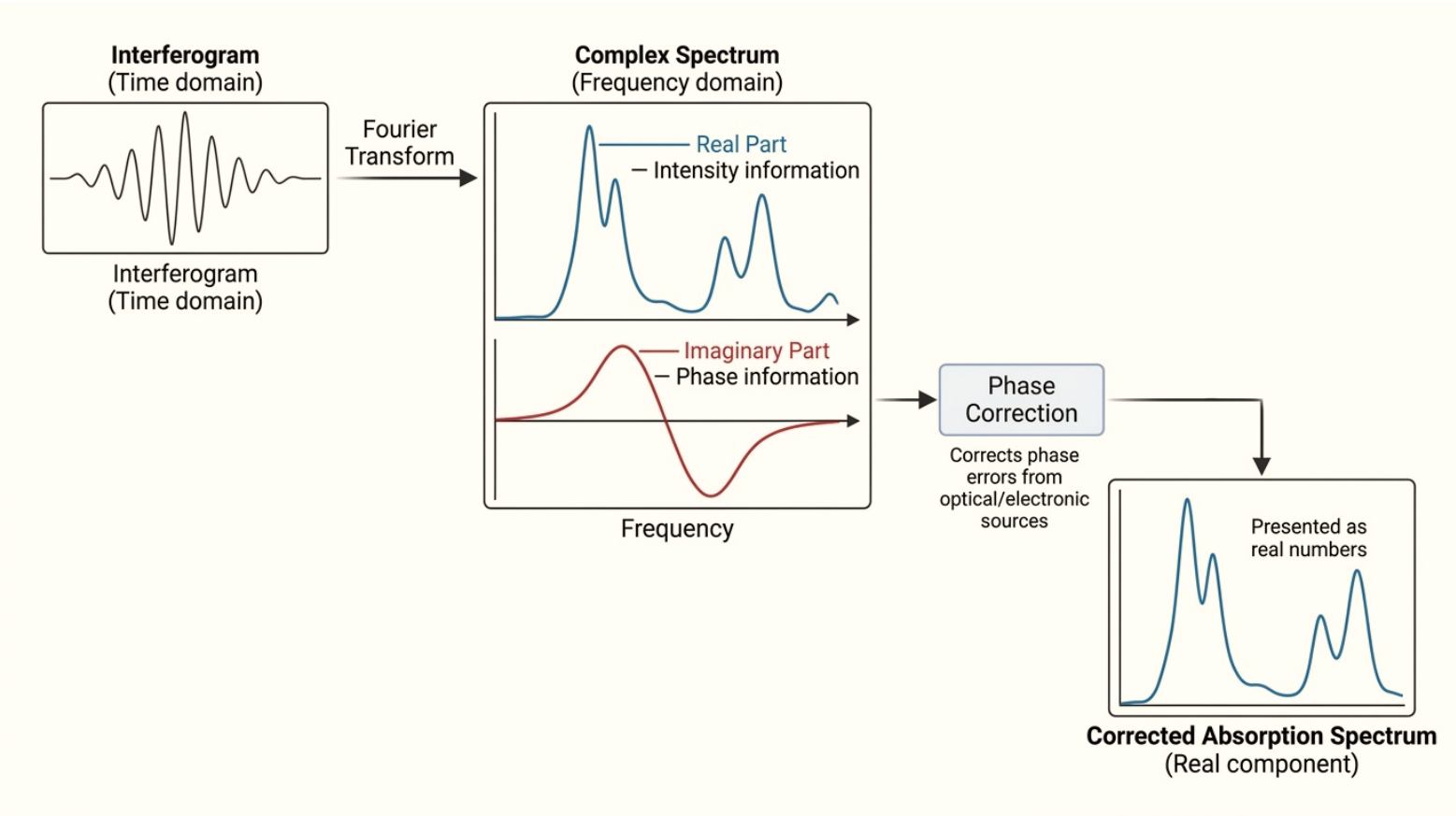

Role of the real and imaginary components in FTIR phase correction. The Fourier transform of an FTIR interferogram produces a complex spectrum. The real part primarily represents intensity, while the imaginary part represents phase. Phase correction removes optical and electronic phase errors, allowing the final absorption spectrum to be presented as a real-valued spectrum.

Fourier Transform IR

- **Interferograms** **IR Spectra**

P(δ) **P($\bar{\nu}$)**

blank/ reference

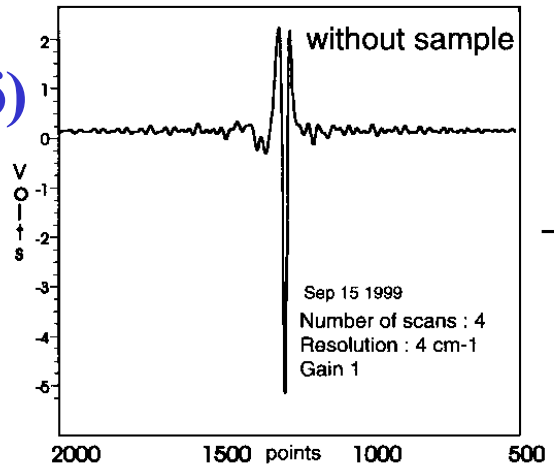

TF

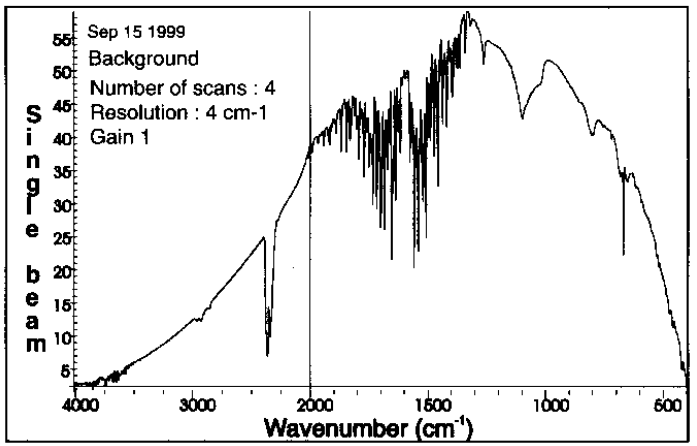

1 Single beam spectrum $I_0 = f(\nu)$ $\bar{\nu}$ (cm $^{-1}$)

sample

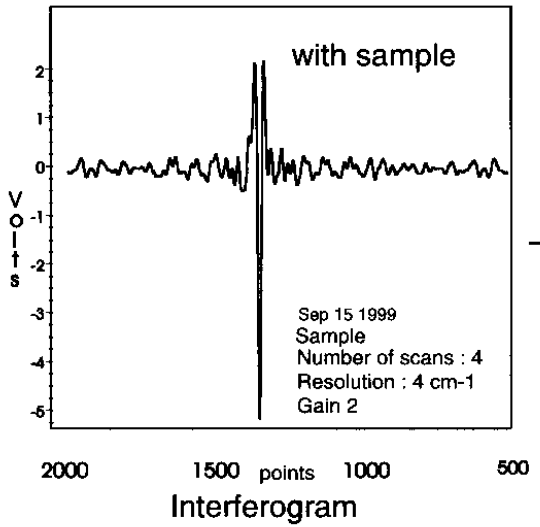

FT

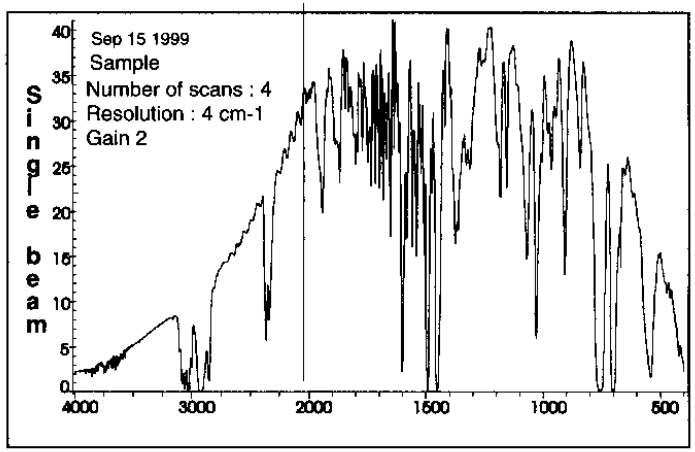

2 Single beam spectrum $I = f(\nu)$

Fig 10-12

Fourier Transform IR

- **Interferograms**

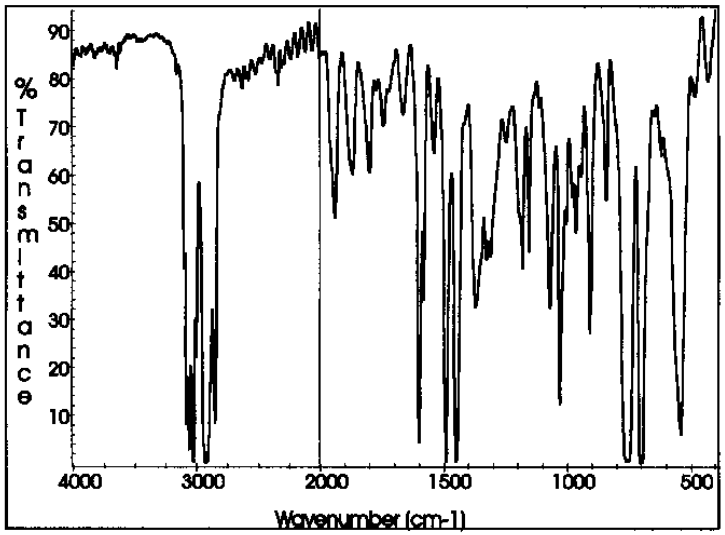

IR Spectra

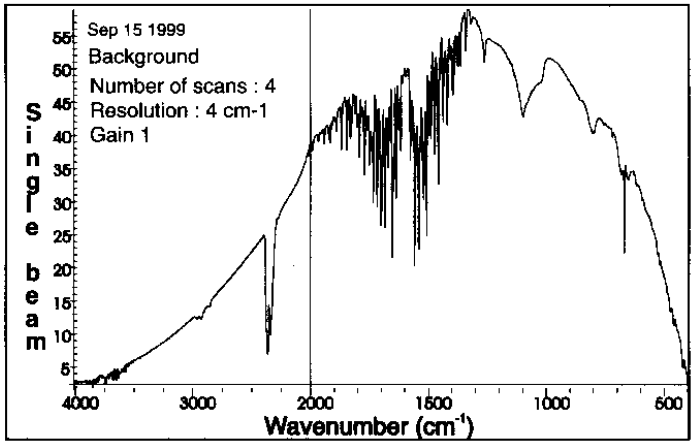

$P(\bar{\nu})$

$T = I/I_0$ *1* Single beam spectrum $I_0 = f(\nu)$ $\bar{\nu}$ (cm $^{-1}$)

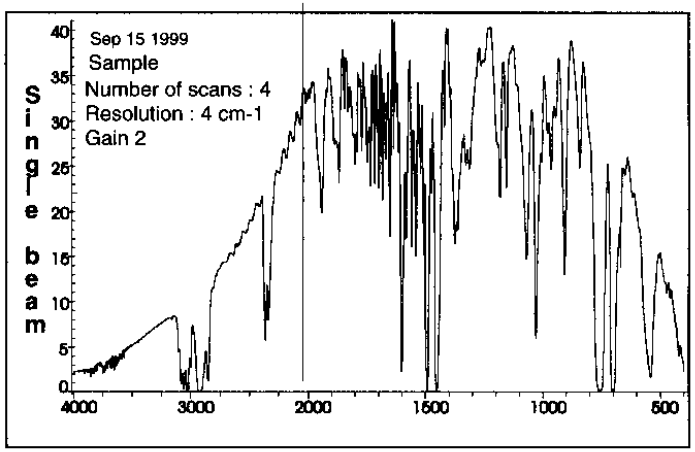

2 Single beam spectrum $I = f(\nu)$

Fig 10-12

Spectral Resolution of FTIR

Spectral resolution of FTIR

$$\Delta v = \frac{1}{2d}$$

$D\Delta v = D(v_1 - v_2)$ = 1 (at least one wavelength difference)

D = $\frac{1}{(v_1 - v_2)}$ $\therefore \Delta v = \frac{1}{D} = \frac{1}{2d}$

***D = 2d* (path difference)**

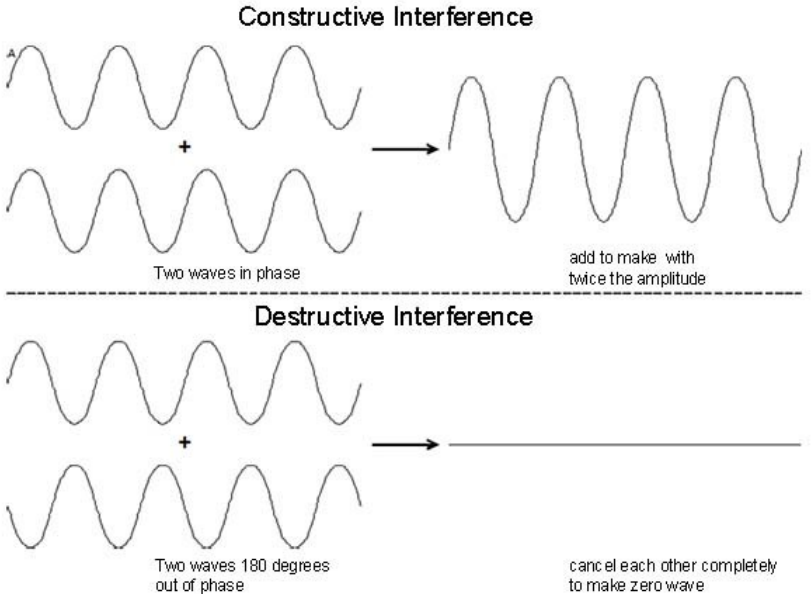

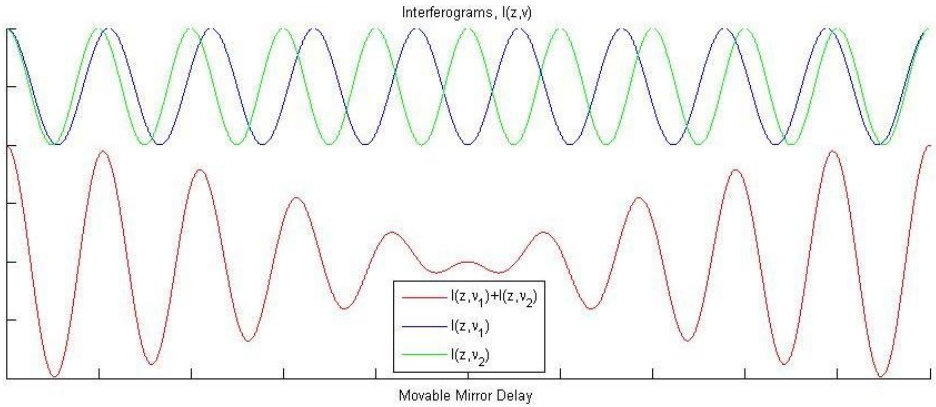

For two closely spaced wavenumbers to be distinguished by the Fourier transform, the corresponding light waves must accumulate at least one full cycle of phase difference within the maximum OPD scanning range. Only then can the Fourier transform identify them as two distinct frequency components.

http://chemwiki.ucdavis.edu/Analytical_Chemistry/Instrumental_Analysis/Spectrometer/How_an_FTIR_instrument_works

$$P(\delta) = B(\tilde{\nu}_1)\cos 2\pi\tilde{\nu}_1\delta$$

$$P(\delta) = B(\tilde{\nu}_2)\cos 2\pi\tilde{\nu}_2\delta$$

$$\Delta\phi = 2\pi\tilde{\nu}_2\delta - \cos 2\pi\tilde{\nu}_1\delta$$
$$= 2\pi\delta_{max}(\tilde{\nu}_2 - \tilde{\nu}_1)$$

In order for the Fourier transform to distinguish two closely spaced wavenumber components, their corresponding interferometric signals **must accumulate a phase difference of at least one complete cycle over the maximum optical path difference, δ_{max}**

$$\Delta\phi \approx 2\pi\delta_{max}(\tilde{\nu}_2 - \tilde{\nu}_1) = 2\pi$$

$$\delta_{max}(\tilde{\nu}_2 - \tilde{\nu}_1) = 1$$

$$\delta_{max} = 1/(\tilde{\nu}_2 - \tilde{\nu}_1)$$

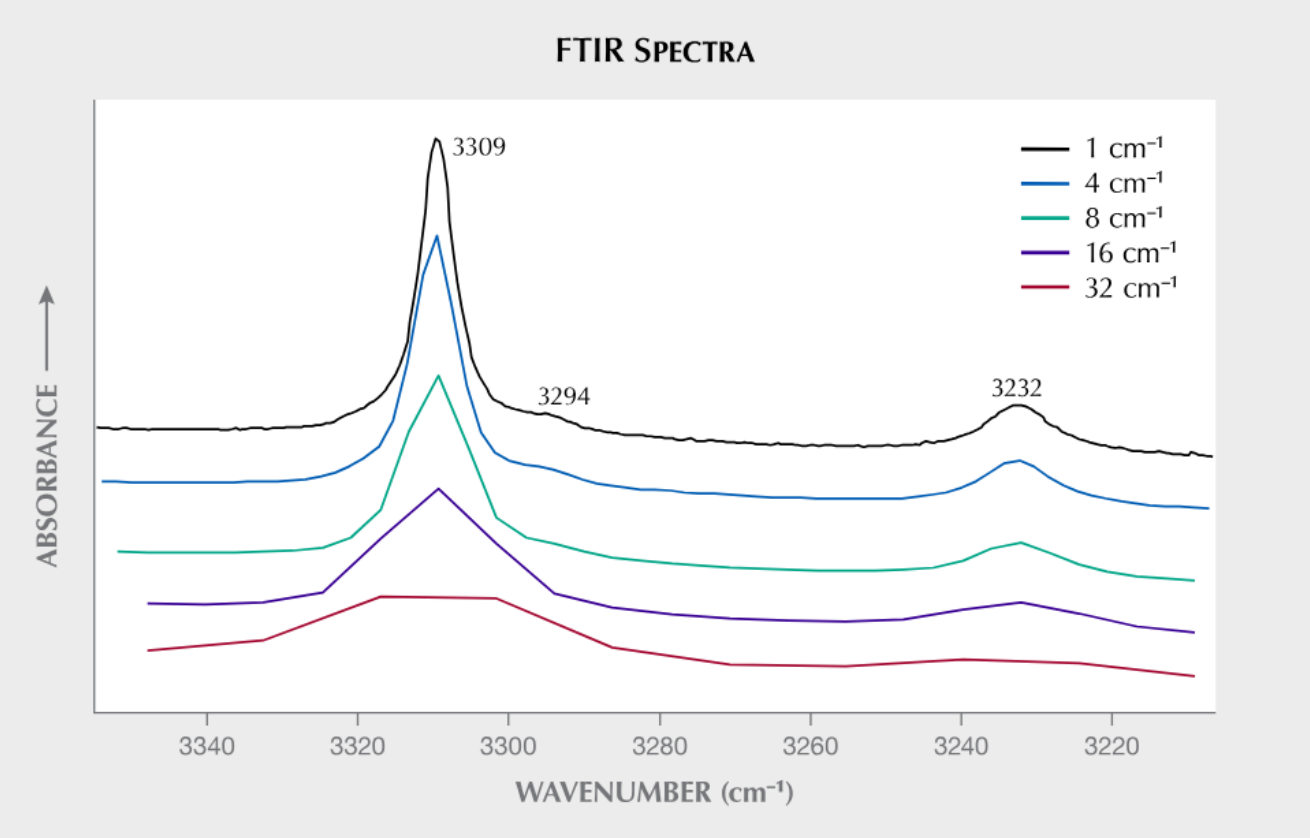

FTIR resolution significantly affects spectral peaks and determines whether closely spaced peaks can be resolved. For example, the 3309 and 3232 cm^{-1} OH absorptions in corundum become very broad and difficult to distinguish with decreased resolution. The effect of increased resolution is shown by the separation of the 3309 and 3294 cm–1 peaks. Spectra are offset vertically for clarity.

IR CRYSTALS AND WINDOW MATERIALS, DESCRIPTIONS AND PROPERTIES

		Incompatible Materials	Cleaning Agents	Refractive Index at 1000 cm^{-1}	Transmission Range (top) and useful ATR Range (bottom)
AgCl	Silver chloride. Reacts with base metals, sensitive to UV radiation, cold flows.	Complexing agents, NH_4OH	Acetone, CH_2Cl_2	1.98	25,000-360 cm^{-1} N/A
AMTIR	Selenium, arsenic and germanium glass. Relatively hard, brittle, may be damaged by uneven pressure. Good with acids.	Alkalies	Alcohol, acetone, H_2O	2.5	11,000-725 cm^{-1} 11,000-725 cm^{-1}
BaF_2	Barium fluoride. Subject to thermal and mechanical shock.	NH_4 salts and acids	Acetone, H_2O	1.42	50,000-740 cm^{-1} N/A
CaF_2	Calcium fluoride. Withstands high pressure, resists most acids and bases.	NH_4 salts and acids	Acetone, H_2O	1.39	50,000-1,111 cm^{-1} N/A
CdTe	Cadmium telluride. Brittle and easily cracked. Tends to be more fragile and more expensive than other crystals.	Acids	Alcohol, acetone, H_2O	2.67	20,000-360 cm^{-1} N/A
CsI	Cesium iodode. A hygroscopic crystal material, easily scratched, soft. Excellent spectral range.	Water, lower alcohols, "wet solvents"	Anhydrous solvents	1.74	40,000-200 cm^{-1} N/A
Diamond	Carbon. Very hard. Non-reactive, pressure and scratch resistant. May fully absorb in 2500/1500 cm^{-1} region (if thick enough).	$K_2Cr_2O_7$, conc. H_2SO_4	Alcohol, acetone, H_2O	2.4	4,500-2,500/1,667-33 cm^{-1} 4,500-2,500/1,667-33 cm^{-1}
Ge	Germanium. Hard and brittle, temperature sensitive, subject to thermal shock. Excellent for highly absorbing samples (ATR).	Hot H_2SO_4, aqua regia	Alcohol, acetone, H_2O	4	5,500-600 cm^{-1} 5,500-830 cm^{-1}

KBr	Potassium bromide. Hygroscopic, withstands thermal and mechanical shock. The most popular material for IR transmission work.	Water, lower alcohols, "wet solvents"	Anhydrous solvents	1.52	40,000-400 cm^{-1} N/A
KRS-5	Eutectic mixture of thallium bromide and thallium iodide. Deforms under pressure. Temperature sensitive. Toxic. Wide spectral range.	Complexing agents, slightly soluble in water	MEK	2.37	20,000-250 cm^{-1} 20,000-400 cm^{-1}
NaCl	Sodium chloride (table salt). A hygroscopic crystal, withstands thermal and some mechanical shock.	Water, lower alcohols, "wet solvents"	Anhydrous solvents	1.49	40,000-625 cm^{-1} N/A
Sapphire	Aluminum oxide. Hard, inert crystal. Ideal for on-line applications. Limited IR range.	Chemically inert	Alcohol, acetone, H_2O	1.74	50,000-1,600 cm^{-1} 50,000-1,780 cm^{-1}
Si	Silicon. Hard and brittle. Withstands thermal shock, chemically inert. ATR range limited by absorption bands (<1,500 cm^{-1})	$HF+HNO_3$	Alcohol, acetone, H_2O	3.4	8,300-660/360-70 cm^{-1} 8,300-1,500/360-70 cm^{-1}
ZnS	Zinc sulfide. Comparable to ZnSe, but slightly harder and more chemically resistant. More limited spectral range.	Acids	Acetone, alcohol	2.2	17,000-720 cm^{-1} 17,000-950 cm^{-1}
ZnSe	Zinc selenide. Most popular ATR material. Withstands limited mechanical and thermal shock. Can be cracked by uneven pressure.	Acids, strong alkalies	Alcohol, acetone, H_2O	2.4	20,000-454 cm^{-1} 20,000-650 cm^{-1}
Zirconia	Zirconium oxide. Very hard. Resistant to acids and bases. Limited spectral range.	Chemically inert	Alcohol, acetone, H_2O	2.4	40,000-2000 cm^{-1} N/A

IV. Principle and Configuration of Attenuated Total Reflection FTIR (ATR-FTIR) for Infrared Spectroscopy

Advantage: ATR-FTIR enables rapid, non-destructive surface analysis with minimal preparation.
Disadvantage: Limited to shallow depths and sensitive to contact and refractive index mismatch.

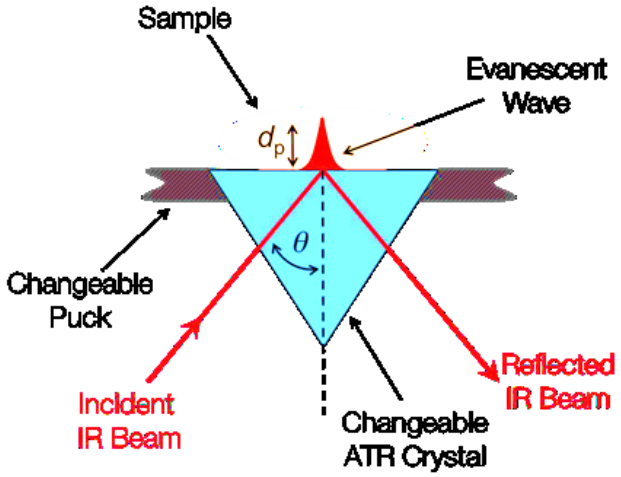

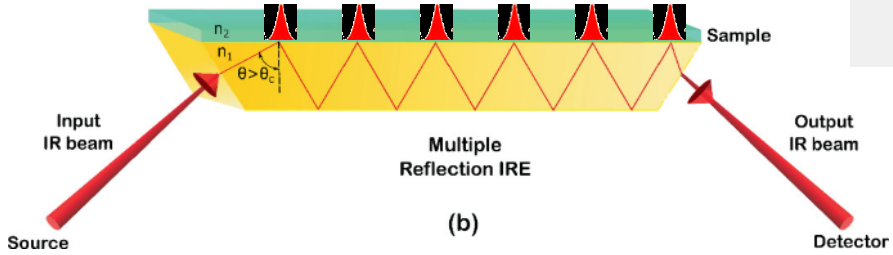

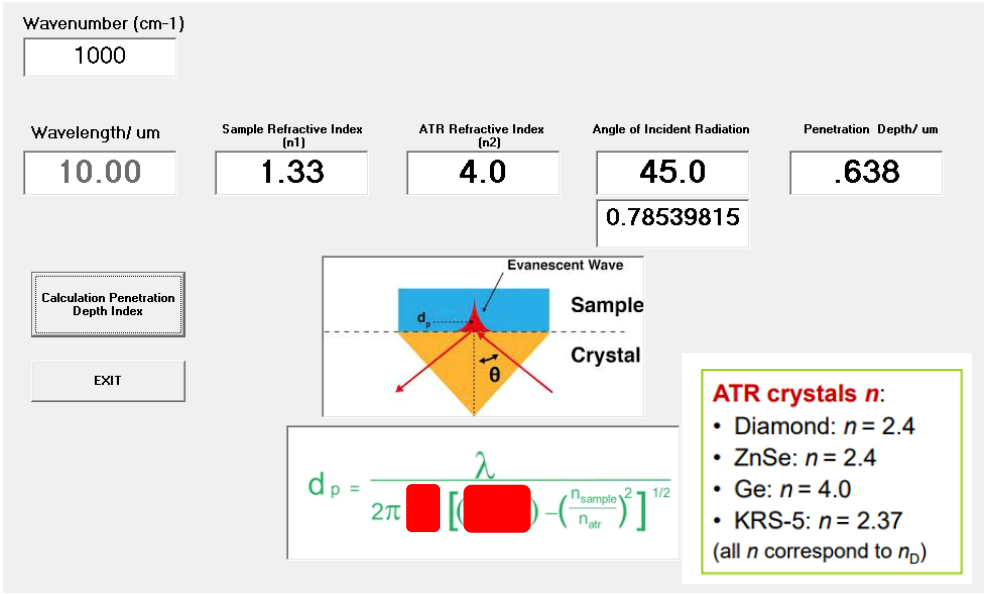

https://qd-europe.com/de/en/product/attenuated-total-reflexion-atr-fundamentals-band-distortion-and-band-shift/
https://qd-europe.com/de/en/product/attenuated-total-reflexion-atr-fundamentals-band-distortion-and-band-shift/
https://link.springer.com/chapter/10.1007/978-981-33-6084-6_1

ATR Crystal	ZnSe	Diamond	Ge
n_{ATR}	2.4	2.4	4.0
n_{Sample}	≤ 1.7	≤ 1.7	≤ 2.8
Penetration Depth	1.5 μm	1.5 μm	0.8 μm
Range	650 - 5500 cm^{-1}	30 - 4500 cm^{-1}	650 – 10000 cm^{-1}
Benefits	Good throughput	Intensity, durability, measurement	Analysis for dark samples
Samples (Best)	General organic substance, liquids	Hard powder, General organic substance	Sample including carbon (EPR,etc.)
Samples (Worst)	Hard powder, acidalkaline, high RI sample	High RI sample	Hard powder, acidalkaline
Notes	In case of hard powder, diamond is recommended	Poor S/N ratio in the region around 2000 cm-1, due to internal absorption	Weak absorption due to small depth of penetration

$$d_p = \frac{\lambda}{2\pi n_{atr}\left[(\sin^2\theta) - \left(\frac{n_{sample}}{n_{atr}}\right)^2\right]^{1/2}}$$

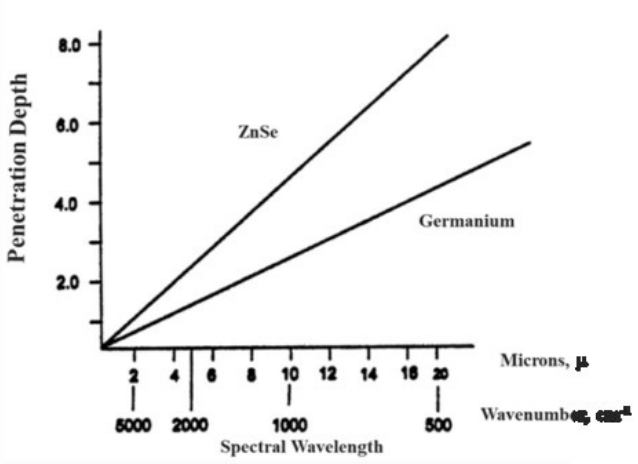

https://jascoinc.com/learning-center/theory/spectroscopy-1/attenuated-total-reflectance/

Penetration Depth and Sample Property

ATR-FTIR

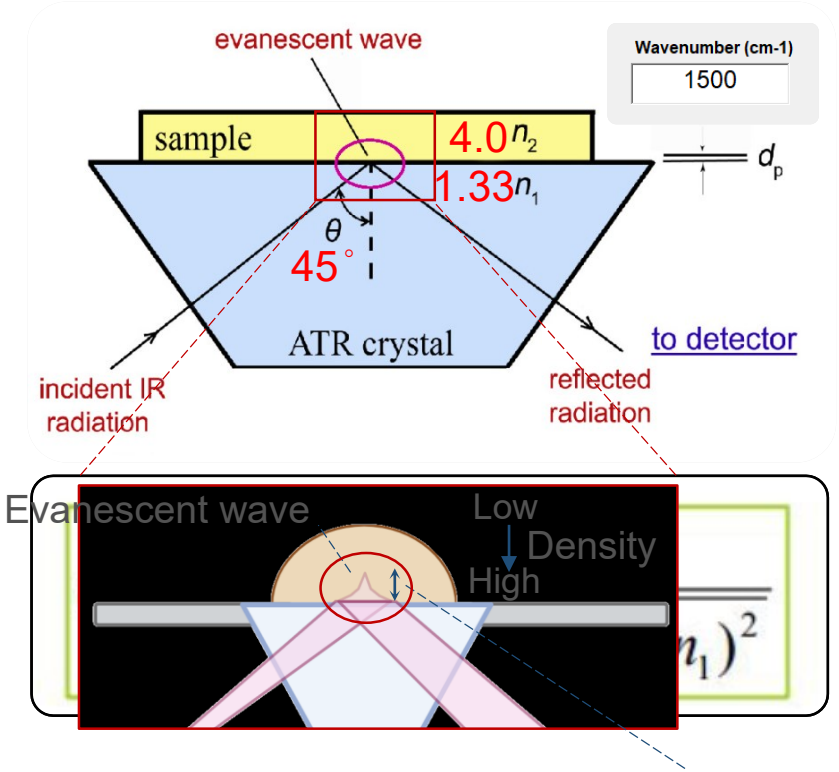

- Penetration depth = 0.43 μm (1500cm^{-1})

Transmission FTIR

Sample distribution in layers

	ATR	Transmission
Homogeneous	Average	Average
	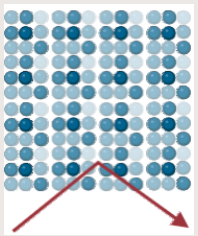	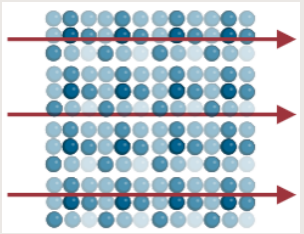
Heterogeneous	High density	X
	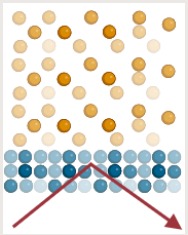	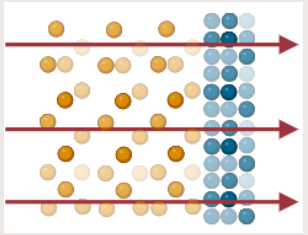

FT-IR Spectra Of Calcite Obtained Using Various Techniques

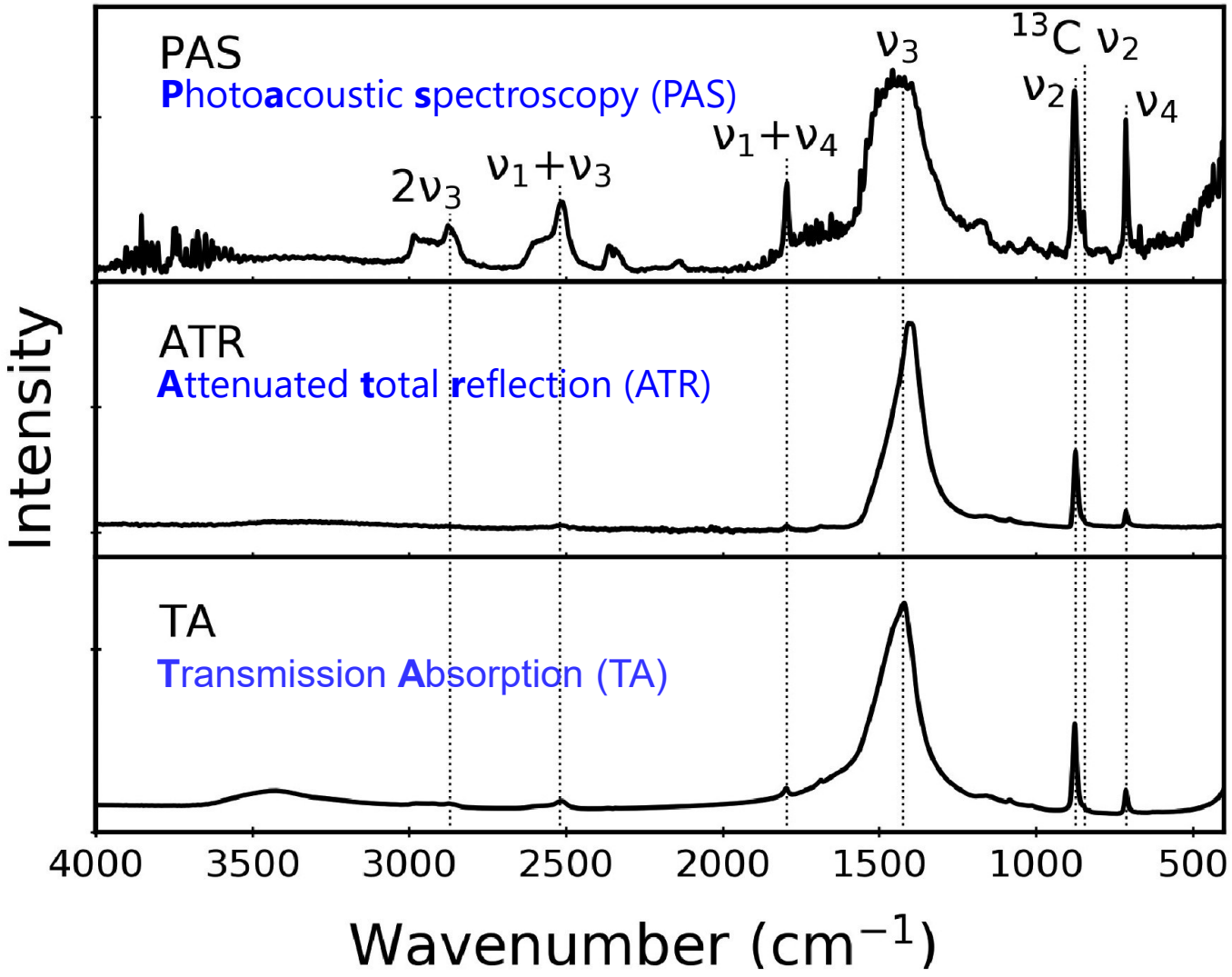

https://journals.sagepub.com/doi/10.1177/000370282110092l2

Fiber Optic ATR Loop Probe

Main features:

- High throughput at Mid InfraRed range
- On-line absorbance spectroscopy of liquids, pastes & soft solid surfaces
- Compatible with all FTIR, QCL and IR-Filter spectrometers
- Cost effective alternative to more expensive ATR-IR-fiber probes
- Replaceable ATR Loop PIR-Fiber Tips

https://artphotonics.com/product/fiber-optic-atr-loop-probe/

Fiber-optic ATR probes

Suitable for reaction monitoring in lab, pilot plant and for full automated process control.

https://kaplanscientific.nl/product/fiber-optic-atr-probes/

Micro ATR-FTIR spectroscopic imaging of colon biopsies with a large area Ge crystal

Cai Li Song, Sergei G. Kazarian

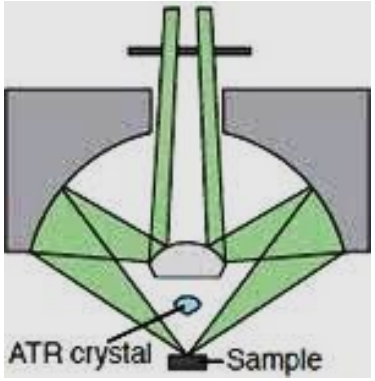

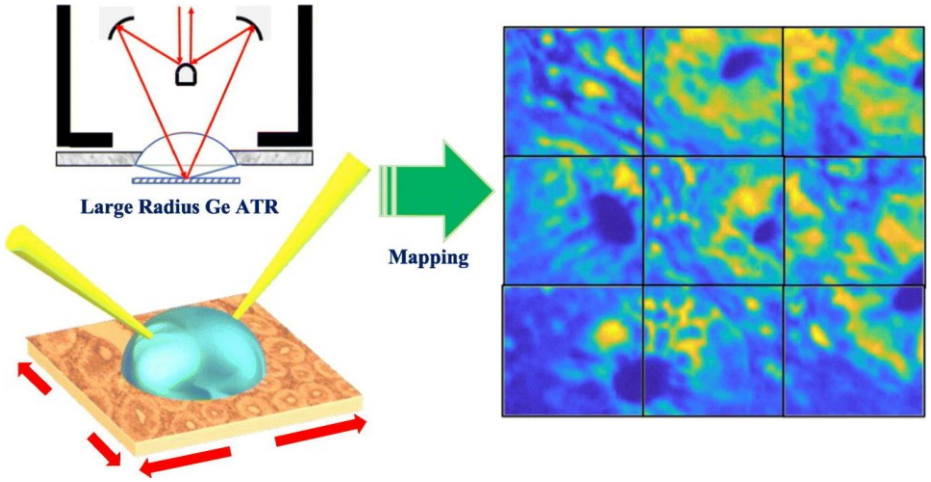

Spectrochimica Acta Part A: Molecular and Biomolecular Spectroscopy, 228, 117695, 2020

Grazing Incidence Reflection Absorption FTIR (GIRA-FTIR)

Isotropic

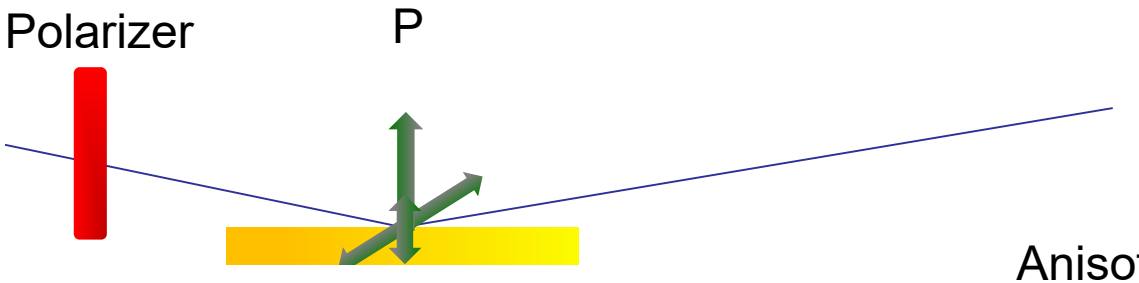

Anisotropic

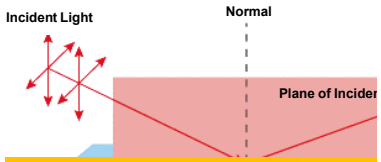

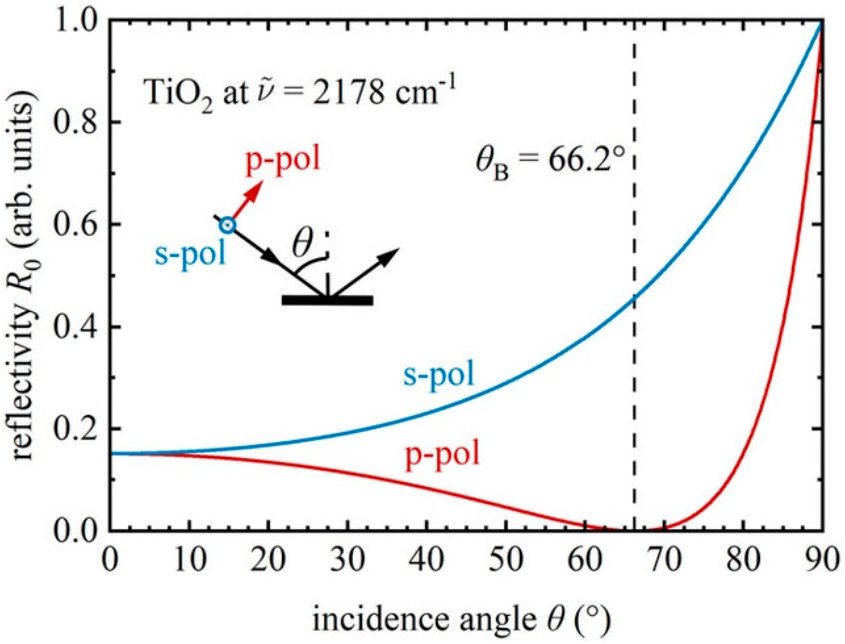

Grazing Angle Objective (GAO) 84 °

At grazing incid… electric field pe… perpendicular m… …TIR because its …s with surface- …ion.

- **High surface s…** …erface regions.
- **Ideal for ultrat…** …single-molecule layer analysis.
- **Enhanced by …** …>70° for stronger absorption.
- **Optimized for metallic or reflective substrates**: Strong IR reflection improves signal-to-noise.
- **Polarization support**: Enables analysis of molecular orientation.
- **UHV-compatible**: Integrates with vacuum systems for surface reaction and adsorption studies.

Chemical speciation techniques: Grazing Incidence Reflection (GIR) FTIR Spectroscopy

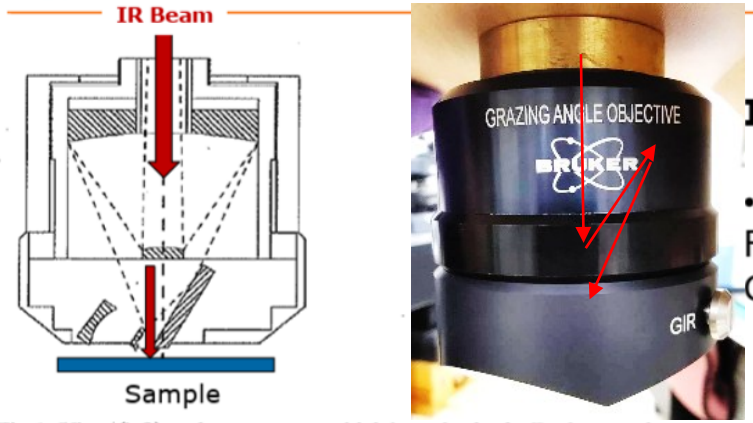

Fig 1: View (left) and measurement (right) modes in the Bruker grazing angle objective.

Courtesy of Bruker Optics, Germany

Instrument:

- Bruker Hyperion 2000 FTIR Microscope with Grazing Angle Objective

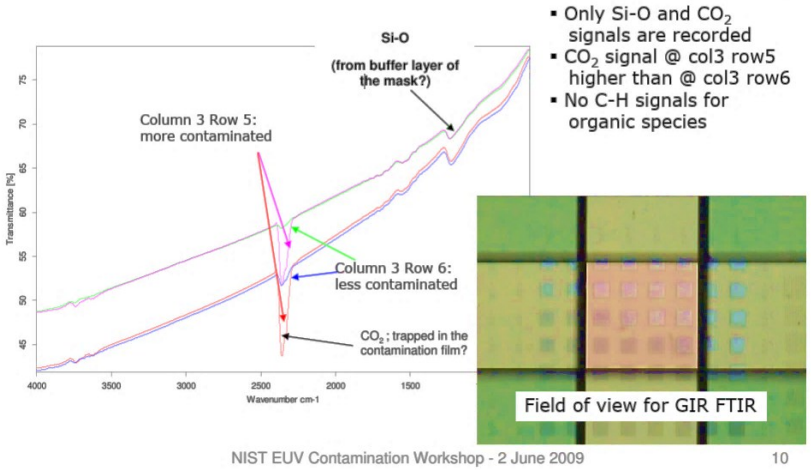

- Only Si-O and CO_2 signals are recorded
- CO_2 signal @ col3 row5 higher than @ col3 row6
- No C-H signals for organic species

https://www.poctok.org/~faradjev/workshop/slides/NISTWorkshop2009_Okoroanyanwu.pdf

V. AI-Driven Spectral Imaging Analysis

Machine Learning for Infrared Spectroscopy and FTIR Imaging
機器學習於紅外光譜與 FTIR 影像分析之應用

監督式學習 Supervised Learning

- 有明確的輸入（特徵）與輸出（標籤）
- 例：細胞光譜（特徵）+ 該細胞是否為癌症（標籤）

pixels to train models for classification, regression, or prediction.

非監督式學習 Unsupervised Learning

（例：分群、
籤（Label）

Discover hidden patterns, clusters, or spectral heterogeneity from unlabeled FTIR spectral data.

深度學習 Deep Learning

自動學習光譜或空間-光譜特徵，用於分類與影像分析。
Automatically learns spectral or spatial-spectral features for classification and image analysis.

Python.NET整合VB.NET 與 Python 的機器學習

Integrating VB.NET and Python using the Python.NET framework

Visual Studio

Community 2022

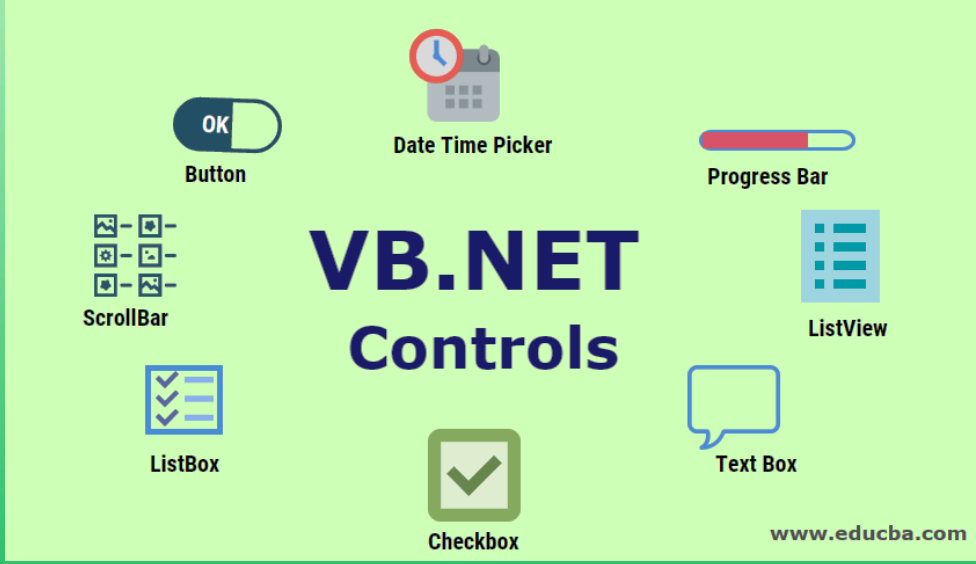

pythonnet/
pythonnet

Python for .NET is a package that gives Python programmers nearly seamless integration with the .NET Common Language Runtime (CLR)...

機器學習於 FTIR 光譜與光譜影像分析之常用方法
Machine Learning Algorithms for FTIR Spectroscopy and Spectral Imaging

線性迴歸
Linear Regression

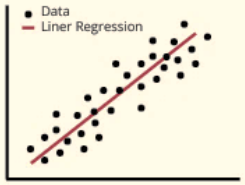

邏輯迴歸
Logistic Regression

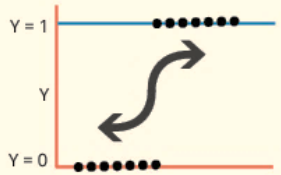

決策樹
Decision Trees

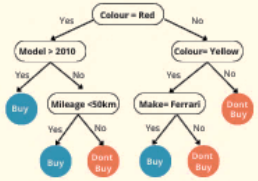

亂數森林
Random Forest

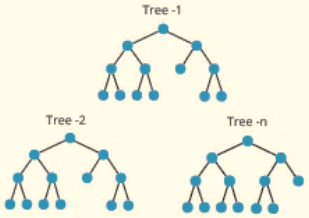

K-最近鄰居
K-Nearest Neighbor

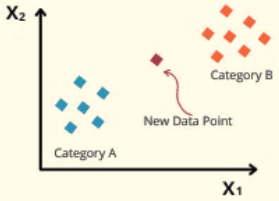

支援向量機器
Support Vector Machine

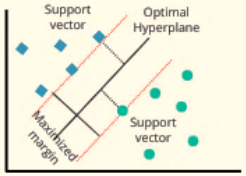

K-平均聚類
K-Means Clustering

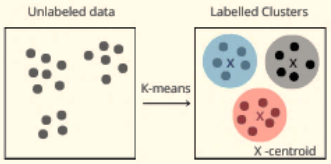

樸素機率
Naïve Bayes

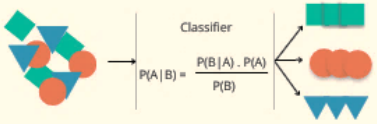

https://datasciencedojo.com/blog/machine-learning-algorithms-explanation/

FTIR 光譜影像機器學習分析流程
AI-Driven FTIR Spectral Imaging Workflow

Step 01
收集資料

Data Acquisition
FTIR spectra / FTIR images/labels

Step 02
準備資料

Spectral Preprocessing
Baseline correction/normalization/smoothing

OpenAI

Step 03
選擇模型

Model Selection
PCA / K-means / SVM / Random Forest / CNN

Step 04
訓練模型

Model Training
Training with labeled spectra or image pixels

Step 05
分析評估

Evaluation
Cross-validation/confusion matrix/performance metrics

Step 06
超參數調整

Hyperparameter Tuning
Optimize model parameters and reduce overfitting

Step 07
預測結果

Prediction and Visualization
Classification map/probability map / chemical image

https://solwen.ai/posts/machine-learning

Workflow for CNN-Based Machine Learning Analysis of ATR-FTIR Spectra

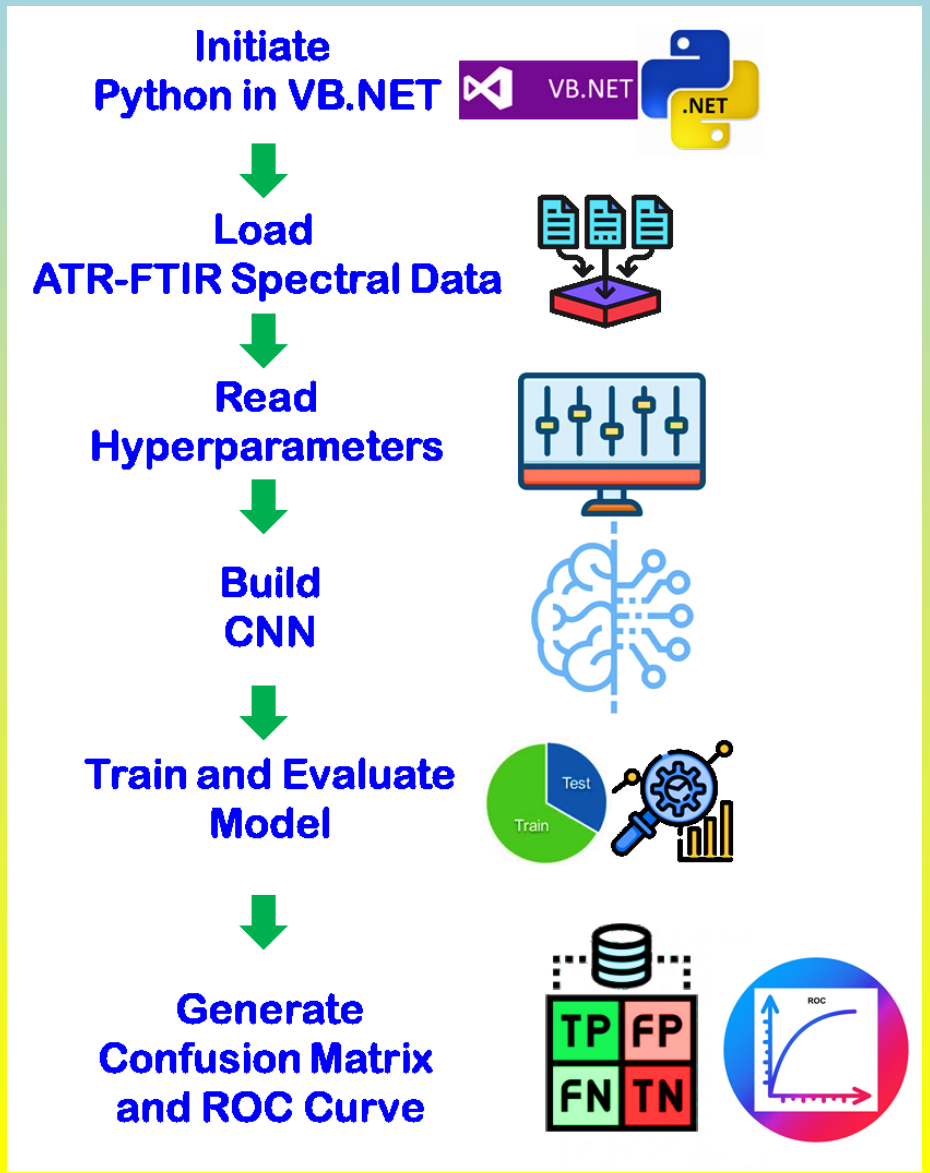

Dimensionality Reduction

Kernel size

Number of filters

Pooling type & size

Number of convolutional layers

Fully connected layers

Automated FTIR Amide I Peak Deconvolution and Protein Secondary Structure Mapping

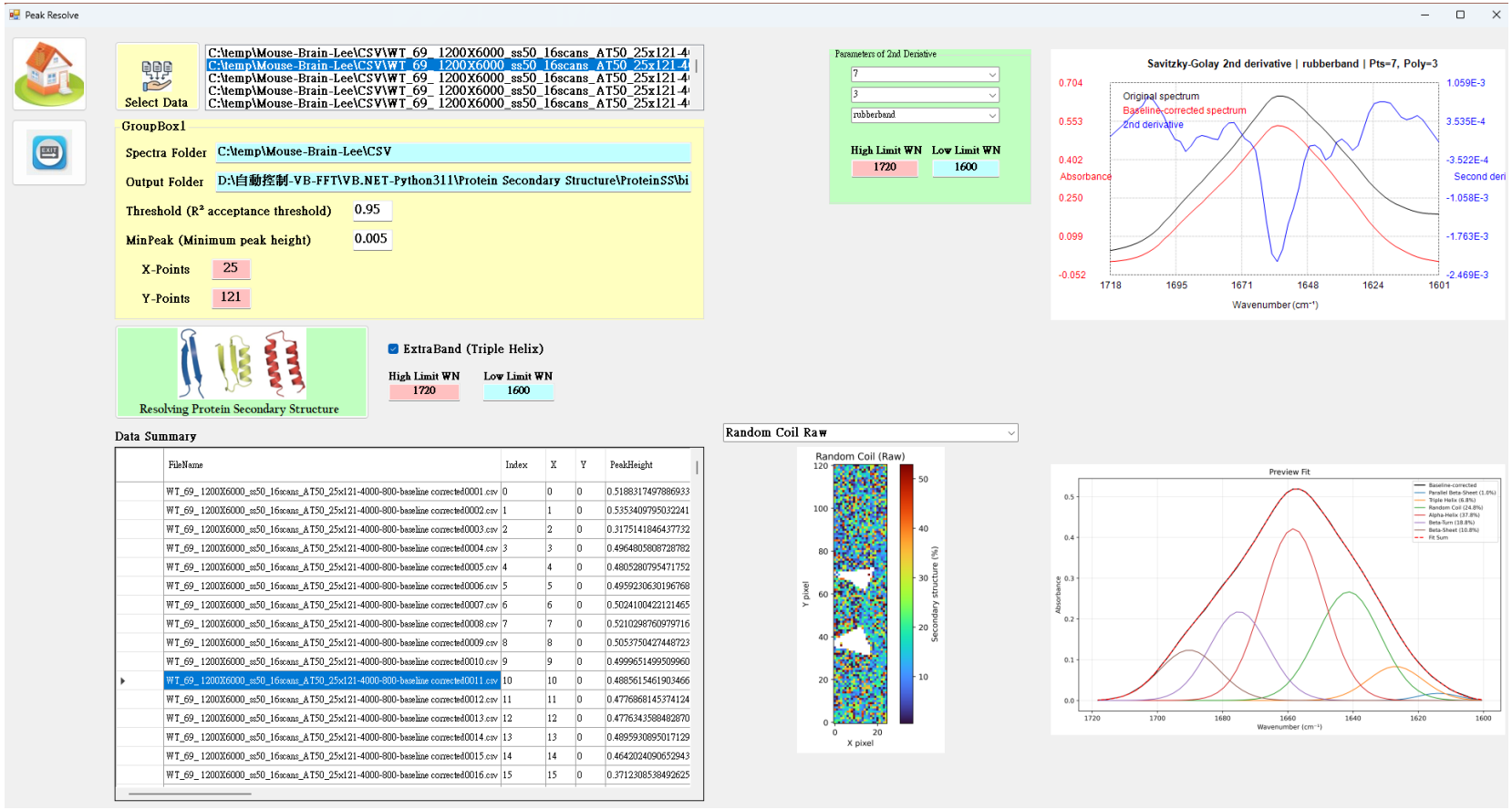

Automated FTIR Amide I deconvolution platform for protein secondary structure imaging.

Automated Peak Deconvolution and CNN-based Spectral Classification for Lupus Nephritis Assessment.

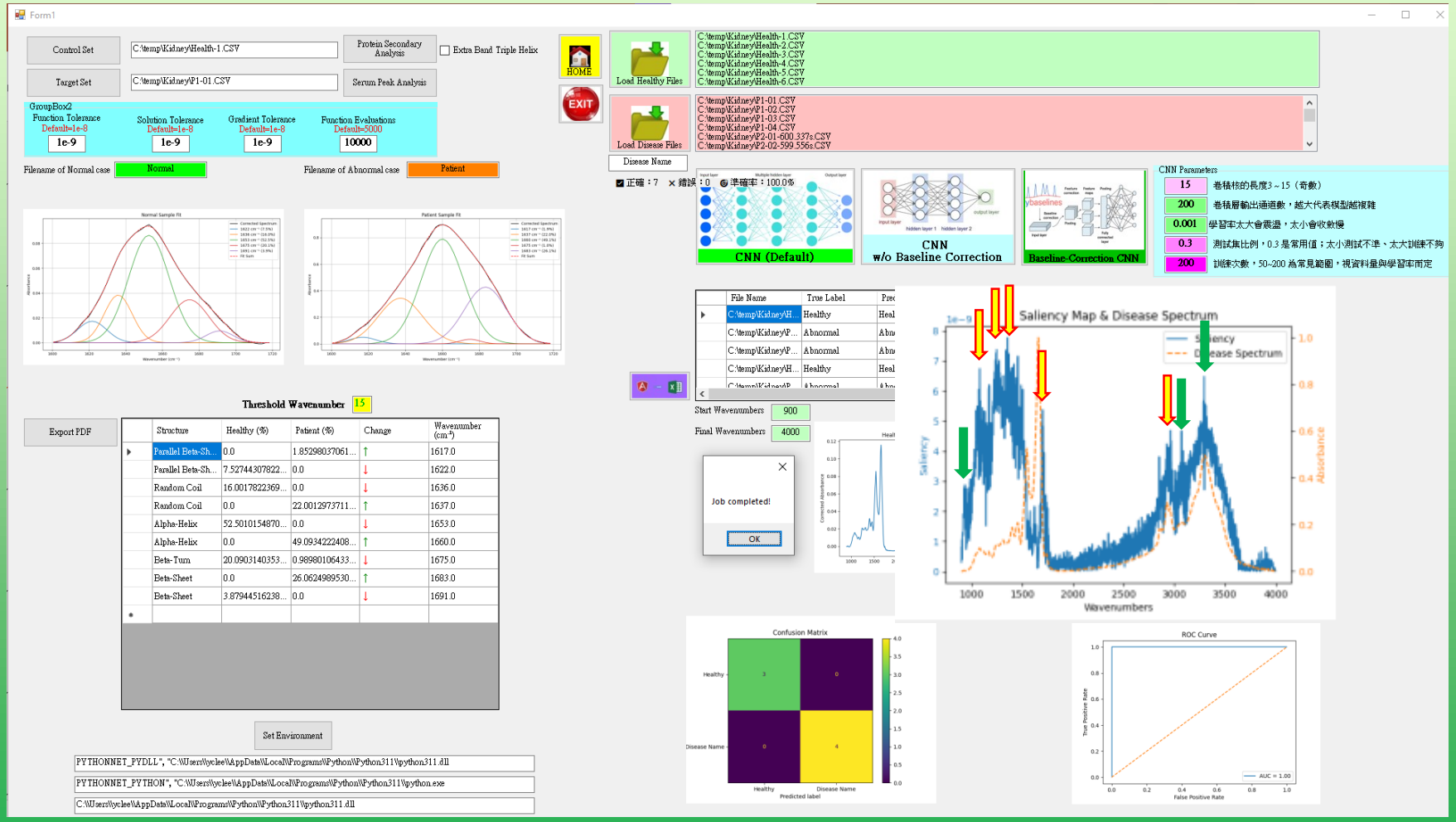

New Cancer Early Detection Technology
Schematic Diagram of Detection Process Combining FTIR Image Analysis

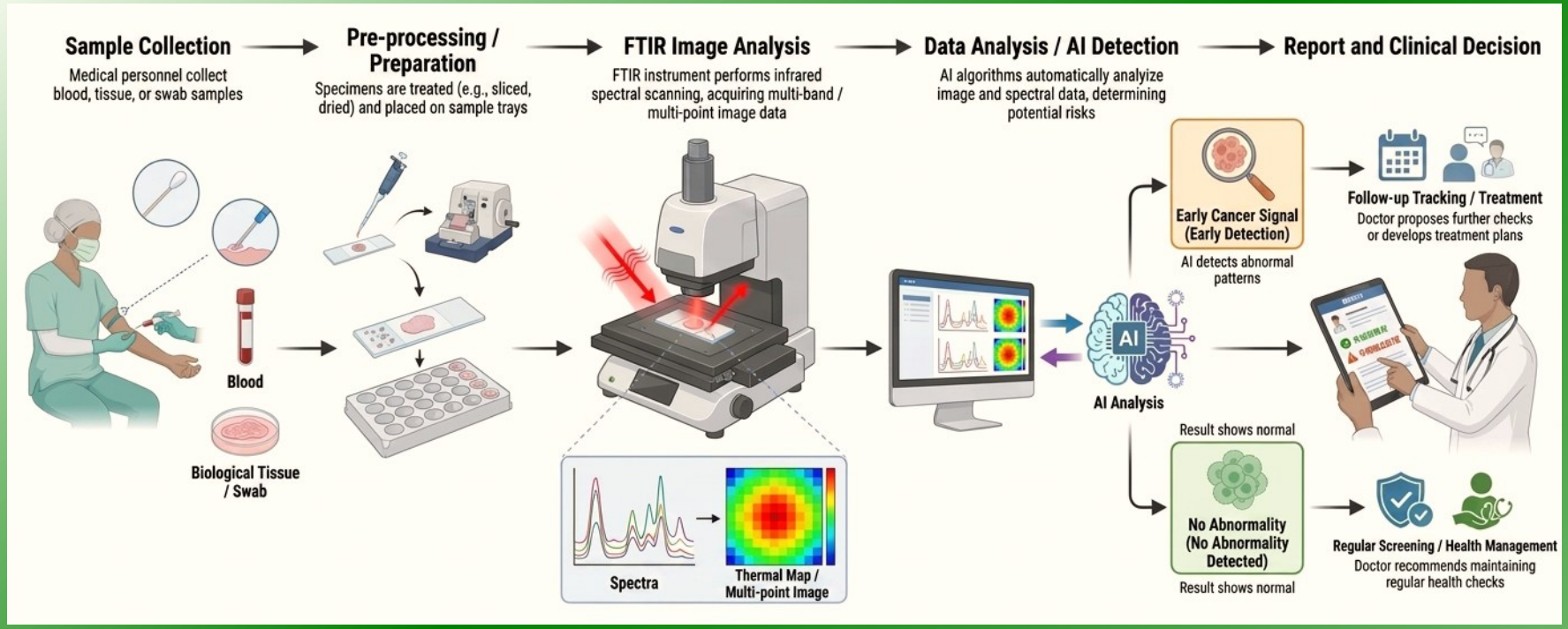

Summary:

This diagram illustrates a cancer early detection method combining innovative 4D Fourier Transform Infrared imaging technology, highlighting its high precision and automated analysis

Wax Physisorption Kinetics with FTIR Imaging for Molecular Characterization and Cancer Screening

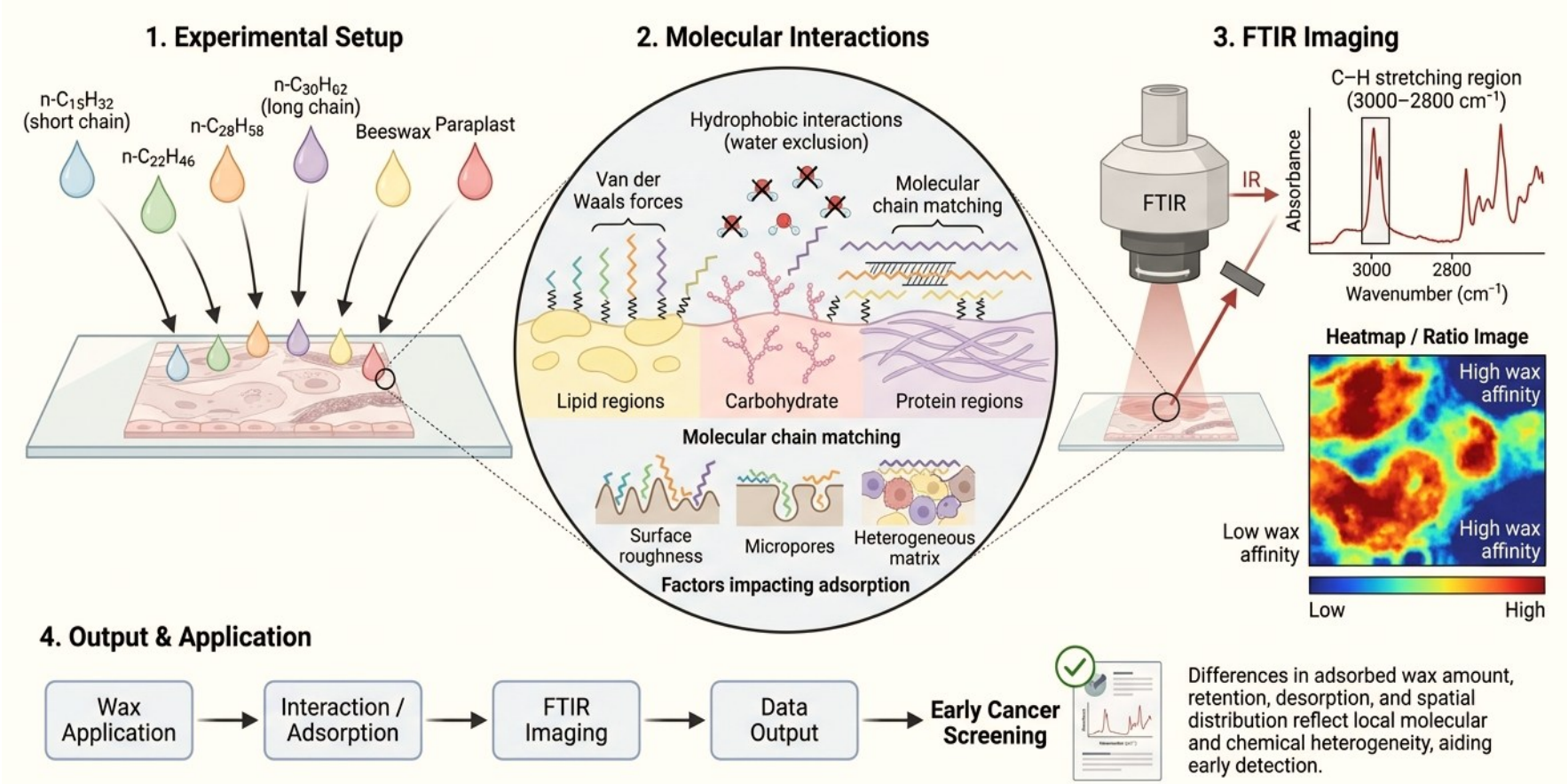

WPK-FTIR/PINN-Based Chemical Imaging Analysis of Colon Cancer Tissue Sections

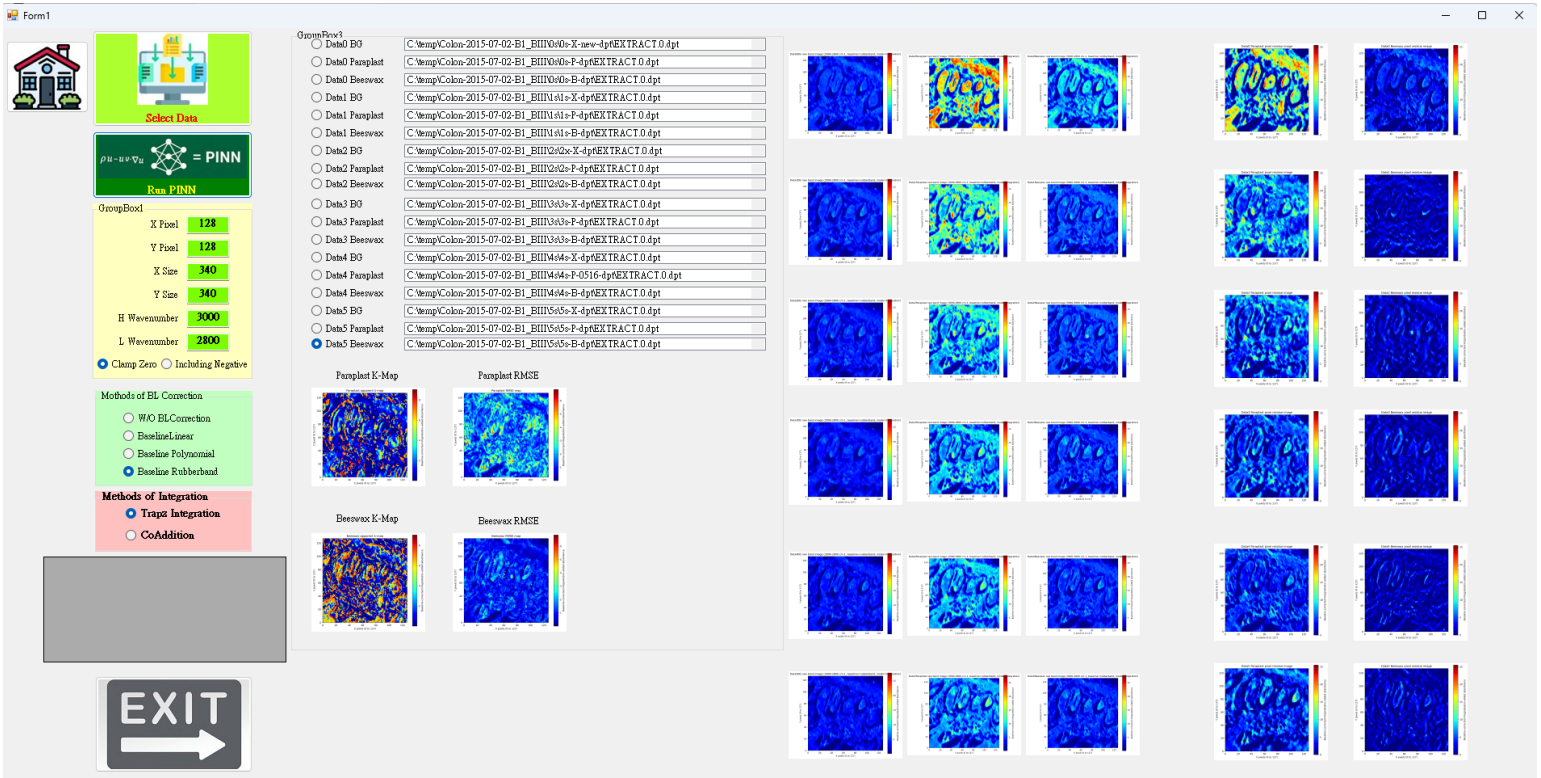

ACH-WPK-FTIR/PINN analysis interface and chemical imaging results of a colon cancer tissue section.The customized UI integrates FTIR spectral image loading, baseline correction, spectral integration, and PINN-based kinetic analysis. Spatially resolved K-maps and RMSE maps are generated for different wax probes, such as paraplast and beeswax, to visualize heterogeneous wax–tissue interactions in colon cancer tissue sections.

Infrared Spectroscopic and Computational Platform for Real-Time Assessment of Lupus Nephritis

- **Multi-marker analysis:** IgG glycosylation, lactate, hydrophobicity, hydrophilicity, albumin.
- **IR platform with Prognosis Prediction Function (PPF):** Spectral markers integrated with renal biomarkers for prognosis.
- **SAXS validation:** Glycosylated IgG shows larger radius of gyration (Rg).
- **Clinical value:** Real-time monitoring and prognosis in lupus nephritis.

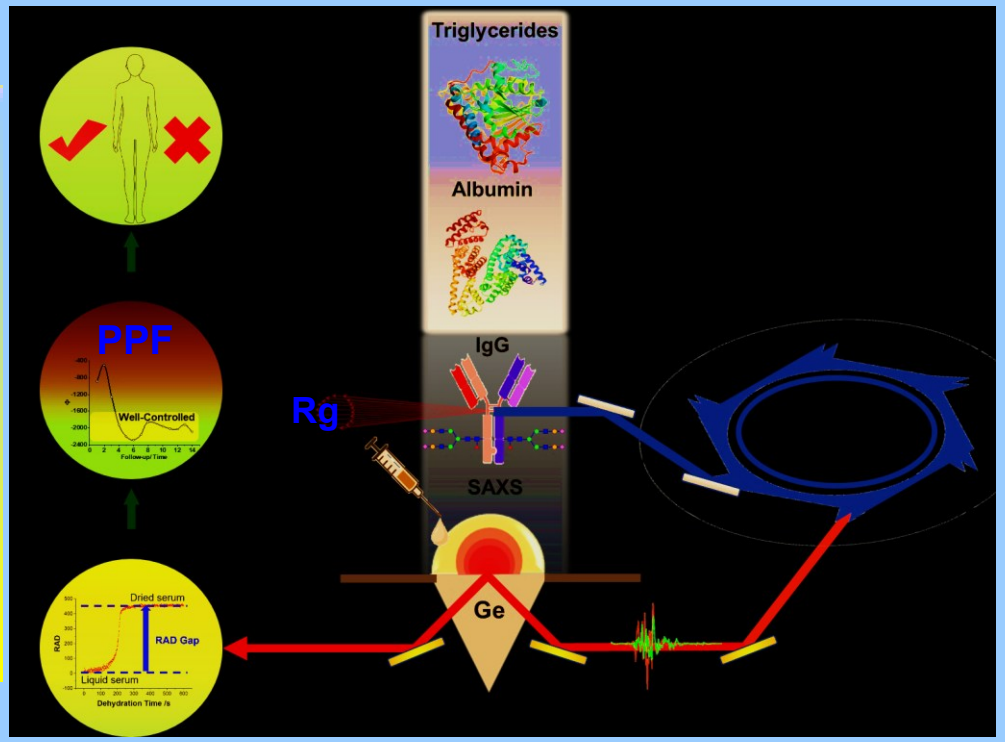

Multi-marker analysis

Biosensors. 2025; 15(1):39. https://doi.org/10.3390/bios15010039

AI-Driven Infrared Spectroscopy for Real-Time Lipid and Metabolic Syndrome (MetS) Assessment

Dyslipidemia (血脂異常) is a hallmark of metabolic syndrome, but current lipid assays are time-consuming (days).

- **AI-assisted ATR-FTIR** enables lipid profiling from **0.5 µl blood in ~10 min**.
- **HGBT model** achieved best lipid prediction (TG R^2 = 0.85; HDL-C R^2 = 0.76).
- **RF model** showed the highest MetS classification accuracy (AUC = 0.978).
- Provides **rapid, accurate monitoring** for MetS diagnosis and intervention.

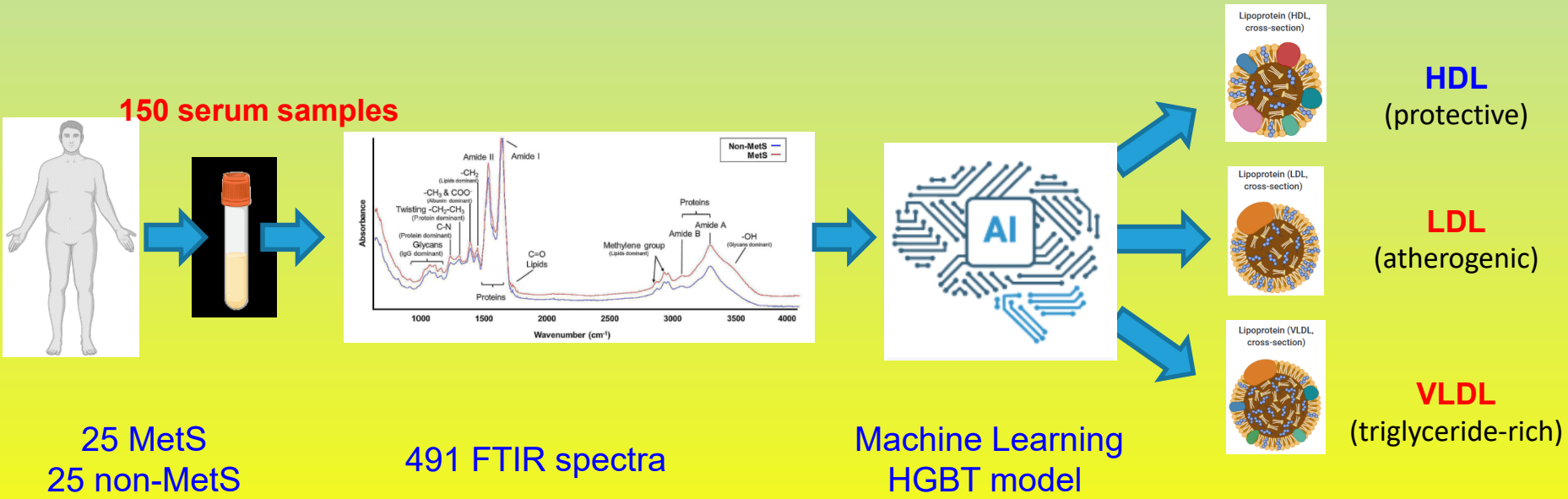

PLoS One. 20(1):e0316522(2025); doi: 10.1371/journal.pone.0316522. PMID: 39883744

VI. Summary and Take-home Message

Key Topic	Summary	Take-home Message
Synchrotron IR / FPA-FTIR	High-brightness IR source and FPA detector enable rapid spectral imaging.	**Fast chemical imaging with high spatial information.**
Lateral Resolution	Far-field FTIR resolution depends mainly on **wavelength and N.A.**	**Light source improves S/N, not the diffraction limit.**
FTIR Spectral Imaging	**Each pixel** contains a full infrared spectrum.	**One pixel = one spectrum = one molecular fingerprint.**
Spectral Processing	Baseline correction, normalization, smoothing, and spectral range selection are essential.	**Good preprocessing gives reliable chemical images.**
Chemical Image Construction	Peak height, peak area, band ratio, PCA, or ML features can generate maps.	**Chemical images are quantitative spectral-feature maps.**
ATR / GIRA / Nano-IR	ATR and GIRA provide surface-sensitive analysis; nano-IR extends resolution to the nanoscale.	**Different IR modes reveal different spatial and surface information.**
AI-Driven Analysis	ML/DL can classify spectra, identify patterns, and generate prediction maps.	**AI converts FTIR images into diagnostic information.**